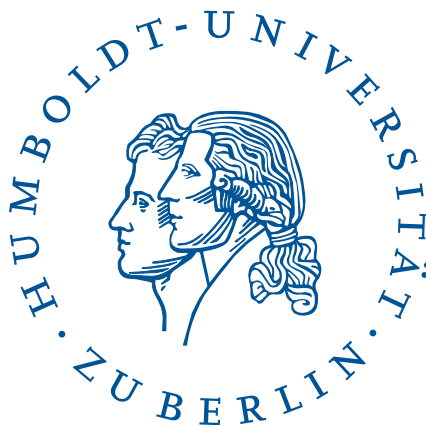Master Thesis:

The Application Of Elliptic Polylogarithms in All Order Solutions Of Massive Two-Loop Integrals

Author: Armin Ralf Kurt Schweitzer

Date: June 28, 2017

Abstract

This thesis is concerned with the computation of the Laurent expansion of scalar Feynman integrals within the framework of dimensional regularization.

For a large class of integrals the computation of their Laurent expansion is well understood within the iterated structure of hyperlogarithms. Beyond hyperlogarithms one enters mostly unknown territory and there are only two known examples of iterated all order solutions in terms of elliptic polylogarithms, the sunrise and the kite [107, 124].

I discuss our all order solution of the kite family in terms of elliptic polylogarithms [124]. Since understanding the sunrise enabled us to obtain this result, I review the iterated solution in [107]. Hereby the emphasis will be on the structure rather than on the explicit solution and crucial technical details are added.

The iterated solutions were computed in the Euclidian regime only. But due to a study of their structure we were able to obtain a simple analytic continuation to the complete kinematic regime [109]. This analytic continuation and the numerical results are reviewed. The numerical results are extended by an explicit comparison of the solution of the sunrise integral with one massive propagator in terms of hyperlogarithms and elliptic polylogarithms. This allows us to study the influence of the finite q-series expansion on the error of the approximation. One finds that already at low orders in the q-expansion the relative error away from the thresholds is $< 10^{-16}$.

For a good understanding of these generalized all order solutions, a knowledge of currently well established approaches and the structures arising therein is important. Therefore the method of IBP-reductions and differential equations as well as the iterated all order solutions of Feynman integrals within the class of hyperlogarithms are reviewed on detailed examples with an emphasis on the structure of the results.

Selbstständigkeitserklärung

Hiermit erkläre ich, dass ich die vorliegende Masterarbeit selbstständig und nur unter Verwendung der angegebenen Literatur und Hilfsmittel angefertigt habe. Die aus fremden Quellen direkt oder indirekt übernommenen Stellen sind als solche kenntlich gemacht.

Die Arbeit wurde bisher in gleicher oder ähnlicher Form keiner anderen Prüfungsbehörde vorgelegt.

_____
Armin Schweitzer

_____
Datum, Ort

Danksagungen

Contents

Chapter 1

Motivation

This master thesis is concerned with the computation of Feynman integrals. Feynman integrals arise as contributions to scattering amplitudes in the treatment of quantum field theories within the framework of perturbation theory. The computation of these scattering amplitudes is the foundation of theoretical predictions on the outcome of high-energy scattering experiments as measured e.g. at LHC. The increasing precision of the experimental tests of the Standard Model of particle physics gives rise to new requirements on the accuracy of the theoretical prediction. This leads to the necessity to compute increasingly numerous and complicated Feynman integrals. These computations soon reach a high mathematical complexity such that the existing methods have to be constantly improved and new approaches need to be developed to allow a successful evaluation of this mathematically challenging task.

Currently a wide class of Feynman integrals can be computed within a class of special functions, known as hyperlogarithms. By improving on the established methods of parametric integration and differential equations [45, 46] these computations could be greatly simplified and systematized [35, 43, 73, 76].
Beyond this well established class of functions, little is known and the results are obtained in a case to case study. In a recent computation of the equal mass 2-loop 3-denominator sunrise topology [26, 93, 95–113] a first iterated all order result of a Feynman integral beyond hyperlogarithms could be obtained in the Euclidian regime [107]. This solution required a generalization of the class of functions towards the elliptic case which was already established in the computation of Feynman integrals [107, 110].

Originating from this result and its beautiful structure are two questions:

- Can a similar class of functions be used to compute other Feynman integrals to all orders in their Laurent expansion?

- Can the results be continued into the whole physical regime?

The answer to both questions is yes.
In a joint work with Luise Adams, Christian Bogner and Stefan Weinzierl we obtained the all order result of the kite, a more involved 5-denominator topology, in terms of elliptic polylogarithms [124].
The analytic continuation of the integrals of the kite and all its sub-topologies has been computed in a recent joint work with Christian Bogner and Stefan Weinzierl [109].

The main goal of this thesis is to establish the methods and structures of the iterated solutions of all order results of Feynman integrals in a comprehensive way, such that the non-standard and non-trivial generalizations necessary to understand our results can be lucidly presented. To achieve this goal I structured the thesis in three parts as followed:

Part I: Short introductions into commonly used tools and concepts in the computation of scalar Feynman integrals with emphasis on their application. The introduced subjects include the necessity of a regularization scheme in chap. 2, the consideration of complete families of Feynman integrals (called topologies) in chap. 3, the method of integration-by-parts in chap. 4 and the parametric representation of Feynman integrals in chap. 5.

Part II This part introduces in chapter 6 the computation of Feynman integrals to all orders in terms of hyperlogarithms. In this part I will emphasize the iterated structure of the results and introduce the class of special functions in which it becomes manifest, the hyperlogarihms. This will be done by investigation of the parametric representation. Furthermore I review the method of differential equations and introduce the concept of a canonical basis. The canonical basis will be introduced by constructing certain dLog-forms in the parametric representation. The canonical basis necessary for the computation of the kite integral will be explicitly derived.

Part III In this part consisting of chapter 7 the iterated structure of Feynman integrals beyond hyperlogarithms is discussed. The result of the all order solution of the equal mass sunrise as obtained by Adams et al will be reviewed in some detail and the elliptic polylogarithms will be introduced. The second part of this chapter presents the results of the master integrals of the kite topology, their analytic continuation and numerical evaluation. Thereby the emphasis will be on the structure rather than the explicit results. The non-trivial technical details of these computations are covered in detail in appendix B.

Chapter 2

Fundamentals and Basic Techniques

Feynman diagrams are the basic objects for visualization as well as computation in quantum field theories within the framework of perturbation theory, meaning a series expansion of the path integral around small coupling constants.

These computations are a crucial part in the understanding of the fundamental interactions between particles described in the standard model and studied in scattering experiments at particle colliders like the LHC. For testing the validity of the standard model and its limits there have to be high precision predictions on the observables accessible by collider experiments.

One of these observables, typically measured by scattering experiments, is the cross section σ. The cross section is related to the probability P that a scattering of incoming particles A will result in outgoing particles B. The relation between the theoretical computation and the measured cross section for a given scattering process is roughly described by

$$\sigma\left(A \to B\right) \propto \left|P\left(A \to B\right)\right|^2 \propto \left|\sum all\ possible\ feynman\ diagrams\right|^2 \quad . \tag{2.0.1}$$

Hereby a *Feynman diagram* is a pictorial representation of the underlying fundamental particle interactions which can be "translated" into mathematical expressions by the so called *Feynman rules*.

2.1 Fundamentals

A Feynman diagram (here: $2 \to 2$) describes, shortly and superficially speaking, the

$$\tag{2.1.1}$$
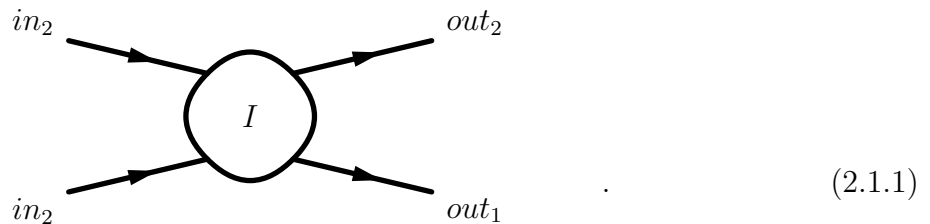
physical process of: some particles come in, they interact (I), some other come out. The incoming and outgoing particles are referred to as *legs* carrying *external momenta*. The interaction of these external particles is graphical depicted by a connection with *internal*

$$\text{(2.1.2)}$$
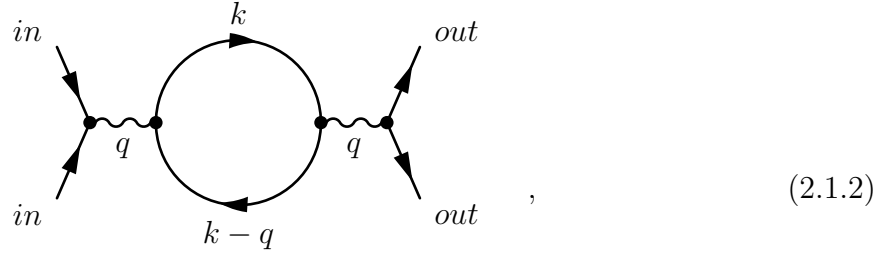
lines called *edges* carrying *internal momenta*. All possible ways of connecting the external particles are completely determined by the order of expansion in the coupling and by the allowed *vertices* (dots in the diagram above), which originate from the underlying field theory. The four momentum is conserved at every vertex such that the incoming and outgoing momenta add to zero.

In higher order perturbation theory the internal momenta are not completely determined by momentum conservation. In that case the internal momenta are referred to as *loop* momenta (k in the graph above). One has to integrate over the undetermined *loop* momenta since they can take any value. Diagrams containing loops are called loop integrals. If a diagram has n loops and m external legs it is referred to as n-loop m-point function. Diagrams with completely determined internal momenta are called *tree-level* diagrams.

The Feynman rules associated to the diagrams of different sorts of quantum fields can be summarized as followed

- $\displaystyle \frac{}{} \propto \frac{T^{\nu_1 \nu_2 \ldots}_{\mu_1 \mu_2 \ldots}}{k^2 - m^2 + i\varepsilon}$:

  is called propagator an describes the propagation of an particle

- : is called vertex and is proportional to the couplings of the fields

- the momentum is conserved at every vertex

- $\displaystyle \int \mathrm{d}^4 k$ integrate over loop momenta .

One recognizes in the rules above, that momentum integrals occur for every Feynman diagram beyond the tree-level and that they might posses a tensor structure resulting from the underlying quantum fields. In general, the analytical evaluation of these types of integrals is far from trivial and they require a continuous improvement of existing mathematical methods, algorithms and in some cases a development of completely new strategies and mathematical functions.

2.2 Basics for Scalar Feynman Integrals

The main subject of this thesis is the investigation and computation of massive scalar 2-loop diagrams. These diagrams do not arise from an interacting theory directly, since there is only one scalar particle described within the standard model, the Higgs-boson. However, tensor integrals which occur in the computation of scattering processes beyond the tree-level can be reduced to scalar integrals. A first systematic reduction of one-loop tensor integrals was developed by Passarino and Veltman in the context of the computation of the $e^+e^- \to \mu^+\mu^-$ scattering process [1]. Reductions of multi-loop integrals are possible as well [2–4], such that the evaluation of the initial Feynman diagram, given by the scattering process under investigation, reduces to the computation of a certain combination of scalar multi-loop integrals.

Therefore, the knowledge of the solution of scalar Feynman integrals is an essential step within the prediction of actual scattering processes observed in collider experiments.

2.2.1 First Example and the Necessity of Regularization Schemes

The investigation of a rather simple massless scalar one-loop integral (2.2.1) reveals some of the difficulties connected to the evaluation of Feynman diagrams already.

$$I_1 = \int_{\mathbb{R}^{1,3}} \frac{\mathrm{d}^4 k}{(2\pi)^4} \frac{1}{k^2(-k)^2} \tag{2.2.1}$$
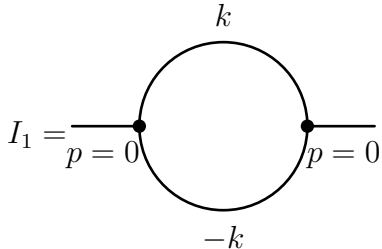
The first problem lies in the measure of the integral. Since the momenta are elements of the Minkowski space $k \in \mathbb{R}^{1,3}$ it is not intuitively obvious how to perform the integration. However, one can show that a suitable change of the k^0 integration contour, the so called Wick-rotation [1], yields "momenta" K in the Euclidean $\mathbb{R}^4$, whereas after the substituting

$$k_0 = iK_0, \tag{2.2.2}$$

$$k_j = K_j \qquad \text{for } j = \{1,2,3\} \tag{2.2.3}$$

the scalar product becomes

$$k^2 = k_\mu k^\mu = k_0^2 - k_j^2 = -K_0^2 - K_j^2 = -K^2 \tag{2.2.4}$$

and the measure changes according to

$$\mathrm{d}^4 k = i\mathrm{d}K_0 \mathrm{d}^3 K = i\mathrm{d}^4 K \ . \tag{2.2.5}$$

---

[1] For a detailed review of the Wick-rotation see e.g. [5].

This change of variables leaves us with "ordinary" scalar products in $\mathbb{R}^4$ and makes the $i\varepsilon$-prescription in the propagator superfluous. Throughout this thesis, momenta in the Euclidean space $\mathbb{R}^4$ are denoted by capital letters (K) and momenta in the Minkowski space $\mathbb{R}^{1,3}$ by small ones (k). Furthermore we work in a mostly minus convention, such that $k_\mu k^\mu < 0$ for space-like momenta k.

How to perform the integral I_1 depicted in (2.2.1) becomes obvious after applying a Wick-rotation (W.R.) and a change to 4d-spherical coordinates (S.C.)

$$I_1 = \int\limits_{\mathbb{R}^{1,3}} \frac{\mathrm{d}^4 k}{(2\pi)^4} \frac{1}{k^4} \stackrel{W.R.}{=} i \int\limits_{\mathbb{R}^4} \frac{\mathrm{d}^4 K}{(2\pi)^4} \frac{1}{K^4} \stackrel{S.C.}{=} i \int\limits_0^\infty \mathrm{d}K_E \frac{-iK_E^3}{K_E^4} \int\limits_{\partial S^4} \frac{\mathrm{d}\Omega}{(2\pi)^4} \tag{2.2.6}$$

$$= \int\limits_0^\infty \frac{\mathrm{d}K_E}{(4\pi)^2} \frac{1}{K_E} \qquad \left(\text{"}\propto \log(K_E)\big|_0^\infty\text{"}\right) \tag{2.2.7}$$

and the second mayor issue becomes obvious. I_1 diverges logarithmically in the limit $K_E \to 0$ as well as $K_E \to \infty$.

These divergences do not stem from some improper integral transformation (W.R. or S.C.) but became only more apparent through them. They are not restricted to the integral I_1 but will arise for certain classes of Feynman integrals beyond tree-level and their physical interpretation is beyond the scope of this thesis (but is given in every proper QFT textbook).

However, it is quite evident, that every physical observable given by means of divergent integrals is in itself ill defined. Therefore one has to find ways to *regularize* these divergences for a further treatment within the framework *renormalization.*

For a further discussion of divergences arising in Feynman integrals, we classify them as followed:

The divergences in the limit $k \to 0$ and thus in the limit $1/k \propto \lambda \to \infty$ of long wavelengths λ are called *infrared* (IR) divergences, whereas the divergences associated with large momenta $k \to \infty$ (short wavelengths) are called *ultraviolet* (UV) divergences.

By studying the analytical structure of the scalar propagators

$$P(K^2) \propto \frac{1}{K^2 + m^2} \stackrel{m \to 0}{\to} \frac{1}{K^2} \tag{2.2.8}$$

it becomes apparent that IR-divergences do arise for massless propagators (e.g. stemming from photons) only. Therefore they are somewhat special, since IR divergent Feynman diagrams have to be completely massless or contain at least a completely massless subdiagram.

UV divergent diagrams on the other hand, do not depend on special properties like massless propagators. They do arise for every Feynman diagram (massless or massive) for which the so called *superficial* degree of UV divergence $G = DL - 2P$ becomes greater or equal zero for itself or one of its sub-graphs. Hereby D denotes the dimension of space time, L the number of loops and P the number of internal edges ($\propto$ propagators).

The diagram shown in (2.2.1) is both IR and UV divergent in $D = 4$ spacetime dimension and its superficial degree of divergence reads $G = 4 \cdot 1 - 2 \cdot 2 = 0$ which manifests itself in the logarithmic UV divergence of the integral.

For the treatment of divergences in Feynman diagrams, several regularization schemes

have been developed. These schemes either modify the propagator [6, 7] or the dimension of the integral measure [8–11].

Dimensional Regularization

During this thesis we will work within the framework of dimension regularization[2]. Within this scheme we consider the momentum integrals in arbitrary D dimensions instead of the original physically motivated $D = 4$. Here, D becomes an additional free parameter of the problem, which does not have to be an integer or even real. After computing the integral we will get a function of the kinematical invariants, the masses and the parameter D. By considering the limit $D \to 4$, we can investigate the divergent behavior of the integral and are able to make it manifest within a suitable chosen expansion parameter.

From now on we will consider the D-dimensional version I_1^D

$$I_1^D = \int\limits_{\mathbb{R}^{1,D-1}} \frac{\mathrm{d}^D k}{(2\pi)^D} \frac{1}{k^4} \tag{2.2.9}$$

of the integral I_1 (2.2.1) and point out some general aspects regarding divergent Feynman integrals within dimensional regularization.

To get a more handy version of the integral (2.2.9) we can apply Wick-rotation once again. Furthermore it is convenient to work in D-dimensional spherical coordinates whereas the measure transforms according to $\mathrm{d}K^D \to \mathrm{d} K_E K_E^{D-1} \mathrm{d}\Omega_D$. The integration of the generalized solid angle $\mathrm{d}\Omega_D$ yields an D dependent closed form such that it suffices to consider the K_E dependent part of the integral for an investigation of the divergences only.

Therefore the interesting part of the integral (2.2.9) is

$$I^D = \int\limits_0^\infty \mathrm{d}K_E \frac{K_E^{D-1}}{K_E^4} \ . \tag{2.2.10}$$

For the analysis of the IR-divergence only, we consider an upper bound on the integration, the so called *cut-off* Λ. This cut-off is taken to be large but finite. Even though it plays a central role in certain regularization schemes (see e.g. [6]), it is only used to make the integral UV-finite here. After introducing the cut-off, we are left with the integral

$$I_{IR}^D = \int\limits_0^\Lambda \mathrm{d}K_E \frac{K^{D-1}}{K_E^4} \ . \tag{2.2.11}$$

From the integral (2.2.11) it becomes obvious that we have to consider initially IR-divergent integrals in generalized D-dimensions with $\mathrm{Re}(D) > 4$ to ensure IR-convergence.

---

[2]Notice that it has been stated in [12] and the references therein (see footnote [1] in [12]), that this regularization scheme and the connected MS-scheme within renormalization is erroneous on the level of the path integral. But we will take a "practical" approach here, since dim. reg. is quite convenient and has not failed in practical applications yet (at least to my knowledge).

To obtain an analogous condition on D for initially UV-divergent integrals, we consider the slightly modified integral

$$I_{UV}^D = \int\limits_0^\infty \mathrm{d}K_E \frac{K_E^{D-1}}{(K^2+m^2)^2} \ , \qquad (2.2.12)$$

where we introduced an additional parameter, which corresponds to a mass. The integral (2.2.12) yields the initial integral I^D (2.2.10) in the limit $m \to 0$ and it convergences for $K_E \to \infty$ only if $\mathrm{Re}(D) < 4$.

Although we considered a special example only, the obtained conditions on D are more general. Integrals with UV-divergences yield well defined results if they are considered in arbitrary dimensions D with $\mathrm{Re}(D) < 4$ (or even $\mathrm{Re}(D) < 2$), whereas initially IR-divergent integrals are convergent in D dimensions iff $\mathrm{Re}(D) > 4$. In $D = 4$ dimensions the integrals have poles [5].

At first sight, these two conditions seem to contradict each other and one would expect, that there is no dimensional regularization scheme, in which the simultaneous regularization of both UV- and IR-divergences is possible. That it is possible to dimensionally regularize both IR- and UV-divergent after all is not trivially seen, such that we will solely outline the main ideas on how to achieve it [3].

Given a both IR- and UV-divergent integral, regularize the IR-divergence with a suitable (non dimensional) regularization scheme by for example introducing massive propagators as in the case of $I^D \to I_{UV}^D$.

Once the IR-divergence is regularized the integration in the domain $\mathrm{Re}(D) < 4$ yields a well defined function of D which will be analytic and can be continued on the whole complex D-plain. The regulators initially introduced for the IR-finiteness of the integral can now be removed in the domain $\mathrm{Re}(D) > 4$ by considering the analytically continued result of the first integration in that region, such that IR- as well as UV-divergences are regularized dimensionally. The poles associated to the divergences in dimensional regularization will enter the result with opposite signs. Therefore it is possible to set integrals without an external scale, meaning no dependence on the external momenta and massless propagators (see e.g. (2.2.9)), to zero [4].

The poles associated to UV-divergences in $D \to 4$ dimensions are treated within the framework of renormalization of the underlying QFT.

The poles originating from IR-divergences cancel, under the assumption of a finite resolution of detectors used in the actual experiments, with IR-divergences of phase-space integrals (Kinoshita-Lee-Nauenberg-Theorem [14, 15]). That means, roughly speaking, that the standard model is IR-finite if detectors can not resolve particles below a certain energy-threshold respectively separate them below a certain distance limit.

A detailed treatment of renormalization or the resolution and canceling of IR-divergences is far beyond the scope of this master thesis, since both are current fields of research in their own right with a high degree of complexity involving different mathematical formalisms respectively approaches.

At this point, I will summarize the main aspects of the preceding paragraphs and emphasize on the results mandatory for understanding the upcoming discussions, since

---

[3] For a more explicit and complete discussion of the here outlined ideas see e.g. [5].

[4] More properties of dimensional regularized Feynman integrals are listed e.g. in [13] (p. 9 ff.).

they may seem rather technical at some points.

If we attempt high precision predictions on observables measured in scattering experiments, we have to compute associated Feynman diagrams, which are a pictorial representation prescribed by the interactions of underlying quantum fields. These diagrams are translated to formulas by using Feynman rules and they yield complicated integrals over loop momenta for higher orders within a perturbative treatment of QFT. These integrals over the loop momenta are mostly tensor integrals, but they are reducible to combinations of scalar integrals. The attempt to compute certain types of Feynman integrals leads to ill defined, divergent expression in $D = 4$ dimensions. It is possible to treat this divergences within the framework of dimensional regularization such that the integration over the loop momenta is performed in arbitrary D dimensions. It is possible to change between momenta k defined as elements of the Minkowski space $\mathbb{R}^{1,D-1}$ and Euclidean "momenta" defined as elements in $\mathbb{R}^D$. Throughout this thesis capital letters are used for Euclidean momenta and we will work in a mostly minus metric for the Minkowski-space.

Chapter 3

A More General Viewpoint

In the previous chapter we discussed some crucial properties of Feynman integrals associated to scattering processes of elementary particles. Up to now we have not solved any integrals, neither in $D = 4$ nor in arbitrary D-dimensions. That is owed to the fact that the methods of the computation of Feynman integrals are, except fo some special cases, highly non trivial. Therefore it is desirable to find methods to relate similar integrals and to evaluate as little integrals as possible explicitly via integration. To specify what similarities to expect and how to use them for the purpose of reductions, we will look at Feynman integrals from a slightly more general viewpoint.

3.1   Topologies

After a successful tensor reduction of the initial integral, we are left with a linear combination of scalar Feynman integrals with g legs, l loops and d internal edges in the generic form

$$\int \mathrm{d}k_1^D \mathrm{d}k_2^D \ldots \mathrm{d}k_l^D \frac{\prod\limits_{i=1}^{N_{sp}} S_i^{n_i}}{\prod\limits_{j=1}^{d} D_j} \tag{3.1.1}$$

where we suppressed constant factors resulting from the Fourier-transform and the dimensional regularization procedure. The D_j in the denominator in (3.1.1) denote the quadrics

$$D_j = q_j^2 - m_j^2 \tag{3.1.2}$$

associated to the internal edges of the Feynman diagram. From now on we will refer to the D_j as propagators since they fully characterize the scalar propagator $\propto 1/D_j$.
The S_i in (3.1.1) are scalar products between either external and internal momenta or between two of the l internal momenta, whereas the $n_i \in \mathbb{N}$ are related exponents. The product of the S_i is over all possible N_{sp} combinations of the l internal and $g - 1$ external momenta, such that $N_{sp} = N_{lg} + N_{ll}$.
The number N_{lg} of possible scalar products between external and internal momenta is

$$N_{lg} = l(g - 1) . \tag{3.1.3}$$

Hereby one has to take the momentum conservation of the whole diagram into consideration, such that one of the external momenta is always expressible through the $g - 1$ remaining ones. The number N_{ll} of scalar products between the loop-momenta is given by

$$N_{ll} = \frac{l(l+1)}{2} \tag{3.1.4}$$

and it follows that there are

$$N_{sp} = l(g-1) + \frac{l(l+1)}{2} \tag{3.1.5}$$

possible scalar products. If only t of the d propagators D_j in (3.1.1) are different, we can denote the integral as

$$\int \mathrm{d}k_1^D \mathrm{d}k_2^D \ldots \mathrm{d}k_l^D \frac{\prod\limits_{i=1}^{N_{sp}} S_i^{n_i}}{\prod\limits_{j=1}^{t} D_j^{m_j}} \tag{3.1.6}$$

with $m_j, n_i \in \mathbb{N}$. Furthermore there are t of the N_{sp} scalar products expressible through the propagators such that only $q = N_{sp} - t$ of the scalar products are *irreducible*. We are left with a so called *topology*

$$\mathcal{T}_{\mu_1,\ldots,\mu_t;\nu_1,\ldots,\nu_1} = \int \mathrm{d}k_1^D \mathrm{d}k_2^D \ldots \mathrm{d}k_l^D \frac{1}{\prod\limits_{j=1}^{t} D_j^{\mu_j} \prod\limits_{i=1}^{q} D_{t+i}^{-\nu_i}} \tag{3.1.7}$$

with $\mu, \nu \geq 0$, where we introduced q additional propagators to denote the irreducible scalar products. Topologies can be drawn and analyzed by the same Feynman rules as the initial Feynman diagrams.

3.1.1 Example: A Feynman Diagram And Its Topology

In the following we are going to emphasize the relations between Feynman diagrams and their associated topologies. This will be done in analogy to an example in [16].

Consider the massive, scalar Feynman digram given by
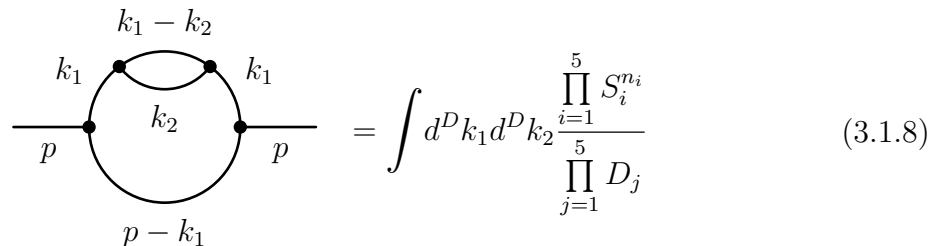
$$= \int d^D k_1 d^D k_2 \frac{\prod\limits_{i=1}^{5} S_i^{n_i}}{\prod\limits_{j=1}^{5} D_j} \tag{3.1.8}$$

with $d = 5$ internal edges, $g = 2$ legs, $l = 2$ loop momenta and $N_{sp} = 2 + 3 = 5$ possible scalar products.

The relations between possible scalar products S_i and a choice of propagators respecting momentum conservation are listed in table (3.1). It is obvious that there exist relations such that only one scalar product, e.g. the arbitrarily chosen $S_5 = p \cdot k_2$, is irreducible. Analogously to (3.1.7) one could define an irreducible propagator

$$D_{irr} = (p - k_2)^2 \tag{3.1.9}$$

encoding the scalar product S_5.

Table 3.1: Relations between scalar products and propagators of the Feynman diagram (3.1.8).

scalar product S_i	corresponding propagator	relation
$S_1 = k_1^2$	$D_1 = k_1^2 - m^2$	$S_1 = D_1 + m^2$
	$D_5 = k_1^2 - m^2 = D_1$	
$S_2 = k_2^2$	$D_2 = k_2^2 - m^2$	$S_2 = D_2 + m^2$
$S_3 = k_1 k_2$	$D_3 = (k_1 - k_2)^2 - m^2$	$S_3 = \frac{1}{2}(D_1 + D_2 - D_3 + m^2)$
$S_4 = p k_1$	$D_4 = (p - k_1)^2 - m^2$	$S_4 = \frac{1}{2}(D_1 - D_4 + p^2)$
$S_5 = p k_2$ (irred.)	$D_{irr} = (p - k_2)^2$ (z.B.)	$S_5 = \frac{1}{2}(D_2 - D_{irr} + p^2)$

Furthermore, as listed in table 3.1, two of the propagators can be chosen identically, such that the Feynman diagram eq. (3.1.8) can be written as an element of a simpler family

$$\int \mathrm{d}^D k_1 \mathrm{d}^D k_2 \frac{(D_1 + m^2)^{n_1}(D_2 + m^2)^{n_2}(\frac{1}{2}(D_1 + D_2 - D_3 + m^2))^{n_3}(\frac{1}{2}(D_1 - D_4 + p^2))^{n_4} S_5^{n_5}}{D_1^2 D_2 D_3 D_4} \tag{3.1.10}$$

with only four propagators and one irreducible scalar product.
Therefore every integral in (3.1.8) is completely governed by the *4-denominator topology*
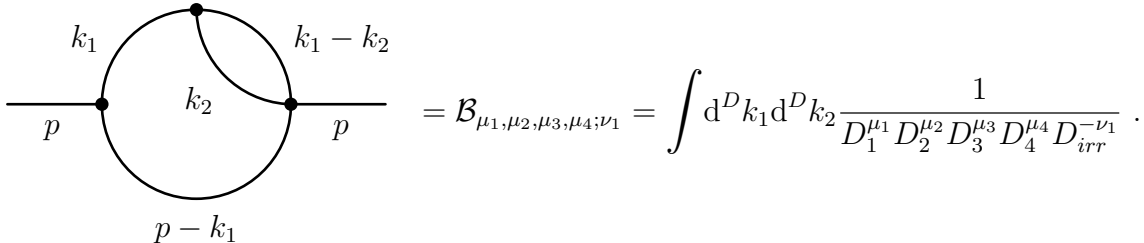
$$= \mathcal{B}_{\mu_1, \mu_2, \mu_3, \mu_4; \nu_1} = \int \mathrm{d}^D k_1 \mathrm{d}^D k_2 \frac{1}{D_1^{\mu_1} D_2^{\mu_2} D_3^{\mu_3} D_4^{\mu_4} D_{irr}^{-\nu_1}} \ . \tag{3.1.11}$$

Consider for example, that we are left with an integral of the type (3.1.8) with $n_1 = n_2 = 1$ and $n_{i>2} = 0$ after the tensor reduction. Inserting the relation from tab. 3.1

yields

$$I = \int d^D k_1 d^D k_2 \frac{k_1^2 k_2^2}{D_1^2 D_2 D_3 D_4} \tag{3.1.12}$$

$$= \int d^D k_1 d^D k_2 \frac{(D_1 + m^2)(D_2 + m^2)}{D_1^2 D_2 D_3 D_4} \tag{3.1.13}$$

$$= \int d^D k_1 d^D k_2 \frac{1}{D_1 D_3 D_4} + \frac{m^2}{D_1^2 D_3 D_4} + \frac{m^2}{D_1 D_2 D_3 D_4} + \frac{m^4}{D_1^2 D_2 D_3 D_4} \tag{3.1.14}$$

$$= \mathcal{B}_{1,0,1,1;0} + m^2 \mathcal{B}_{2,0,1,1;0} + m^2 \mathcal{B}_{1,1,1,1;0} + m^4 \mathcal{B}_{2,1,1,1;0} \tag{3.1.15}$$

and we see that this integral contains elements of 4-denominator topology only. The rewriting of scalar Feynman integrals by expressing reducible scalar products in terms of the propagators is called *trivial tensor reduction* [16].

In (3.1.15) the trivial tensor reduction canceled the propagator D_2 in the first two terms completely. These two terms can be associated to a simpler *3-denominator sub-topology*, whereby the complete cancellation of a propagator is called *contraction*. These contractions have a pictorial counterpart by means of a shrinking of the associated propagator, such that the contraction of D_2 in (3.1.15) is depicted as

$$\tag{3.1.16}$$

The elements of the "new" 3-denominator sub-topology can be translated into integrals by applying Feynman rules directly since the "old" and the "new" propagators are related by translations only, under which dimensionally regularized Feynman integrals are invariant [11].

For the initial integral (3.1.15) we find by using the topology $\mathcal{B}$ as well as the sub-topology $\mathcal{J}$

$$I = \mathcal{J}_{1,1,1;0,0} + m^2 \mathcal{J}_{2,1,1;0,0} + m^2 \mathcal{B}_{1,1,1,1;0} + m^4 \mathcal{B}_{2,1,1,1;0} \ , \tag{3.1.17}$$

whereas the integral representation can be obtained by applying the Feynman rules directly.

In the upcoming section, the advantage of the topology notation becomes apparent and we will therefore summarize its main points.

In the topology notation we denote Feynman integrals as a linear combination of integrals with minimal set of propagators and only irreducible scalar products. A topology is completely characterized by its propagators and irreducible scalar products. A specific set of indices yields a Feynman integral of the topology. If this Feynman integral does not have the complete set of propagators, it can be associated to a simpler sub-topology, whereas contractions of a propagators correspond to the shrinking of the associated internal edges.

Chapter 4

IBP-Reduction to Master Integrals

In the following, the advantage of the compact notation of families of Feynman integrals as topology becomes apparent, since, as we will see soon, the elements of a given topology are related by so called *integration-by-part*-identities [17]. Therefore the computation of topologies with arbitrary indices is reducible to the evaluation of so called *master integrals* (MI's) [1]. The main point behind the IBP-reduction is the vanishing of an integral of a total divergence, such that the identity

$$\int \mathrm{d}^D k_1 ... \mathrm{d}^D k_l \frac{\partial}{\partial k_i^\sigma} \left[v^\sigma T_{\mu_1,...,\mu_t;\nu_1,...,\nu_q} \right] = 0 \tag{4.0.1}$$

holds and can be used to derive relations between different integrals $T_{\mu_1,...,\mu_t;\nu_1,...,\nu_q}$ and $T_{\mu_1+a_1,...,\mu_t+a_t;\nu_1+a_{t+1},...,\nu_q+a_{t+q}}$ with $a_i \in \{-1,0,1\}$ of a given topology. The k_i in (4.0.1) denote loop momenta and the v can be either a loop or an external momentum.

4.1 Examples of IBP-Reduction

One of the easiest examples for IBP-reductions is given by the tadpole topology

$$\mathcal{I}_\mu = \underbrace{}_{} = \int \frac{\mathrm{d}^D k}{(k^2 - m^2)^\mu} \ , \tag{4.1.1}$$

since there exists only one IBP-relation

$$\int \mathrm{d}^D k \frac{\partial}{\partial k^\nu} \frac{k^\nu}{D_1^\mu} = 0 \ . \tag{4.1.2}$$

---

[1] For more complete overviews see e.g. [18] or [19]. The choice of examples is following [19].

This IBP-relation yields

$$\int \left(\left(\frac{\partial}{\partial k^\nu} k^\nu \right) \frac{1}{D_1^\mu} + k^\nu \left(\frac{\partial}{\partial k^\nu} \frac{1}{(k_\sigma k^\sigma - m^2)^\mu} \right) \right) \mathrm{d}^D k \tag{4.1.3}$$

$$= \int \left(\frac{D}{D_1^\mu} - 2\mu \underbrace{\frac{k^2}{D_1^{\mu+1}}}_{k^2 = D_1 + m^2} \right) \mathrm{d}^D k = \int \left(\frac{D - 2\mu}{D_1^\mu} - \frac{2\mu m^2}{D_1^{\mu+1}} \right) \mathrm{d}^D k \tag{4.1.4}$$

$$= (D - 2\mu)\mathcal{I}_\mu - 2\mu m^2 \mathcal{I}_{\mu+1} \tag{4.1.5}$$

$$= 0 \quad . \tag{4.1.6}$$

and after relabeling $\mu \to \mu - 1$ we are left with the recurrence relation

$$\mathcal{I}_\mu = \frac{D - 2\mu + 2}{2(\mu - 1)m^2} \mathcal{I}_{\mu-1} \quad . \tag{4.1.7}$$

In (4.1.7) it becomes obvious that there is only one MI, e.g. $\mathcal{I}_1$, for the whole tadpole topology and that every integral $\mathcal{I}_{\mu>1}$ is reducible to it.

A second slightly more involved but still rather simple example of an IBP-reduction is given by the integrals associated with the massive one loop two denominator topology

$$\mathcal{J}_{\mu_1,\mu_2} = \underset{p \qquad\qquad p}{\underset{D_2}{\overset{D_1}{\bigcirc}}} = \int \mathrm{d}^D k_1 \frac{1}{D_1^{\mu_1} D_2^{\mu_2}} \tag{4.1.8}$$

$$= \int \mathrm{d}^D k_1 \frac{1}{(k_1^2 - m^2)^{\mu_1}((p - k_1)^2 - m^2)^{\mu_2}} \quad . \tag{4.1.9}$$

For this topology there are already two IBP-identities, namely

$$\int \mathrm{d}^D k \frac{\partial}{\partial k^\nu} \frac{p^\nu}{(k_1^2 - m^2)^{\mu_1}((p - k_1)^2 - m^2)^{\mu_2}} = 0 \tag{4.1.10}$$

$$\int \mathrm{d}^D k \frac{\partial}{\partial k^\nu} \frac{k^\nu}{(k_1^2 - m^2)^{\mu_1}((p - k_1)^2 - m^2)^{\mu_2}} = 0 \tag{4.1.11}$$

to consider. After performing the trivial tensor reduction as usual, these identities can be rewritten as the following relations on the level of the topology:

$$(4.1.10) \Leftrightarrow 0 = (-\mu_1 + \mu_2 - p^2 \mu_1 \mathbb{1}^+ + p^2 \mu_2 2^+ - \mu_2 2^+ \mathbb{1}^- + \mu_1 \mathbb{1}^+ 2^-) \mathcal{J}_{\mu_1,\mu_2} \tag{4.1.12}$$

$$(4.1.11) \Leftrightarrow 0 = \left(D - 2\mu_1 - \mu_2 - 2m^2 \mu_1 \mathbb{1}^+ - 2m^2 \mu_2 2^+ + p^2 \mu_2 2^+ - \mu_2 2^+ \mathbb{1}^- \right) \mathcal{J}_{\mu_1,\mu_2} , \tag{4.1.13}$$

where we introduced the ladder operators $\mathbb{1}^\pm \mathcal{J}_{\mu_1,\mu_2} = \mathcal{J}_{\mu_1\pm1,\mu_2}$ and $2^\pm \mathcal{J}_{\mu_1,\mu_2} = \mathcal{J}_{\mu_1,\mu_2\pm1}$ which act on the exponents of the propagators by lowering (resp. raising) its value by ±1.

By performing the shifts in (4.1.13), (4.1.12) and after relabeling $\mu_i + 1 \to \mu_i$ we arrive at the following recursion relations

$$\mathcal{J}_{\mu_1,\mu_2} = \frac{(p^2(-D+\mu_1+2\mu_2-1)+2m^2(\mu_1-\mu_2-1))}{(\mu_1-1)p^2\,(p^2-4m^2)}\mathcal{J}_{\mu_1-1,\mu_2}$$

$$+\frac{2m^2\mu_2}{(\mu_1-1)p^2\,(p^2-4m^2)}\mathcal{J}_{\mu_1-2,\mu_2+1}+\frac{(p^2-2m^2)}{p^2(p^2-4m^2)}\mathcal{J}_{\mu_1,\mu_2-1} \qquad (4.1.14)$$

$$\mathcal{J}_{\mu_1,\mu_2} = \frac{(p^2(-D+\mu_2+2\mu_1-1)+2m^2(\mu_2-\mu_1-1))}{(\mu_2-1)p^2\,(p^2-4m^2)}\mathcal{J}_{\mu_1,\mu_2-1}$$

$$+\frac{2m^2\mu_1}{(\mu_2-1)p^2\,(p^2-4m^2)}\mathcal{J}_{\mu_1+1,\mu_2-2}+\frac{(p^2-2m^2)}{p^2(p^2-4m^2)}\mathcal{J}_{\mu_1-1,\mu_2} \ , \qquad (4.1.15)$$

where the sum of the exponents on the r.h.s. is always lesser than on the l.h.s..
Moreover the relations (4.1.14) and (4.1.15) are symmetric under the interchange of the indices $\mu_1 \leftrightarrow \mu_2$. This symmetry of the IBP-relations reflects the symmetry $\mathcal{J}_{\mu_1,\mu_2} = \mathcal{J}_{\mu_2,\mu_1}$ of the diagram (4.1.9) in the equal mass case.
Furthermore we can read off the MI's of the $\mathcal{J}$-topology from the recursion relations directly.
Therefore we notice, that we have a singularity at $(\mu_1 = 1, \mu_2)$ in the r.h.s of (4.1.14) and at $(\mu_1, \mu_2 = 1)$ in (4.1.15) respectively. Hence, a further reduction is not possible and we can use for example (4.1.14) to reduce until $\mu_1 - 1 = 1$. The symmetry of the problem (or equivalently (4.1.15)) can then be used to reduce until $\mu_2 - 1 = 1$ from which follows, that one of the MI's of the $\mathcal{J}$-topology will be $\mathcal{J}_{1,1}$.
To see the second MI which is mandatory to express every integral in the $\mathcal{J}$-topology we have to look at the underlined part of (4.1.14) and (4.1.15). These terms will yield integrals of the form $\mathcal{J}_{\sigma,0}$ with $\sigma \in \mathbb{N}_{>0}$ for $(\mu_1 - 1, \mu_2 - 1) = (1,1)$. But, as already shown in (4.1.7), integrals of this type are completely reducible to the MI $\mathcal{I}_1$.

From the considerations above it follows that every integral of the one loop two denominator equal mass topology (4.1.9) is expressible via

$$J_{\mu_1,\mu_2} = C_1(\mu_1,\mu_2,D,p^2,m^2)\mathcal{J}_{1,1} + C_2(\mu_1,\mu_2,D,p^2,m^2)\mathcal{I}_1 \qquad (4.1.16)$$

in terms of the only two MI's $\mathcal{J}_{1,1}$, $\mathcal{I}_1$ and rational prefactor functions C_i depend on the indices μ_i, the scales and the dimension D.

4.2 The Main Idea behind Laportas Algorithm

In the last preceding section we looked at two quite simple IBP-reductions whereas we did not even bother to compute the second one explicitly. Since for topologies with l loops and g legs there are $l(g-1+l)$-IBP-relations the concrete calculations, even though the main idea and the way to tackle the reduction problem seems quite clear, tend to be rather tedious and grow fast beyond human manageability. Furthermore, for actual computations in particle physics one is mainly interested in expressing certain integrals of a topology in terms of MI's and not in universal recursion relations like (4.1.7) and (4.1.16) which are valid for every element of the topology. Therefore one started to consider IBP-relations as a set of equations between integrals of a topology with a fixed set of indices $(\mu_1, \ldots, \mu_t, \nu_1, \ldots, \nu_q)$ as variables. The observation [20] that the number of relations between the integrals grows faster than the number of additional, unknown integrals [2] transfers the problem of an IBP-reduction of a specific integral into the solution of an overdetermined system of linear equations. The solution of such an overdetermined system of linear equations is far from being a trivial computational task and it defines relations between integrals, in which the MI's are arbitrary.

Laportas algorithm introduces an alternative approach to the solution of IBP-relations by assigning a global ordering in terms of suitable chosen criteria to the integrals [25, 26]. By means of this ordering different integrals differ in their degree of complexity and the system of IBP-relations is solved by systematically expressing complicated integrals in terms of easier integrals, starting with the most complicated one.

The degree of complexity of an integral is e.g. defined by the following experience based conjectural criteria[3] (similar to [25] but shortened):

1. Integrals with less propagators are easier to solve, that means:

$$\mathcal{T}_{\mu_1,\ldots,\mu_t,\nu_1,\ldots,\nu_q} \succ \mathcal{T'}_{\sigma_1,\ldots,\sigma_{t-a},\lambda_1,\ldots,\lambda_{\bar{q}}} \text{ with } a > 0 \ . \tag{4.2.1}$$

2. Integrals with an equal number of propagators for which

$$\sum_{n=1}^{t}(\mu_n) < \sum_{n=1}^{t}(\sigma_n) \tag{4.2.2}$$

   is fulfilled are ordered by

$$\mathcal{T'}_{\sigma_1,\ldots,\sigma_t,\lambda_1,\ldots,\lambda_{\bar{q}}} \succ \mathcal{T}_{\mu_1,\ldots,\mu_t,\nu_1,\ldots,\nu_q} \tag{4.2.3}$$

   such that integrals for which the sum of the exponents of the propagators is higher are said to be more complicated.

---

[2] In [21] it had been proven, that the number of MI's in standard topologies is limited and therefore the observation, that the number of relations grows faster than the number of additional, unknown integrals is valid. Furthermore, it was shown in [22], that it is possible to count the number of MI's in a given topology without explicitly performing IBP-reductions by the analysis of its critical properties only. This counting method is implemented in the *Mathematica* package Mint and is part of the most recent version of the IBP-reduction program LiteRed [23, 24].

[3]We will see, that these criteria might not be optimal later in this thesis.

In general these two criteria will not suffice to order the system completely and in actual implementations a variety of subcriteria are added to ensure a complete ordering (see e.g. [25, 27, 28]). Hereby a variation of the criteria will in general result in a different set of MI's.

For example, if we want to express the integrals F_k in terms of MI's we have to generate the associated $i = l(g - 1 + l)$ IBP-relations for every of the k integrals. These relations are solved with respect to the most complicated integral $S_{j,k}$ specified by the introduced ordering. Afterwards we determine, if every of the integrals V_j in the defining equations of $S_{j,k}$ can be expressed in terms of simpler integrals. If that is not the case we would increase the indices and generate new IBP-relations. At some point, the algorithm will stabilize and every new set of relations will yield integrals which are expressible in terms of simpler ones (the systems becomes overdetermined) [4] . At that point the algorithm terminates, the system is ordered completely and the integrals for which no expression in terms of simpler integrals exists, the simplest independent set $M \in V$, are declared to be MI's. Since the system is ordered completely now and every integral (except fo the MI's) depends on simpler integrals only, the IBP-relations are substituted in reversed order, starting with the simplest ones until every of the F_k is expressed as a linear combination of the determined MI's [25].

The main takeaway of this chapter is, that instead of looking at individual Feynman diagrams one should consider a basis of MI in which every of the integrals of the complete family can be expressed. These MI can be derived in an algorithmic way by introducing an ordering to the elements of the family. There are numerous programs for IBP-reduction (see e.g. [24, 29–31] for the more recent ones) which are partly based on Laporta's algorithm whereby Reduze 2 [28, 30] has been used for the reductions during the course of this thesis.

---

[4]This stabilization usually occurs at a high index numbers, such that systems of many thousands of relations have to be ordered and solved [19] which seems to be the bottleneck of current computational approaches.

Chapter 5

Parametric Representation of Feynman Integrals

In the preceding chapters some basic properties of Feynman integrals as well as the topology notation and IBP-reduction were introduced. We outlined, that in order to compute whole families of Feynman integrals only a limited number of representatives, the so-called MI's, have to be computed. We are able to express every integral of the associated topology by simply resubstituting the MI's in the previously derived IBP-relations. The method of IBP-reduction is a powerful tool for simplifications only, if we are able to compute the MI's. Therefore, the next step is to present methods which are suitable for practical computations. But beforehand, I will take a short detour and introduce another representation of Feynman integrals, the parametric representation [1].
Even though it is not the main focus of the thesis, this representation will often be used for explicit examples and by using it some integral points of the following approaches become more transparent.

The typical form of Feynman integrals without irreducible scalar products is given by D-dimensional loop integrals of the form

$$I \propto \int \frac{1}{\prod_i D_i^{\nu_i}} \mathrm{d}^D k_1 \dots \mathrm{d}^D k_l \ , \tag{5.0.1}$$

where the D_i are some quadrics taken to the ν_i-th power. We already mentioned in section 2.2, that it is possible to try a "direct" integration by introducing D-dimensional spherical coordinates after performing a Wick-rotation. This approach, however, becomes rather complicated quickly and there are only some simple integrals where it can be applied successfully.
Therefore, already in the 50s, alternative approaches which yield integrals of rational functions over parameter spaces had been developed [2]. These tricks are based on rewriting

---

[1] For a more extensive overview see e.g. [32] or [19] and [33] respectively.

[2] These parameter representations were mainly developed by Feynmann, Schwinger, Symanzik and Nambu. Recently another representation in terms of a single graph polynomial has been introduced in [22].

denominators as integrals over parameters and are called Schwinger trick[3]

$$\frac{1}{\prod_{i=1}^{d} A_i^{n_i}} = \prod_{i=1}^{d} \frac{1}{\Gamma(n_i)} \int\limits_{0}^{\infty} \mathrm{d}x_i x_i^{n_i-1} e^{-x_i A_i} \qquad \text{with } A, \mathrm{Re}(n_i) > 0 \qquad (5.0.2)$$

and Feynman trick[4]

$$\frac{1}{\prod_{i=1}^{d} A_i^{n_i}} = \frac{\Gamma(\sum_{i=1}^{d} n_i)}{\prod_{i=1}^{d} \Gamma(n_i)} \int_{0}^{1} \mathrm{d}x_1 \cdots \int_{0}^{1} \mathrm{d}x_n \frac{\delta(1 - \sum_{i=1}^{d} x_i) \prod_{i=1}^{d} x_i^{n_i-1}}{\left(\sum_{k=1}^{d} x_k A_k\right)^{\sum_{k=1}^{d} n_k}} \ . \qquad (5.0.3)$$

These tricks are useful in their own right but their main feature is, that they can be used as a starting point to derive formulas which allow us to write down a suitable parametric representation from the associated Feynman diagram G directly.

Therefore one can e.g. use (5.0.3) to express the loop momenta dependent numerator in (5.0.1) where the A_i are now quadrics of the form $A_i = q_i^2 - m_i^2$ with some linear combination of external and loop momenta q_i and masses m_i. Since Feynman integrals are translational invariant, we can shift the loop momenta k_i to complete the square, such that the numerator depends on k_i^2 only. Now, the integration about the loop momenta can be performed and we are left with an integration over the parameters [5] given by

$$I = \int \frac{1}{\prod_{i=1}^{d} D_i^{\nu_i}} \mathrm{d}^D k_1 \ldots \mathrm{d}^D k_l \qquad (5.0.4)$$

$$= (-1)^n \frac{(i\pi^{\frac{D}{2}})^l \Gamma(n - l\frac{D}{2})}{\prod_{i=1}^{d} \Gamma(n_i)} \int\limits_{0}^{\infty} \mathrm{d}x_1 \cdots \int\limits_{0}^{\infty} \mathrm{d}x_d \delta(1 - \sum_{i=1}^{d} x_i) \left(\prod_{i=1}^{d} x_i^{n_i-1}\right) \frac{\mathcal{U}^{n-(l+1)\frac{D}{2}}}{\mathcal{F}^{n-l\frac{D}{2}}} \ . \qquad (5.0.5)$$

In (5.0.5) n denotes the sum over all exponents of the propagators, d the number of internal edges, $\mathcal{U}$ and $\mathcal{F}$ are the so-called first and second Symanzik polynomial which are homogeneous and of degree l and $l+1$ respectively. These polynomials can be derived in several ways [6] but we will restrict ourself to only give a recipe of their direct construction from the graph here.

Therefore we need the notion of a *spanning tree* and a *spanning 2-tree*[7]. A spanning tree T of a graph G is any connected subgraph of G without loops containing all vertices

---

[3]Notice that this trick follows immediately from the integral representation $\Gamma(n) = \int_0^\infty z^{n-1} e^{-z} \, \mathrm{d}x$ with $z = xA$.

[4]The derivation of the Feynman trick is not as easy as the Schwinger trick and can be found e.g. in [34] p. 190.

[5]For a complete derivation by using the here outlined steps see [33] chap. 7 and notice the slightly differently defined V (compared to $\mathcal{F}$) in eq. (7-72) therein. For an alternative derivation starting by using the Schwinger trick see [19]. Furthermore notice, that because of the δ-function the integration domain can be further restricted, such that (5.0.5) is commonly written with an integration domain over the cube $[0, 1]^d$ or as an projective integral (see e.g. [35] eq. (2.1.35)). The fact, that it is a projective integral allows to replace $\delta(\sum_i x_i - 1)$ in (5.0.5) by $\delta(x_j - 1)$ where x_j is an arbitrary Feynman parameter and the integration of the remaining integrals has to be performed from zero to infinity. This fact is commonly known among physicists as the *Cheng-Wu* theorem [36].

[6]see e.g. the review [32]

[7]For an extensive introduction to graph theory with emphasis on Feynman diagrams see [33].

of G.

If we consider for example the graph

$$G = \hspace{3cm} \tag{5.0.6}$$
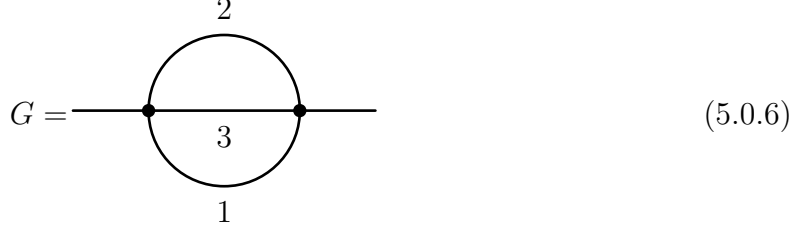
we immediately see its three spanning trees

$$\tag{5.0.7}$$
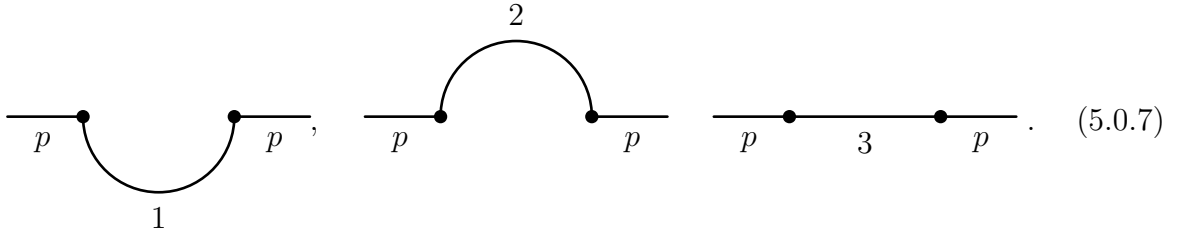
Similarly, a spanning 2-tree $S = T_1 \cup T_2$ is defined as any subgraph of G, consisting of two connected components which are trees such that S contains all vertices of G. For the graph defined in (5.0.6) there is only one spanning 2-tree

$$\tag{5.0.8}$$

and it is obvious, that we get a spanning 2-tree by deleting one additional internal edge from a spanning tree.

By using the lingo of graph theory, the first Symanzik polynomial is defined by

$$\mathcal{U} = \sum_{T_i \in T \subset G} \prod_{e \notin T} x_e \, , \tag{5.0.9}$$

where the sums is over all spanning trees T_i of G and the product is over all internal edges e of G, which are not in the spanning tree T_i. For the example graph G (5.0.6) we have to consider the spanning trees in (5.0.7) to arrive at

$$\mathcal{U} = x_2 x_3 + x_1 x_3 + x_1 x_2 \, . \tag{5.0.10}$$

The second Symanzik polynomial is defined as

$$\mathcal{F} = \mathcal{U} \sum_{e \in E_{int}} m_e^2 x_e - \underbrace{\sum_{(T_1, T_2) \in S} \prod_{e \notin S} x_e (q_S)^2}_{\mathcal{F}_0} \tag{5.0.11}$$

where the summation in the massive part is over all internal edges of G. In the massless part $\mathcal{F}_0$ of the second Symanzik polynomial, the summation is over all spanning 2-trees, the product is over all internal edges of G, which are not in S and q_S denotes the total

23

momentum[8] entering T_1 (resp. T_2).

The second Symanzik polynomial of the fully massive graph G in (5.0.6) is hence given by considering the only spanning 2-tree (5.0.8) and (5.0.11) yields

$$\mathcal{F} = (x_2 x_3 + x_1 x_3 + x_1 x_2)(m_1 x_1 + m_2 x_2 + m_3 x_3) - \underbrace{x_1 x_2 x_3 p^2}_{\mathcal{F}_0} \ . \tag{5.0.12}$$

---

[8]in Minkowski metric

Chapter 6

Computing Feynman Integrals in Terms of Hyperlogarithms

In the preceding chapter we gave a brief introduction into the parametric representation of Feynman integrals. The main focus thereby lay to present a detailed enough recipe, to write down the graph polynomials.

In the following, we use this parametric representation to study examples of the iterated structures arising in the computations of Feynman integrals [35, 37–44]. As we will see, the parametric representation is, in a way, a natural entry point into these subjects, since many relations can be seen directly on the integral level. Nonetheless, the main focus of the following chapter will be on methods necessary to understand the further calculations during this thesis. In the second part I will introduce the methods of differential equations [45, 46] and attempt to motivate some of its recent developments [47–55]. .

6.1 Normalization of Feynman Integrals

But before we start, there are some slight adjustments to be taken in the notation, since from now on and till the end of this thesis we are mainly concerned with actual computations. In the remaining part of this thesis Feynman integrals will be normalized as

$$I_{\nu_1,...,\nu_N} = (-1)^\nu (\mu^2)^{\nu - l\frac{D}{2}} \int \frac{\mathrm{d}^D k_1}{i\pi^{\frac{D}{2}}} \cdots \frac{\mathrm{d}^D k_l}{i\pi^{\frac{D}{2}}} \frac{1}{D_1^{\nu_1} \cdots D_N^{\nu_N}} \text{ with } \nu = \sum_{i=1}^N \nu_i \qquad (6.1.1)$$

whereby μ is an arbitrary mass scale with mass dimension 1. The normalization is motivated by following aspects:

- Wick rotating the integrals will result in Euclidian momenta whereas we have to replace the squared momenta according to $k^2 \to -K^2$ and the measure $\mathrm{d}k_0$ by $i\mathrm{d}K_0$ (see sec. 2.2.1). Therefore it is advantageous to normalize the integrals by $(-1)^\nu$ and the measure by i to compensate for the replacement $(q^2 - m^2) \to (Q^2 + m^2)$ and the change $\mathrm{d}k_0 \to i\mathrm{d}K_0$.

- The $\pi^{D/2}$ takes into consideration, that the momentum integrals are obtained by a Fourier transform of correlation functions defined in the position space were we have chosen a symmetrical convention for the Fourier transform.

- The prefactor $(\mu^2)^{n-l\frac{D}{2}}$ ensures (mass) dimensionless integrals and function arguments. It furthermore introduces an additional scale which becomes necessary within the framework of renormalization.

- Last but not least, by choosing this specific normalization, the defining equation of the associated parameter representation (5.0.5) simplifies.

6.2 Iterated Structures Arising in Computations of Feynman Integrals

In the previous section we showed, that it is always possible to rewrite a momentum space Feynman integral with d internal edges as a parametric integral with $d-1$ non trivial integrations and the question of how to perform these still remains open.

To introduce the class of functions in which a large class of Feynman integrals can be computed, I will compute an easy explicit example and point out general features afterwards.

6.2.1 An Illustrative Example

In the following computation we are, as it was mostly done during this thesis, mainly concerned with the illustration of some general points supported by explicit calculations. Therefore we consider the rather simple integral

$$
I = \text{(diagram)} = (\mu^2)^{2-\frac{D}{2}} \int \frac{\mathrm{d}k^D}{i\pi^{\frac{D}{2}}} \frac{1}{(k^2 - m^2)(k-p)^2}
$$

$$
\overset{D=4-2\varepsilon}{=} \Gamma(\varepsilon) \left(\mu^2\right)^\varepsilon \int\limits_0^1 \mathrm{d}x_1 \int\limits_0^1 \mathrm{d}x_2 \frac{\delta(1 - x_1 - x_2)(x_1 + x_2)^{-2+2\varepsilon}}{\left((x_1 + x_2)m^2 x_1 - t x_1 x_2\right)^\varepsilon}
$$

$$
\overset{a=\frac{t}{m^2}}{=} \underbrace{\Gamma(\varepsilon) \left(\frac{\mu}{m}\right)^{2\varepsilon}}_{C(\varepsilon,\mu,m)=:C} \int\limits_0^1 \mathrm{d}x((1-x)(1-ax))^{-\varepsilon}
$$

(6.2.1)

where the dashed line denotes a massless propagator and the infinitesimal parameter ε had been introduced to describe the deviation from the physical $D = 4$ dimensions. Since, at the end of the day, we are interested in the limit $D \to 4$ ($\varepsilon \to 0$ respectively), our goal is, to obtain an series expansion in ε where the divergences become manifest in the pole structure of the result.

The first attempt to achieve an ε-expansion is to integrate the parametric form (6.2.1) directly, which can be done easily by using Mathematica [56] and immediately, for $0 < a < 1$, yields the result

$$
I = \frac{\Gamma(\varepsilon) \left(\frac{\mu}{m}\right)^{2\varepsilon}}{2a} \left(\frac{\sqrt{\pi}(a-1)(-4)^\varepsilon(1-a)^{-2\varepsilon}a^\varepsilon\Gamma(1-\varepsilon)}{\Gamma\left(\frac{3}{2} - \varepsilon\right)} - \frac{2\left(\frac{a}{a-1}\right)^\varepsilon {}_2F_1\left(1 - \varepsilon, \varepsilon; 2 - \varepsilon; \frac{1}{1-a}\right)}{\varepsilon - 1} \right)
$$

(6.2.2)

where ${}_2F_1$ denotes Gauss hypergeometric function. Hypergeometric functions and their multivariate generalizations will often appear as soon as we attempt to solve slightly more involved integrals with their full D (respectively ε) dependence. The main obstacle in this approach is the ε-expansion of these functions, even though it can be done for that

specific example without further effort by using expansion programs like [57] or [58], we will pursue another approach here.

Therefore we expand (6.2.1) on the level of integrand already and obtain

$$I = C \int_0^1 \mathrm{d}x \left(\underbrace{1}_{\mathcal{I}^{(0)}} - \underbrace{\log((1-x)(1-ax))}_{-\mathcal{I}^{(1)}} \varepsilon + \frac{1}{2} \underbrace{\log^2((1-x)(1-ax))}_{2\mathcal{I}^{(2)}} \varepsilon^2 + \mathcal{O}(\varepsilon^3) \right)$$

(6.2.3)

where we attempt to solve the integrals order per order in ε [1].

Before we solve the bubble integral (6.2.3) we anticipate that we will have to deal with integrals of powers of logarithms. Therefore it is helpful to compute the recursion relation

$$\int \log^n(1-ax)\mathrm{d}x \overset{x \to ax}{=} \frac{1}{a} \left(x \log^n(1-x) - \int x \mathrm{d}\log^n(1-x) \right)$$

(6.2.4)

$$= \frac{1}{a} \left(x \log^n(1-x) - n \underbrace{\int \frac{x}{x-1} \log^{n-1}(1-x)\mathrm{d}x}_{\text{partial fraction decomposition}} \right)$$

(6.2.5)

$$= \frac{1}{a} \left((x-1) \log^n(1-x) - n \int \log^{n-1}(1-x)\mathrm{d}x \right)$$

(6.2.6)

from which we can read off [2]

$$\int_0^1 \log^n(1-x) = (-1)^n n!$$

(6.2.7)

directly. With this short preparation we can tackle the bubble expansion (6.2.3) by computing

$$-\mathcal{I}^{(1)} = \int_0^1 (\log(1-x) + \log(1-ax))\, \mathrm{d}x = -\frac{1}{a} \left(2a + (1-a) \int_0^a \frac{\mathrm{d}x}{x-1} \right)$$

(6.2.8)

---

[1]Notice that this approach requires convergent integrals at every intermediate integration in every order in ε. This will in general not be the case, in particular if a diagram contains sub-divergences originating from divergent sub-diagrams. In that instance one can convert them to finite integrals by applying partial integration [59]. If one deals with UV divergent integrals only, a renormalization on level of the integrand [60] is possible, such that the parameter integrals become finite. Alternatively it is possible to choose an quasi finite basis of integrals [61, 62] in which propagators are raised to higher powers and the dimensions are shifted, but the ε expansion becomes trivial.

[2]since $\lim_{x \to 0} x \log^n(x) = 0$

and

$$2\mathcal{I}^{(2)} = \int\limits_0^1 \left(2 \underbrace{\log(1-x)\log(1-ax)}_{\text{part. int. and part. frac. decomp.}} + \underbrace{\log^2(1-ax)}_{(6.2.6)} + \underbrace{\log^2(1-x)}_{(6.2.7)} \right) \mathrm{d}x \qquad (6.2.9)$$

$$= 2\frac{1}{a} \left(2a - (a-1) \int_0^a \frac{\mathrm{d}x}{x-1} + (a-1) \int_0^a \frac{\mathrm{d}x}{x-1} \int_0^x \frac{\mathrm{d}y}{y-a} \right) \qquad (6.2.10)$$

$$+ \frac{2}{a} \left(a - (a-1) \int_0^a \frac{\mathrm{d}x}{x-1} + (a-1) \int_0^a \frac{\mathrm{d}x}{x-1} \int_0^x \frac{\mathrm{d}y}{y-1} \right) + 2 \qquad (6.2.11)$$

$$= \frac{2}{a} \left(4a - 2(a-1) \int_0^a \frac{\mathrm{d}x}{x-1} + (a-1) \int_0^a \frac{\mathrm{d}x}{x-1} \int_0^x \frac{\mathrm{d}y}{y-1} \right. \qquad (6.2.12)$$

$$\left. + (a-1) \int_0^a \frac{\mathrm{d}x}{x-1} \int_0^x \frac{\mathrm{d}y}{y-a} \right) \qquad (6.2.13)$$

in the kinematic regime of $a < 1$ [3].

The expansion of the ε depended prefactor in (6.2.1) yields

$$C = \underbrace{\frac{1}{\varepsilon}}_{\mathcal{C}^{(-1)}\varepsilon^{-1}} + \underbrace{(L - \gamma_E)}_{\mathcal{C}^{(0)}} + \underbrace{\frac{1}{12} \left(6L^2 - 12\gamma_E L + 6\gamma_E^2 + \pi^2 \right) \varepsilon}_{\mathcal{C}^{(1)}\varepsilon} + \mathcal{O}\left(\varepsilon^2\right) \qquad (6.2.14)$$

where γ_E denotes the Euler-Mascheroni constant, $L = \log(\mu^2/m^2)$ and the final result of the ε-expansion[4] of the bubble integral to $\mathcal{O}(\varepsilon)$ reads

$$I = \frac{\mathcal{C}^{(-1)}\mathcal{I}^{(0)}}{\varepsilon} + (\mathcal{C}^{(0)}\mathcal{I}^{(0)} + \mathcal{C}^{(-1)}\mathcal{I}^{(1)}) + (\mathcal{C}^{(0)}\mathcal{I}^{(1)} + \mathcal{C}^{(1)}\mathcal{I}^{(0)} + \mathcal{C}^{(-1)}\mathcal{I}^{(2)})\varepsilon + \mathcal{O}\left(\varepsilon^2\right) \ . \qquad (6.2.15)$$

6.2.2 Upshot on Iterated Integrals and the Method of Hyperlogarithms

In the computation of the expansion of the bubble integral in (6.2.8) and (6.2.13) we used partial fraction decomposition and partial integration to rewrite the problem. We obtained a result in which every *iterated integral* [63] except for the last marked by the dotted underline, evaluates to a power of the classical logarithm given by a n-fold iterated

---

[3]The result can be continued in the "physical" regime $a > 1$ by means of an analytical continuation.

[4]One reason for the necessity of expansions beyond $\mathcal{O}(\varepsilon^0)$ will become clear in the next section.

integral with the one-form $\omega_1 = \mathrm{d}x/(x-1)$ of the form

$$
\begin{aligned}
\frac{\log^n(1-x)}{n!} &= \int_0^x \left(\int_0^{t_n} \cdots \left(\int_0^{t_2} \frac{1}{t_1 - 1} \mathrm{d}t_1 \right) \cdots \frac{1}{t_{n-1} - 1} \mathrm{d}t_{n-1} \right) \frac{1}{t_n - 1} \mathrm{d}t_n \\
&= \int_{0 \leq t_1 \leq \ldots \leq t_n \leq x} \frac{1}{t_1 - 1} \mathrm{d}t_1 \cdots \frac{1}{t_{n-1} - 1} \mathrm{d}t_{n-1} \frac{1}{t_n - 1} \mathrm{d}t_n \\
&= \int_\gamma \underbrace{\omega_1 \ldots \omega_1}_{\text{n-times}} \,,
\end{aligned} \tag{6.2.16}
$$

where γ denotes a path on $\mathbb{C} \backslash \{1\}$ with $\gamma(0) = 0$ and $\gamma(1) = x$.

The first natural generalization of the logarithm are so-called *classical polylogarithms*[5], which are given by iterated integrals of the form

$$
\mathrm{Li}_{n \geq 1}(z) = \int_0^z \mathrm{Li}_{n-1}(t) \frac{\mathrm{d}t}{t} \;; \qquad\qquad \mathrm{Li}_0 = \frac{z}{1-z} \tag{6.2.17}
$$

and therefore by an iterated integration of the one forms

$$
\mathcal{A}_{\text{poly}} = \{ \omega_0 = \frac{\mathrm{d}t}{t}, \omega_1 = \frac{\mathrm{d}t}{1-t} \} \tag{6.2.18}
$$

and the short notation

$$
\mathrm{Li}_n(z) = \int_\gamma \omega_1 \underbrace{\omega_0 \ldots \omega_0}_{n-\text{times}} \tag{6.2.19}
$$

and γ being a piecewise smooth path from 0 to z in $\mathbb{C} \backslash \{0, 1\}$.

In particle physics classical polylogarithms became insufficient soon, such that iterated integrals of additional one-forms in arbitrary order [37] and multivariate extensions [38–40] of the classical polylogarithms (6.2.19) were introduced. They are called harmonic [46], two-dimensional harmonic [38, 39] and cyclotomic harmonic polylogarithms [40] [6] and form a subclass of the most general setup of iterated integrals currently established in computations in particle physics, the *hyperlogarithms*.

Hyperlogarithms [44] are defined by the iterated integral

$$
G(z_1, \vec{z}; y) := \int_0^y \frac{\mathrm{d}t}{t - z_1} G(\vec{z}; t) \;; \qquad G(\underbrace{0, \ldots, 0}_{n}; z) := \frac{\log^n(z)}{n!} \tag{6.2.20}
$$

with $z_i \in \mathbb{C}$ and we denote

$$
G_{n_1, \ldots, n_l}(z_1, \ldots, z_l; y) = G(\underbrace{0, \ldots, 0}_{n_1 - 1}, z_1, \ldots, z_{l-1} \underbrace{0, \ldots, 0}_{n_l - 1}, z_l; y) \tag{6.2.21}
$$

---

[5]See e.g. [64] for an extensive discussion of their properties.

[6]To express cyclotomic harmonic polylogarithms by hyperlogarithms (and polynomials) partial fraction decomposition and partial integration have to be used.

with $z_j \neq 0$, $\forall j \in \{1, \ldots, l\}$.

In the notation analogously to (6.2.19) we write

$$G(z_1, \ldots, z_l; y) = \int_\gamma \omega_{z_l} \ldots \omega_{z_1} \tag{6.2.22}$$

with $\gamma : [0, 1] \to \mathbb{C} \backslash \{z_1, \ldots, z_l\}$ together with $\gamma(0) = 0$ and $\gamma(1) = y$.

The one-form ω_{z_i} (or the z_i respectively) are referred to as *letters*, the set of all letters is called an *alphabet* and $w = \omega_{z_1} \ldots \omega_{z_l}$ denotes a *word*. Furthermore one defines the *weight* of a hyperlogarithm to be the number of iterated integrations or the length of the vector $\vec{z}$ respectively. The alphabet of harmonic polylogarithms is $\mathcal{A}_{hpl} = \{-1, 0, 1\}$ whereas the letters of the alphabet of cyclotomic harmonic polylogarithms might be expressed as a set of letters with z_i being a root of unity or zero.

Since it is often the case, that we have to integrate from (to) a point which is not in $\mathbb{C} \backslash \{z_1, \ldots, z_l\}$ the integrals in (6.2.22) need to be regularized. Therefore one uses, that the singularities of the integrals at $y \to \tau \in \{z_1, \ldots, z_l\} \cup \{\infty\}$ are at most logarithmic and can be expanded as

$$G(z_1, \ldots, z_l; y) = \sum_{i=0}^{l} \alpha_\tau^{(i)}(y) \begin{cases} \log^i(y) & \tau = \infty \\ \log^i(y - \tau), & \tau \neq \infty \end{cases}. \tag{6.2.23}$$

The regularized value is defined by formally setting $\log(y - \tau)$ for $y \to \tau$ to zero and taking the limit afterwards such that

$$\operatorname*{Reg}_{y \to \tau} G(\vec{z}; y) := \alpha_\tau^{(0)}(\tau) , \tag{6.2.24}$$

where a detailed description of the whole regularization scheme can be found e.g. in chapter 6 in [42] or in [35].

The iterated integrals (6.2.20) can further be expressed as nested sums in terms of *multiple polylogarithms* [41, 65]

$$\operatorname{Li}_{n_1, \ldots, n_l}(z_1, \ldots, z_l) = \sum_{0 < k_1 < \ldots < k_l} \frac{z_1^{k_1}}{k_1^{n_1}} \cdots \frac{z_l^{k_l}}{k_l^{n_l}} \tag{6.2.25}$$

by the relation

$$\operatorname{Li}_{n_1, \ldots, n_l}(z_1, \ldots, z_l) = (-1)^l G_{n_1, \ldots, n_l} \left(\frac{1}{z_1}, \frac{1}{z_1 z_2}, \ldots, \frac{1}{\prod_{i=1}^{l} z_i}; 1 \right) . \tag{6.2.26}$$

Furthermore hyperlogarithms form a *shuffle-* and the multiple polylogarithms a *stuffle-*algebra [7]. Hyperlogarithms and an alternative class of iterated integrals with the same universality as the hyperlogarithm are discussed in great detail in [42]. Programs suited for numerical evaluation of harmonic [66–68], harmonic cyclotomic [69] and multiple polylogarithms [70] as well as analytical computations [66, 67, 71, 72] are already publicly available.

---

[7]See e.g. [5] for an easy to understand introduction.

In the explicitly computed example (6.2.3) of an ε-expansion, all the iterated integrals are easily expressed in the class of hyperlogarithms. But in the general case, where we have to perform more than one parameter integration, the naive try to express the full integrand such that we can read off an iterated structure, will most certainly fail, since we are concerned with integrals: [8]

$$
\begin{aligned}
I &= (\mu^2)^{n-l\frac{D}{2}} \frac{\Gamma(n-l\frac{D}{2})}{\prod_{i=1}^{d}\Gamma(n_i)} \int_0^\infty \mathrm{d}x_1 \cdots \int_0^\infty \mathrm{d}x_d \delta(1-x_j) \left(\prod_{i=1}^{d} x_i^{n_i-1}\right) \frac{\mathcal{U}^{n-(l+1)\frac{D}{2}}}{\mathcal{F}^{n-l\frac{D}{2}}} \\
&= (\mu^2)^{n-l\frac{D}{2}} \frac{\Gamma(n-l\frac{D}{2})}{\prod_{i=1}^{d}\Gamma(n_i)} \int_0^\infty \mathrm{d}x_1 \cdots \int_0^\infty \mathrm{d}x_d \left[\delta(1-x_j)\left(\prod_{i=1}^{d} x_i^{n_i-1}\right)\mathcal{F}^{2l-n}\mathcal{U}^{n-2(l+1)}\right. \\
&\quad \left. \cdot\left(1 - (l\log(\mathcal{F})-(l+1)\log(\mathcal{U}))\varepsilon + \frac{1}{2}(l\log(\mathcal{F})-(l+1)\log(\mathcal{U}))^2\varepsilon^2 + \mathcal{O}(\varepsilon^3)\right)\right]
\end{aligned}
$$
(6.2.27)

where d denotes the number of internal edges, n the sum over all exponents of the propagators, x_j an arbitrary Feynman parameter and we work $D = 4 - 2\varepsilon$ dimensions.

In the above equation we notice the following "problems": Even though ε-expansion naturally yields logarithms of the Symanzik polynomials with rational functions as prefactor, the graph polynomials are (up to some special cases) not factorizable and depend on multiple parameters. Therefore it is ad hoc not clear, in which order we should attempt to integrate them. Furthermore, the integration domain is from zero to infinity and it is not clear at first, how to arrive at an iterated representation.

An algorithm for performing a certain class of integrals of the type (6.2.27) was first explained in [73, 74], further refined in [35] and implemented in [71, 72].
Suppose now, some polynomial f (e.g. $\mathcal{U}$ or $\mathcal{F}$) is linear in one of its variables, say x_i, such that

$$
f = \underbrace{a(x_1,\ldots,x_{i-1},x_{i+1},\ldots,x_d)}_{a_{\cancel{x_i}}} x_i + \underbrace{b(x_1,\ldots,x_{i-1},x_{i+1},\ldots,x_d)}_{b_{\cancel{x_i}}} .
$$
(6.2.28)

For such a polynomial, the typical logarithmic terms in (6.2.27) can then, after partial fraction decomposition, be written as

$$
\propto \tilde{a}_{\cancel{x_i}} \cdot \left(1 + x_i + \ldots + x_i^k + \frac{1}{(x_i - \tilde{b}_{\cancel{x_i}})^{\tilde{k}}} + \ldots + \frac{1}{(x_i - \tilde{b}_{\cancel{x_i}})}\right) \log(x_i - \tilde{c}_{\cancel{x_i}}) ,
$$
(6.2.29)

where $k, \tilde{k} \in \mathbb{N}$. If the integrand of (6.2.27) can be brought in a similar form (allowing hyperlogarithms instead of only logarithms), then we can, by using partial integration if necessary, find a primitive for every term, which will be in the class of hyperlogarithms as well. In short, for one integration step

$$
\int_0^\infty \ldots \int_0^\infty f_k \mathrm{d}x_{k+1} \ldots \mathrm{d}x_d = \int_0^\infty \ldots \int_0^\infty f_{k-1} \mathrm{d}x_k \mathrm{d}x_{k+1} \ldots \mathrm{d}x_d ,
$$

---

[8]See footnote 5 and notice, that this formula only holds for graphs without divergent subgraphs. For graphs with divergent subgraphs the form of the integrand will differ (see footnote 1) but the outlined algorithm remains applicable without the need of further adjustments.

we need perform the following three steps

1. Convert $f_{k-1}(x_k)$, such that it involves hyperlogarithms in x_k only

2. Find its primitive $F_{k-1}(x_k)$

3. Evaluate the limits $f_k = \lim_{x_k \to \infty} F_{k-1}(x_k) - \lim_{x_k \to 0} F_{k-1}(x_k) = \text{Reg}_{x_k \to \infty} F_{k-1}$ since $\text{Reg}_{x_k \to 0} G(\vec{z}, x_k) = 0$ for some $z_i \neq 0$ [9]

at every parameter integration and it becomes already apparent, that one has to find a sequence of integrations, such that the integrand is linear in one of the parameters at every intermediate integration. Graphs for which such an sequence can be found are called *linearly reducible* [35, 73–75] and there are known examples, in which linear reducibility is not apparent in the Feynman parametrization but can be constructed by a suitable change of variables [59].

---

[9]This follows from analyticity near zero (see e.g. [35], Lemma 3.3.14 for a proof).

6.3 The Method Of Differential Equations

In the previous section the solution of Feynman integrals was computed by a direct integration of their parametric representation within the method of hyperlogarithms. Even though this direct, systematic approach became more accessible through its implementation in [35, 72], within the course of this thesis I omitted many crucial and intriguing details since it served merely as a first introduction to the iterated structure and the associated class of functions arising in the Laurent expansion of Feynman integrals.

An indirect approach for computing Feynman integrals, introduced by Kotikov [45] in the 90's, is the so-called *method of differential equations*[10]. It is initially based on differentiating MI's of a given topology and its relevant subtopologies with respect to their internal masses followed by an IBP-reduction which results in a linear, coupled system of first order differential equations (deq's), whose solution are the corresponding MI's. In [46] Remiddi suggested a generalization of the method by considering deq's obtained by a differentiation with respect to the kinematic invariants formed by the external momenta, such that massless integrals became accessible as well. In [76] Henn pointed out, that the solution of these coupled systems of differential equations can become a trivial task, if a suitable, so-called *canonical basis* of MI's can be found. This observation led to an high amount of interest in a further development of the method of differential equations towards a more systematic and general approach [47–55, 77], such that it is currently the most powerful and versatile method for the analytical computation of Feynman integrals. Since a coverage of all these recent developments and their interplay[11] is beyond the scope of this thesis, I will only try to summarize its main points of [47], while neglecting others completely.

6.3.1 The General Setup for the Laurent Expansion around D=4

In the following we work in $D = 4 - 2\varepsilon$ dimensions, denote $\mathbf{s}$ as the set of all kinematic invariants corresponding to the external momenta p_i and $\mathbf{m}$ as the set of all internal masses in a given topology.

While the differentiation with respect to the masses m_i^2 is done easily, since it just raises the exponent of the corresponding propagators by one, taking the derivative with respect to the kinematic invariants $p_i p_j$ involves the solution of the system

$$\sum_\alpha \left(p_{j,\mu} \frac{\partial s_a}{\partial p_{k,\mu}} \right) \frac{\partial I(\mathbf{s}, \mathbf{m}, \varepsilon)}{\partial s_\alpha} = p_{j,\mu} \frac{\partial I(\mathbf{s}, \mathbf{m}, \varepsilon)}{\partial p_{k,\mu}} \tag{6.3.1}$$

with respect to $\frac{\partial I(\mathbf{s},\mathbf{m},\varepsilon)}{\partial s_\alpha}$ in terms of $p_{j,\mu} \frac{\partial I(\mathbf{s},\mathbf{m},\varepsilon)}{\partial p_{k,\mu}}$ [16]. The sum over α denotes the sum over all (independent) kinematic invariants $p_i p_j$. Since we are only concerned with two-point functions in this thesis, the only relevant differentiation reads

$$\frac{\partial}{\partial s} I(s = p_\mu p^\mu, \mathbf{m}, \varepsilon) = \frac{1}{2s} p_\mu \frac{\partial}{\partial p_\mu} I(s = p_\mu p^\mu, \mathbf{m}, \varepsilon) \tag{6.3.2}$$

---

[10]For reviews see [16, 19].

[11]It is fair to say, that a complete understanding from a generalized viewpoint, which relates them is still missing.

where the r.h.s yields higher powers of propagators by simply applying the chain rule. As already seen in chapter 4, the IBP-reduction of the r.h.s of the deq will in general involve integrals associated to subtopologies and an additional differentiation of the MI's of all relevant (sub)topologies yields an inhomogeneous, linear system of first order differential equations

$$\frac{\partial \vec{I}(\mathbf{s}, \mathbf{m}, \varepsilon)}{\partial s_\alpha} = A(\mathbf{s}, \mathbf{m}, \varepsilon)\vec{I}(\mathbf{s}, \mathbf{m}, \varepsilon) \tag{6.3.3}$$

where $\vec{I} = (I_1, I_2, \ldots, I_N)^T$ denotes the vector of all relevant MI's of the topology and its sub-toplogies. The boundary condition of such a differential equation can be obtained by looking at singular points of the differential equations, which are non-singular for the integral itself. By requiring finiteness of the result at these *pseudo-thresholds*, it is often possible to fix the constants of integration, if the solution of the integral at a certain kinematical point is unknown[12].

In the following we assume for the sake of simplicity, that we normalized every integral with a suitable power of ε, such that its Laurent expansion reads

$$I_k(\mathbf{s}, \mathbf{m}, \varepsilon) = \sum_{j=0}^{\infty} \varepsilon^j \mathcal{I}_k^{(j)}(\mathbf{s}, \mathbf{m}) \tag{6.3.4}$$

and the elements of the matrix A can be written as

$$A_{i,j}(\mathbf{s}, \mathbf{m}, \varepsilon) = \sum_{k=0}^{\infty} \varepsilon^k \mathcal{A}_{i,j}^{(k)}(\mathbf{s}, \mathbf{m}) . \tag{6.3.5}$$

The Laurent expansion of the deq (6.3.3) with N different MI's to order for an certain MI I_l translates directly in the deq for its Laurent coefficients $\mathcal{I}_l^{(k)}$[13] and yields

$$\frac{\partial}{\partial s_\alpha} \mathcal{I}_l^{(k)}(\mathbf{s}, \mathbf{m}) = \mathcal{A}_{l,l}^{(0)}(\mathbf{s}, \mathbf{m})\mathcal{I}_l^{(k)}(\mathbf{s}, \mathbf{m})$$
$$+ \sum_{\{i,j \in \mathbb{N} | j < k, i+j=k\}} \mathcal{A}_{l,l}^{(i)}(\mathbf{s}, \mathbf{m})\mathcal{I}_l^{(j)}(\mathbf{s}, \mathbf{m}) \tag{6.3.6}$$
$$+ \sum_{\{i,j \in \mathbb{N} | i+j=k\}} \left(\sum_{\{o | 1 \leq o \leq N, o \neq l\}} \mathcal{A}_{l,o}^{(i)}(\mathbf{s}, \mathbf{m})\mathcal{I}_o^{(j)}(\mathbf{s}, \mathbf{m}) \right) .$$

Since under the redefinition of the MI's $\vec{\tilde{I}} = M(\mathbf{s}, \mathbf{m}, \varepsilon)\vec{I}$ the system (6.3.3) transforms according to

$$\frac{\partial \vec{\tilde{I}}(\mathbf{s}, \mathbf{m}, \varepsilon)}{\partial s_\alpha} = \left(\frac{\partial M(\mathbf{s}, \mathbf{m}, \varepsilon)}{\partial s_\alpha} + M(\mathbf{s}, \mathbf{m}, \varepsilon) \underbrace{A(\mathbf{s}, \mathbf{m}, \varepsilon)}_{\partial_{s_\alpha}\vec{I}=A\vec{I}} \right) M^{-1}(\mathbf{s}, \mathbf{m}, \varepsilon)\vec{\tilde{I}}(\mathbf{s}, \mathbf{m}, \varepsilon) , \tag{6.3.7}$$

---

[12]See e.g. [78] for a more detailed presentation.
[13]By a simple comparison of the rhs and the lhs at order $\mathcal{O}(\varepsilon^k)$.

a normalization of the *l-th* MI with its homogeneous solution at order ε^0

$$\tilde{I}_l = \frac{1}{I^0_{l,\text{homo}}} I_l \tag{6.3.8}$$

yields the differential equation

$$
\frac{\partial}{\partial s_\alpha} \tilde{\mathcal{I}}_l^{(k)}(\mathbf{s},\mathbf{m}) = \sum_{\{i,j\in\mathbb{N}|j<k,i+j=k\}} \mathcal{A}_{l,l}^{(i)}(\mathbf{s},\mathbf{m})\tilde{\mathcal{I}}_l^{(j)}(\mathbf{s},\mathbf{m})
$$
$$
+ \frac{1}{e^{\int ds_\alpha A_{l,l}^{(0)}(\mathbf{s},\mathbf{m})}} \sum_{\{i,j\in\mathbb{N}|i+j=k\}} \left(\sum_{\{o|1\leq o\leq N,o\neq l\}} \mathcal{A}_{l,o}^{(i)}(\mathbf{s},\mathbf{m})\mathcal{I}_o^{(j)}(\mathbf{s},\mathbf{m}) \right) \tag{6.3.9}
$$

and it becomes obvious, that an iterated structure is associated with an iterated integration over the homogeneous solution of lesser order Laurent coefficients of $\tilde{I}_l$ and other MI's of the topology[14]. Before we proceed in the discussion of the solution of these systems of deq's, which of course depends strongly on the particular form of the matrix A, we will compute the bubble integral with one massive propagator (6.2.1) in the regime $p_\mu p^\mu < m^2$ which served already as an example in section 6.2.1.

An Illustrative Example of Solving Differential Equations

The bubble topology with one massive propagator, as seen already in chapter 4, has two associated MI's from which one is the simple tadpole vacuum diagram called $\mathcal{I}_{1,0}$ therein. The system of differential equations obtained by differentiation with respect to the square of the external momentum normalized by the mass square $y = \frac{p_\mu p^\mu}{m^2}$ reads

$$\begin{pmatrix} I_{1,0} \\ I_{1,1} \end{pmatrix} = \begin{pmatrix} 0 & 0 \\ \left(\frac{\mu}{m}\right)^2 \left(\frac{\varepsilon}{(y-1)^2} - \frac{1}{(y-1)^2}\right) & \varepsilon\left(\frac{1}{y} - \frac{2}{y-1}\right) \end{pmatrix} \begin{pmatrix} I_{1,0} \\ I_{1,1} \end{pmatrix} \tag{6.3.11}$$

---

[14]Notice that we will e.g. need the *l-th* coefficient of the Laurent expansion of an integral of a sub-topology to compute the *(l-k)-th* coefficient of the integral we are interested in. Therefore all order expansions are desirable.

after normalization of the bubble integral with its homogeneous solution $\mathcal{I}_{1,1}^{(0),homo} = \frac{1-y}{y}$ at order ε^0. As expected, there is no differential equation for the tadpole, since it is a vacuum integral. A solution of the tadpole can easily be computed (see A.0.1) and is given by

$$I_{1,0} = -\varepsilon \left(\left(\frac{\mu}{m} \right)^2 \right)^{-\varepsilon} \Gamma(\varepsilon - 1) \ . \tag{6.3.12}$$

From the normalization with the homogeneous solution it is clear, that a suitable point for the boundary condition of the integral $I_{1,1}$ is $y = 0$, since it and therefore all of its Laurent coefficients $\mathcal{I}_{1,1}^{(n)}$ are zero there.

From (6.3.11) the deq for the Laurent coefficients can be directly read off to

$$\frac{d}{dy} \mathcal{I}_{1,1}^{(n)}(y) = \left(\frac{1}{y} - \frac{2}{y-1} \right) \mathcal{I}_{1,1}^{(n-1)} + \frac{1}{(y-1)^2} \underbrace{\left(\frac{\mu}{m} \right)^2 \left(\mathcal{I}_{1,0}^{(n-1)} - \mathcal{I}_{1,0}^{(n)} \right)}_{=: \mathcal{C}^{(n)}} \tag{6.3.13}$$

where the Laurent coefficients of the tadpole are accessible by the series expansion of (6.3.12).

The solution of (6.3.13) at order $\mathcal{O}(\varepsilon^0)$ yields

$$\mathcal{I}_{1,1}^{(0)}(y) = -\frac{\mathcal{C}^{(0)}}{y-1} + \text{const} \overset{\mathcal{I}_{1,1}^{(0)}(0)=0}{=} -\mathcal{C}^{(0)} \frac{y}{y-1} \ . \tag{6.3.14}$$

After inserting this solution into the deq for the Laurent coefficient at order $\mathcal{O}(\varepsilon^1)$ we get

$$\frac{d}{dy} \mathcal{I}_{1,1}^{(1)}(y) = \left(2\mathcal{C}^{(0)} + \mathcal{C}^{(1)} \right) \frac{1}{(y-1)^2} + \mathcal{C}^{(0)} \frac{1}{y-1} \tag{6.3.15}$$

which integrates to

$$\mathcal{I}_{1,1}^{(1)} = -\left(2\mathcal{C}^{(0)} + \mathcal{C}^{(1)} \right) \frac{y}{(y-1)} + \mathcal{C}^{(0)} G(1,y) \ . \tag{6.3.16}$$

For the order $\mathcal{O}(\varepsilon^2)$ coefficient we have to solve the deq

$$\frac{d}{dy} \mathcal{I}_{1,1}^{(2)}(y) = \frac{2 \left(2\mathcal{C}^{(0)} + \mathcal{C}^{(1)} \right) + \mathcal{C}^{(2)}}{(y-1)^2} + \frac{2\mathcal{C}^{(0)} + \mathcal{C}^{(1)}}{y-1} + \mathcal{C}^{(0)} \left(\frac{1}{y} - \frac{2}{y-1} \right) G(1,y) \tag{6.3.17}$$

where the first term, after fixing the boundary conditions, yields something $\propto y/(y-1)$, the second term will integrate $\propto G(1,y)$ and the last term yields the hyperlogarithms $G(0,1,y)$ and $G(1,1,y)$ of weight two.

In the above integration algorithm we notice, that for the Laurent coefficients of higher order we need to integrate over kernels which correspond to the alphabet of harmonic polylogarithms. Therefore we get hyperlogarithms of higher weight for every additional order in the Laurent expansion. Additional to these HPL-kernels we have a term $\propto 1/(y-1)^2$ in the deq's, which yields the rational function in the result. This term, originating from the prefactor in tadpole inhomogeneity and the homogeneous solution of (6.3.10), is responsible for the mixed weight of the hyperlogarithms in the Laurent coefficient at a given order.

6.4 The Form of the Systems of DEQ's and the Canonical Basis

The previous example is probably the simplest deq possible for Feynman integrals, since it only contains two MI's from which the tadpole is trivial and the exploited approach is only that easy, if there is only one MI for every involved (sub-)topology, since the deq becomes

$$\frac{\partial \vec{I}(\mathbf{s}, \mathbf{m}, \varepsilon)}{\partial s_\alpha} = \begin{pmatrix} \times & & & \mathbf{0} \\ \times & \times & & \\ \vdots & \cdots & \ddots & \\ \times & \cdots & \cdots & \times \end{pmatrix} \vec{I}(\mathbf{s}, \mathbf{m}, \varepsilon) \qquad (6.4.1)$$

for an ordering of the topologies according to their number of propagators. In more realistic cases, there is more than one MI for a given topology, such that the system becomes coupled which results in matrices of lower triangular block form, e.g.

$$\frac{\partial \vec{I}(\mathbf{s}, \mathbf{m}, \varepsilon)}{\partial s_\alpha} = \begin{pmatrix} \times & \times & & \mathbf{0} \\ \times & \times & & \\ \vdots & \cdots & \ddots & \\ \times & \cdots & \cdots & \times \end{pmatrix} \vec{I}(\mathbf{s}, \mathbf{m}, \varepsilon) \ . \qquad (6.4.2)$$

In this case, a decoupling of the differential equation at order ε can be obtained often, by choosing a suitable so-called *canonical basis*, as was pointed out in [76].

6.4.1 An Introduction through dLog-Forms

For the following discussion we should keep in mind, that the IBP-identities define an equivalence relation in the space of all integrals in the topology under consideration and that the MI form basis in the quotient space. This basis, as obtained with Laporta's algorithm, depends solely on experience based ordering prescriptions, as explained in section 4.2 and it is in a way natural to ask: Which basis choice is the best?
To answer this question we start by considering the already treated example 6.3.1, since it can be used as a nice starting point for more general considerations.
In the result for the chosen MI $I_{1,1}$, we noticed that the integral has an iterated structure, which is in a sense not pure, since we obtained a not purely ascending weight in the harmonic polylogarithms for higher orders in its expansion. We recall the parametric

representation of the bubble integral (6.2.1), but now with arbitrary powers n_1, n_2

$$
I_{n_1,n_2} = \underbrace{\left(\frac{\mu^2}{m^2}\right)^{n_1+n_2-\frac{4-2\varepsilon}{2}} \frac{\Gamma(n_1+n_2-\frac{4-2\varepsilon}{2})}{\Gamma(n_1)\Gamma(n_2)}}_{C_{n_1,n_2}}
$$

$$
\cdot \int\limits_0^\infty dx_1 dx_2 \frac{\delta(1-(x_1+x_2))x_1^{n_1-1}x_2^{n_2-1}(x_1+x_2)^{n_1+n_2-4+2\varepsilon}}{\left((x_1+x_2)x_1 - \underbrace{\frac{t}{m^2}}_{a^{-1}} x_1 x_2\right)^{n_1+n_2-\frac{4-2\varepsilon}{2}}}
\tag{6.4.3}
$$

$$
= C_{n_1,n_2} \left(\frac{-1}{a}\right)^{2-(n_1+n_2)} a^\varepsilon \underbrace{\int\limits_0^1 dx_2 \underbrace{\frac{(1-x_2)^{1-n_2} x_2^{n_2-1}}{(x_2-a)^{n_1+n_2-2}}}_{g_{n_1,n_2}(x_2)} ((a-x_2)(1-x_2))^{-\varepsilon}}_{\mathcal{I}_{n_1,n_2}}
$$

where t denotes the external momentum squared. If we now consider $\mathcal{I}_{n_1,n_2}^{(k)}$, the k-th coefficient of the Laurent expansion of the integral I_{n_1,n_2},

$$
\mathcal{I}_{n_1,n_2}^{(k)} = \int\limits_0^1 dx\; g_{n_1,n_2}(x) \left(\log(1-x) + \log(a-x)\right)^k
$$

$$
= \int\limits_0^1 dx\; g_{n_1,n_2}(x) \sum_{i=0}^k \binom{k}{i} G^{k-i}(1;x) \left(G(a;x)+\log(a)\right)^i
$$

$$
= \int\limits_0^1 dx\; g_{n_1,n_2}(x) \sum_{i=0}^k \sum_{j=0}^i \binom{k}{i}\binom{i}{j} G^{k-i}(1;x) G^j(a;x) \log^{i-j}(a)
$$

$$
= \int\limits_0^1 dx\; g_{n_1,n_2}(x) \sum_{i=0}^k \sum_{j=0}^i \binom{k}{i}\binom{i}{j} (k-i)!j! G(\underbrace{1,\ldots,1}_{(k-i)\text{-times}};x) G(\underbrace{a,\ldots,a}_{j\text{-times}};x) \log^{i-j}(a)
$$

$$
\tag{6.4.4}
$$

we see by using the shuffle relations on the underlined term in the last line [15], that we will deal with integrals of the form

$$
\int\limits_0^1 dx \frac{(1-x)^{1-n_2} x^{n_2-1}}{(x-a)^{n_1+n_2-2}} \log^{i-j}(a) G\left(\text{a permutation of }(k-i)\text{ 1's and } j \text{ a's}; x\right)\;. \tag{6.4.5}
$$

---

[15] Namely $\int_\gamma \omega \int_\gamma \omega' = \int_\gamma (\omega \shuffle \omega')$ where $(\omega \shuffle \omega')$ denotes the set of all permutations of the union of the words ω and ω', that preserves the (relative) orderings within ω and ω'.

This form is of course suggestive with respect to a suitable choice of the propagator powers n_1 and n_2, since we immediately notice that for $n_1 = 2$ and $n_2 = 1$ these integrals

$$\log^{i-j}(a) \int\limits_0^1 \mathrm{d}x \frac{1}{(x-a)} G \left(a \text{ permutation of } (k-i) \text{ 1's and } j \text{ a's}; x\right) \tag{6.4.6}$$

evaluate directly to expressions of the form

$$\mathcal{I}_{2,1}^{(k)} = \sum_{i=0}^{k} c_i \cdot G(a; \dots \text{word of length } (i-1) \dots ; 1) \cdot \log^{k-i}(a) \tag{6.4.7}$$

for some constants $c_i \in \mathbb{Q}$.

To make this first observation a bit more tangible, let us evaluate the first three Laurent coefficients by using (6.4.4) with $n_1 = 2$ and $n_2 = 1$. We get

$$\mathcal{I}_{2,1}^{(0)} = \int\limits_0^1 \mathrm{d}x \frac{1}{x-a} = G(a; 1) \tag{6.4.8}$$

$$\begin{aligned} \mathcal{I}_{2,1}^{(1)} &= \int\limits_0^1 \mathrm{d}x \frac{1}{x-a} \left(G(1; x) + \log(a) + G(a; x)\right) \\ &= G(a, 1; x) + G(a; 1) \log(a) + G(a, a; 1) \end{aligned} \tag{6.4.9}$$

and

$$\begin{aligned} \mathcal{I}_{2,1}^{(2)} &= \int\limits_0^1 \mathrm{d}x \frac{1}{x-a} \Big(2(G(1, 1; x) + G(a, a; x)) + \underbrace{G(1, a; z) + G(a, 1; z)}_{=G(1; z)G(a; z)} \\ &\quad + (G(1; x) + G(a; x)) \log(a) + \log^2(a) \Big) \\ &= 2(G(a, 1, 1; 1) + G(a, a, a; 1)) + G(a, 1, a; 1) + G(a, a, 1; 1) \\ &\quad + (G(a, 1; 1) + G(a, a; 1)) \log(a) + G(a; 1) \log^2(a) . \end{aligned} \tag{6.4.10}$$

Until now, it may not be obvious how the bubble integral with the chosen propagator powers helps simplifying the differential equations, since we need the differentiation with respect to a variable on which the letters are depending as well. This differentiation is treated in **Lemma 3.3.30.** in [35] and reads (shortened and adapted to the here used notation):

The total differential of any hyperlogarithm can be written in the form:

$$\mathrm{d}G(\sigma_1, \dots, \sigma_n; z) = G(\cancel{\sigma_1}, \dots; z) \mathrm{d}\log(z - \sigma_1) - G(\dots, \cancel{\sigma_n}; z) \mathrm{d}\log(\sigma_n)$$

$$+ \sum_{k=1}^{n-1} \left(G(\dots, \cancel{\sigma_{k+1}}, \dots; z) - G(\dots, \cancel{\sigma_k}, \dots; z)\right) \mathrm{d}\log(\sigma_k - \sigma_{k+1})$$

$$\tag{6.4.11}$$

40

where ... $\sigma_{\!\!\!\!/k}$ *... denotes the word after deleting the k-th letter* σ_k *and summands with* $\sigma_k = \sigma_{k+1}$ *do not contribute* $(\mathrm{d}\log(0) := 0)$[16]*.*

We are now able to determine some crucial properties of the differential equation satisfied by the Laurent coefficients of the integral $\mathcal{I}_{2,1}$ and MI's with a similar structure. Our example had the structure

$$I_{2,1} = -C_{2,1} \cdot a \cdot (a^\varepsilon \mathcal{I}_{2,1}) \tag{6.4.12}$$

$$= -C_{2,1} \underbrace{\cdot a \cdot}_{\text{normaliz.}} \left(\mathcal{I}_{2,1}^{(0)} + \varepsilon \left(\mathcal{I}_{2,1}^{(0)} \log(a) + \mathcal{I}_{2,1}^{(1)} \right) \right. \tag{6.4.13}$$

$$\left. + \varepsilon^2 \left(\frac{1}{2} \mathcal{I}_{2,1}^{(0)} \log^2(a) + \mathcal{I}_{2,1}^{(1)} \log(a) + \mathcal{I}_{2,1}^{(2)} \right) + \mathcal{O}\left(\varepsilon^3 \right) \right) \tag{6.4.14}$$

where the overall factor a corresponds to the normalization of the integral with the homogeneous solution, as used by going from $I \to I/\mathcal{I}_{homo.}^{(0)}$ in (6.3.6) to (6.3.9). We will comment on $C_{2,1}$ a bit later, but at this moment one can think of it as an overall normalization of all involved MI's. The last and the structurewise most important term is the underlined term. From the above discussion of the Laurent coefficients $\mathcal{I}_{2,1}^{(k)}$ we see now, that every summand in this bracket has the form

$$\varepsilon^k \log(a)^{k-i} G(a, \sigma_2, \ldots, \sigma_i; 1) \ . \tag{6.4.15}$$

where $\sigma_{1<k}$ is either 1 or a. Before taking the derivative of these summands with respect to a notice, that due to the special form of the word, where the first letter is always a and furthermore $z = 1$, only the last letter determines the complete derivative. To see this, consider

$$\partial_a G(a, \ldots, a, 1, \ldots, 1, a, \ldots, \sigma_n; 1)$$

$$= G(\cancel{a}, \ldots, a, 1, \ldots, 1, a, \ldots, a, \sigma_n; 1) \frac{1}{a-1}$$

$$+ \left(G(a, \ldots, a, \cancel{1}, \ldots, 1, a, \ldots, a, \sigma_n; 1) - G(a, \ldots, \cancel{a}, 1, \ldots, 1, a, \ldots, a, \sigma_n; 1) \right) \frac{1}{a-1}$$

$$+ \left(G(a, \ldots, a, 1, \ldots, 1, \cancel{a}, \ldots, a, \sigma_n; 1) - G(a, \ldots, a, 1, \ldots, \cancel{1}, a, \ldots, a, \sigma_n; 1) \right) \frac{1}{a-1}$$

$$+ \begin{cases} \left(G(a, \ldots, a, 1, \ldots, 1, a, \ldots, a, \cancel{\sigma_n = 1}; 1) - G(a, \ldots, a, 1, \ldots, 1, a, \ldots, \cancel{a}, \sigma_n = 1; 1) \right) \frac{1}{a-1} \\ -G(a, \ldots, a, 1, \ldots, 1, a, \ldots, \cancel{\sigma_n = a}; 1) \frac{1}{a} \end{cases}$$

$$= \frac{G(a, \ldots, \sigma_{\!\!\!\!/n})}{a-1} - \frac{G(a, \ldots, \sigma_{\!\!\!\!/n})}{a} \partial_a \sigma_n$$

$$\tag{6.4.16}$$

where dots denote the same letter and equally marked terms always cancel against each other. We see, that due to this cancellation only the last letter determines the derivative

---

[16]See the remarks on the regularization in section 6.2.2.

consisting at most of two terms. With this preparation it is clear, that

$$\varepsilon^k \partial_a \left(\log(a)^{k-i} G(a, \sigma_2, \ldots, \sigma_i; 1) \right) = \varepsilon^k \left((k-i) \frac{\log(a)^{k-i-1}}{a} G(a, \sigma_2, \ldots, \sigma_i; 1) \right.$$
$$\left. + \log(a)^{k-i} \left(\frac{G(a, \sigma_2, \ldots, \cancel{\sigma_i}; 1)}{a-1} + \frac{G(a, \sigma_2, \ldots, \cancel{\sigma_i}; 1)}{a} \partial_a \sigma_i \right) \right) \; .$$

$$(6.4.17)$$

In this derivative it is explicit, that, by a proper normalization, the differential equation for the MI $I_{2,1}$ will have only first order poles as singular points and is therefore completely solvable within the class of hyperlogarithms without additional rational terms as in the solution of $I_{1,1}$ in subsection 6.3.1. Furthermore, by the computation within the parametric representation we obtained the normalization which ensures, that the differential equation for the k-th Laurent coefficient of the MI $\tilde{I}_{2,1} = \frac{t}{m^2} \frac{1}{C_{2,1}} I_{2,1}$ will only depend on the $(k-1)$-th one. Indeed we find:

$$\partial_y \tilde{I}_{2,1} = \varepsilon \left(\frac{1}{y} - \frac{2}{y-1} \right) \tilde{I}_{2,1} + \frac{1}{y-1} \qquad (6.4.18)$$

It is important to point out, that such an MI will in general not be considered as a "good" MI by standard Laporta reduction algorithms, since it has a squared propagator (see chapter 4) and that any MI which possesses a representation of the discussed form with linear letters in the hyperlogarithm, will have a differential equation with poles of order one in the kinematic invariant (due to the dLog-form in (6.4.11)).

6.4.2 The DEQ in a Canonical Basis and Its Solution

A similar but more general observation has first been made explicitly in [76], whereas a more detailed review can be found in [47] and the results may be summarized as followed:

1. For integrals which evaluate within the class of hyperlogarithms, it is often possible to find a basis in which the differential equation takes the particular simple form

$$\mathrm{d}\vec{I}(\varepsilon, s_1, \ldots, s_n) = \varepsilon \left(\sum_i A_i \mathrm{d} \log(f_i(s_1, \ldots, s_n)) \right) \vec{I}(\varepsilon, s_1, \ldots, s_n) \;, \qquad (6.4.19)$$

   where the s_i denote the kinematic invariants, the A_i are matrices without ε or s_i dependence and the f_i are functions, which determine the alphabet. In this basis, the dependence on the dimension factorizes completely and it is therefore often referred to as ε- or *canonical* form.

2. A good basis is formed by integrals of uniform (*"transcendental"*) weight.

3. The basis can be obtained by manipulation of the initial system of differential equations as obtained by standard IBP-approaches (pursued in [47, 48, 53–55, 79]) or by an a priori investigation of the relevant topologies (further discussed in [47, 50, 77, 80]).

A comment on the second point is in order, since it needs some further explanation of what is meant by uniform (*"transcendental"*) weight. In the explicitly computed example we found, that the solution of the integral $\tilde{I}_{2,1}$ at order ε^k has the form of an logarithm of power $k - i$ times an hyperlogarithm of weight i (see (6.4.15)). This product could be transformed into a sum of hyperlogarithms of weight k due to the shuffle relations. Furthermore, any multiplication of i hyperlogarithms of weight k_i will result in principle in a sum of hyperlogarithms of weight $\sum_i k_i$.

The idea is, to assign to ε the (*"transcendental"*) weight -1, such that expressions of the form (6.4.15) have all *uniform weight* zero in analogy to the weight addition of hyperlogarithms. This implies differential equations similar to $\partial_z \mathcal{I}^{(k)} = 1/(a - z)\mathcal{I}^{(k-1)}$ with the boundary $I(0) = 0$. This boundary condition of course, does not hold for general Feynman integrals. Therefore a *"transcendental"* weight is assigned to every special number like e.g the weight γ_E or π is one. Furthermore one assigns to ζ_k the weight k, which seems problematic, since there is little known about their transcendentality yet. Therefore we will not use this terminology and only refer to a weight whenever needed.

Before discussing the solution of a general deq in a canonical basis, let us first consider the special case of (6.4.19) for only one integration variable. In that case we have to solve the differential equation

$$\frac{\mathrm{d}}{\mathrm{d}x}\vec{I}(x,\varepsilon) = \varepsilon A(x)\vec{I}(x) \ , \tag{6.4.20}$$

which is equivalent to the integral equation

$$\vec{I}(t) - \vec{I_0} = \varepsilon \int\limits_{x_0}^{x} \mathrm{d}x A(x)\vec{I}(x) \tag{6.4.21}$$

with $I_0 = I(x_0)$. The approximative solution of either the differential or the integral equation is well known to physicists, since it is usually encountered by considering the time dependent Schrödinger equation

$$\frac{\mathrm{d}}{dt}\Psi(t,t_0) = \frac{i}{\hbar}H(t)\Psi(t,t_0) \tag{6.4.22}$$

with an explicit time dependent Hamiltonian. This problem is well formulated in terms of the Dyson series and the differential equation (6.4.19) admits the same method but with simpler objects involved, since we are dealing with matrices instead of operators acting on a Hilbert space.

The solution of (6.4.20) by the Dyson series approach therefore reads

$$\vec{I}(t,\varepsilon) = T(x,x_0)\vec{I_0} \tag{6.4.23}$$

$$= \left(\mathbb{1} + \varepsilon \int\limits_{x_0}^{x} A(s)\mathrm{d}s + \varepsilon^2 \int\limits_{x_0}^{x} A(s)\int\limits_{x_0}^{s} A(s')\mathrm{d}s'\mathrm{d}s\dots\right)\vec{I_0} \tag{6.4.24}$$

$$= \left(\mathbb{1} + \sum_{n>1}\varepsilon^n \int_{x_0 \leq s_1\dots\leq s_n\leq x} A(s_n)A(s_{n-1})\dots A(s_1)\mathrm{d}s_1\dots\mathrm{d}s_n\right)\vec{I_0} \tag{6.4.25}$$

$$= \mathbb{P}e^{\varepsilon \int_{x_0}^{x} A(s)\mathrm{d}s}\vec{I_0} \tag{6.4.26}$$

Figure 6.1: The contour deformation $\gamma \simeq \gamma_1 \star \gamma_2$ in the complex space of the kinematic invariants yields a factorization of a Chen iterated integrals into hyperlogarithms.

where $\mathbb{P}$ denotes the *path ordering* [17] operator and the matrix $T(x_0, x)$ the *transport* of (6.4.20). The convergence is granted because of the infinitesimal ε and we furthermore notice, that the iterated integration will naturally result in the already introduced hyperlogarithms.

For the general case (6.4.19) with multiple kinematic variables, the iterative solution in terms of a path ordered exponential $\vec{I}(t, \varepsilon) = \mathbb{P} e^{\varepsilon \int_\gamma \mathrm{d}A} \vec{I}_0$ still holds, but the integration is now performed along γ, a path in the space of the kinematic invariants, connecting the boundary point $(s_{1,0}, \ldots, s_{n,0})$ and the point $(s_1, \ldots, s_n)$ while avoiding the singularities. The path ordered exponential yields a solution in terms of Chen iterated integrals. For a representation in terms of hyperlogarithms, the homotopy invariance of Chen iterated integrals can be used to deform the path continuously such that the integration along γ becomes $\gamma \simeq (\ldots ((\gamma_1 \star \gamma_2) \star \gamma_3) \ldots \star \gamma_n)$, on which the integration on the k-th path is performed along one variable s_k while the others stay constant. Here, $\star$ denotes the concatenation of two paths, whereas a possible path deformation for two kinematic invariants is depicted 6.1. The resulting integral will be a sum of products of hyperlogarithms[18].

6.4.3 Example I: Solving the Bubble with One Massive Propagator by Using a Canonical Basis

In section 6.4.1 we established, that the integral

$$\tilde{I}_{2,1} = \varepsilon \frac{t}{m^2} \cdot \text{} \tag{6.4.27}$$

is a suitable element of a canonical basis, since it is a pure function of weight zero. The second topology involved in the deq of the bubble is the tadpole

$$I_\nu = (-1)^\nu \left(\mu^2\right)^{\nu - \frac{D}{2}} \int \frac{\mathrm{d}k^D}{i\pi^{\frac{D}{2}}} \frac{1}{(k^2 - m^2)^\nu} \stackrel{\text{A.0.1}}{=\!=\!=} \left(\frac{\mu^2}{m^2}\right)^{\nu - \frac{D}{2}} \frac{\Gamma(\nu - \frac{D}{2})}{\Gamma(\nu)} \tag{6.4.28}$$

---

[17]Known as time ordering operator in QM.

[18]By using $\int_{\gamma_1 \star \gamma_2} \omega = \sum_{i=0}^n \int_{\gamma_1} \omega_1 \ldots \omega_i \cdot \int_{\gamma_2} \omega_{i+1} \ldots \omega_n$. See e.g. [35] section 3.2.3. for more details.

which can be expanded around $D = 4 - 2\varepsilon$ by using e.g. Mathematica. We find

$$\varepsilon e^{\varepsilon \gamma_E} I_2 = 1 + \varepsilon \log\left(\frac{\mu^2}{m^2}\right) + \frac{1}{12}\varepsilon^2\left(6 \log^2\left(\frac{\mu^2}{m^2}\right) + \pi^2\right) + \mathcal{O}\left(\varepsilon^3\right) \qquad (6.4.29)$$

to be uniform of weight zero whereby the prefactor $e^{\varepsilon \gamma_E}$ had been included to cancel the terms $\propto \gamma_E$ in the expansion of the Γ function. The system of differential equations for the canonical basis reads

$$\frac{\mathrm{d}}{\mathrm{d}y}\begin{pmatrix} \varepsilon e^{\varepsilon \gamma_E} \cdot \rule{2cm}{0pt} \\ \varepsilon e^{\varepsilon \gamma_E} y \cdot \rule{2cm}{0pt} \end{pmatrix} = \varepsilon\left(\frac{1}{y}A_0 + \frac{1}{y-1}A_1\right)\begin{pmatrix} \varepsilon e^{\varepsilon \gamma_E} \cdot \rule{2cm}{0pt} \\ \varepsilon e^{\varepsilon \gamma_E} y \cdot \rule{2cm}{0pt} \end{pmatrix} \qquad (6.4.30)$$

with $y = p_\mu p^\mu / m^2$ and

$$A_0 = \begin{pmatrix} 0 & 0 \\ 0 & 1 \end{pmatrix} \quad \text{and} \quad A_1 = \begin{pmatrix} 0 & 0 \\ -(\frac{\mu}{m})^2 & -2 \end{pmatrix}. \qquad (6.4.31)$$

The solution of this system in terms of the Dyson series is

$$\vec{I}(y) = \Bigg(\mathbb{1} + \varepsilon \int_{y_0}^{y}\left(\frac{A_0}{s} + \frac{A_1}{s-1}\right)\mathrm{d}s$$

$$+ \varepsilon^2 \int_{y_0}^{y}\int_{y_0}^{s_2}\left(\frac{A_0 A_0}{s_2 s_1} + \frac{A_0 A_1}{s_2(s_1-1)} + \frac{A_1 A_0}{(s_2-1)s_1} + \frac{A_1 A_1}{(s_2-1)(s_1-1)}\right)\mathrm{d}s_1 \mathrm{d}s_2\Bigg)\vec{I}(y_0)$$

$$(6.4.32)$$

and a suitable boundary point is $y \to 0$, since the MI chosen for the bubble topology goes to zero proportional to y. Therefore, every term where the rightmost matrix A_0 is zero, since the associated hyperlogarithms diverge at most logarithmic. With this observation we get

$$\vec{I}(y) = \Bigg(\mathbb{1} + \varepsilon \int_{0}^{y}\left(\frac{A_1}{s-1}\right)\mathrm{d}s + \varepsilon^2 \int_{0}^{y}\int_{0}^{s_2}\left(\frac{A_0 A_1}{s_2(s_1-1)} + \frac{A_1 A_1}{(s_2-1)(s_1-1)}\right)\mathrm{d}s_1 \mathrm{d}s_2\Bigg)\vec{I}(0)$$

$$= \Bigg(\mathbb{1} + \varepsilon A_1 G(1; y) + \varepsilon^2\left(G(0, 1; y)A_0 A_1 + G(1, 1; y)A_1 A_1\right)\Bigg)\vec{I}(0)$$

$$= \begin{pmatrix} 1 + \log\left(\frac{\mu^2}{m^2}\right)\varepsilon + \frac{1}{12}\left(6 \log^2\left(\frac{\mu^2}{m^2}\right) + \pi^2\right)\varepsilon^2 + \mathcal{O}\left(\varepsilon^3\right) \\ -\frac{\mu^2}{m^2}G(1, y)\varepsilon + \frac{\mu^2}{m^2}\left(-G(0, 1, y) + 2G(1, 1, y) - G(1, y)\log\left(\frac{\mu^2}{m^2}\right)\right)\varepsilon^2 + \mathcal{O}\left(\varepsilon^3\right) \end{pmatrix},$$

$$(6.4.33)$$

where the only thing to do was an expansion of the boundary tadpole, which is trivial.

45

6.4.4 Example II: Solving the Sunrise with One Massive Propagator by Using a Canonical Basis

The next slightly more involved example is the sunrise topology with one massive propagator given by the integrals

$$
\begin{aligned}
I_{\nu_1,\nu_2,\nu_3}(m,t=p_\mu p^\mu) &= (-1)^\nu \left(\mu^2\right)^{\nu-D} \int \frac{\mathrm{d}^D k}{i\pi^{\frac{D}{2}}} \frac{\mathrm{d}^D l}{i\pi^{\frac{D}{2}}} \frac{1}{(k^2-m^2)^{\nu_1}(l^2)^{\nu_2}((l+k-p)^2)^{\nu_3}} \\
&= (-1)^{\nu_1} \left(\mu^2\right)^{\nu_1-\frac{D}{2}} (-1)^{\nu_2+\nu_3} \left(\mu^2\right)^{\nu_2+\nu_3-\frac{D}{2}} \\
&\quad \cdot \int \left(\frac{1}{(k^2-m^2)^{\nu_1}} \int \frac{\mathrm{d}^D l}{i\pi^{\frac{D}{2}}} \frac{1}{(l^2)^{\nu_2}((l+k-p)^2)^{\nu_3}} \right) \frac{\mathrm{d}^D k}{i\pi^{\frac{D}{2}}}
\end{aligned}
$$

$$= \qquad . \tag{6.4.34}$$

For this family, there are two master integrals and a choice according to the conditions in chapter 4 will result in a coupled system of differential equations. Such a coupled system, as depicted in (6.4.2) can not be decoupled at $\mathcal{O}(\varepsilon)$ by normalizing every MI separately by its homogeneous solution as presented in section 6.3.1. We therefore seek a canonical basis of this family of integrals, since the general form of the canonical basis 6.4.19 automatically comes with a decoupling at $\mathcal{O}(\varepsilon)$.

In the topology depicted in (6.4.34), the red part corresponds to massless bubble with the "external" momentum $q = p - k$ and we may perform the integration over l in (6.4.34) directly. The computation of the massless bubble can be found in appendix A and inserting it into (6.4.34) yields

$$
I_{\nu_1,\nu_2,\nu_3}(m,t=p_\mu p^\mu) = (-1)^{\nu_1} \left(\mu^2\right)^{\nu_1-\frac{D}{2}} C_{\nu_2,\nu_3} \int \frac{\mathrm{d}^D k}{i\pi^{\frac{D}{2}}} \frac{1}{(k^2-m^2)^{\nu_1}} \frac{1}{((k-p)^2)^\lambda} \tag{6.4.35}
$$

with $\lambda = \nu_2 + \nu_3 - \frac{D}{2}$ and

$$
C_{\nu_2,\nu_3} = \left(-\mu^2\right)^{\nu_2+\nu_3-\frac{D}{2}} \frac{\Gamma\left(\nu_2+\nu_3-\frac{D}{2}\right)}{\Gamma(\nu_2)\Gamma(\nu_3)} \frac{\Gamma\left(\frac{D}{2}-\nu_2\right)\Gamma\left(\frac{D}{2}-\nu_3\right)}{\Gamma(D-(\nu_2+\nu_3))} . \tag{6.4.36}
$$

This integral is of course nothing else than the already in great detail studied semi-massive bubble with a slightly generalized propagator λ. We write down its parametric representation analogous to (6.4.3) in $D = 4 - 2\varepsilon$ dimension

$$
I_{\nu_1,\nu_2,\nu_3} = C_{\nu_1,\nu_2,\nu_3} a^{\nu_1+\nu_2+\nu_3-4} \int_0^1 \frac{(1-\xi)^{3-(\nu_2+\nu_3)}\xi^{\nu_2+\nu_3-3}}{(a-\xi)^{\nu_1+\nu_2+\nu_3-4}} \left(\frac{\xi}{((1-\xi)(a-\xi))^2} \right)^\varepsilon \mathrm{d}\xi \tag{6.4.37}
$$

with $a = m^2/t$ and

$$
C_{\nu_1,\nu_2,\nu_3} = a^{2\varepsilon} \left(\frac{\mu^2}{m^2}\right)^{(\nu_1+\nu_2+\nu_3-4+2\varepsilon)} \frac{\Gamma(2-\varepsilon-\nu_2)\Gamma(2-\varepsilon-\nu_3)\Gamma(\nu_1+\nu_2+\nu_3-4+2\varepsilon)}{\Gamma(\nu_1)\Gamma(\nu_2)\Gamma(\nu_3)\Gamma(4-2\varepsilon-\nu_2-\nu_3)} . \tag{6.4.38}
$$

Let us now, analogously to the bubble, consider the integrand

$$\mathcal{I}_{\nu_1,\nu_2,\nu_3} = a^{\nu_1+\nu_2+\nu_3-4} \int_0^1 \frac{(1-\xi)^{3-(\nu_2+\nu_3)}\xi^{\nu_2+\nu_3-3}}{(a-\xi)^{\nu_1+\nu_2+\nu_3-4}} \left(\frac{\xi}{((1-\xi)(a-\xi))^2}\right)^\varepsilon d\xi \qquad (6.4.39)$$

only. As in the bubble case we want to choose the propagator powers such that the denominator has power one and corresponds to a derivative of a logarithm. Therefore we have the condition $\sum_i \nu_i - 4 = 1$ with two possible, distinct choices, namely $\nu_1 = \nu_2 = 2$ and $\nu_3 = 1$ as well as $\nu_1 = 1$ and $\nu_2 = \nu_3 = 2$

The First MI of the Sunrise Topology With One Massive Propagator

The ε-expansion for the first case $\nu_1 = \nu_2 = 2$ and $\nu_3 = 1$ reads

$$\tilde{\mathcal{I}}_{2,2,1} = a \int_0^1 \left(\frac{\xi}{((1-\xi)(a-\xi))^2}\right)^\varepsilon \frac{d\xi}{(a-\xi)}$$

$$= a \int_0^1 \left(1 + (-2\log(a-\xi) - 2\log(1-\xi) + \log(\xi))\varepsilon\right) \frac{d\xi}{(a-\xi)} + \mathcal{O}(\varepsilon^2) \qquad (6.4.40)$$

and we observe from the structure, that there will be no terms of mixed weight. Furthermore, we have to check, that the prefactor $C_{2,2,1}$ has uniform weight and indeed, we find

$$C_{2,2,1} = \frac{\mu^2}{m^2}\left[\left(-2\log(a) - \frac{1}{\varepsilon} - 2\log\left(\frac{\mu^2}{m^2}\right) + 2\gamma_E\right)\right.$$

$$\left. + \varepsilon\left(2\left(-\log(a) - \log\left(\frac{\mu^2}{m^2}\right) + 2\gamma_E\right)\left(\log(a) + \log\left(\frac{\mu^2}{m^2}\right)\right) - 2\gamma_E^2 - \frac{\pi^2}{6}\right)\right] + \mathcal{O}(\varepsilon^2)$$
$$(6.4.41)$$

that it is of weight one. The integral is therefore a good choice for an element of the canonical basis. Notice, that we basically recycled the knowledge about the bubble with one massive propagator.

The Second MI of the Sunrise Topology With One Massive Propagator

The second natural choice, $\nu_2 = \nu_3 = 2$ and $\nu_1 = 1$ is the sunrise integral, with the massless propagators dotted (raised to the power two), reads

$$\tilde{\mathcal{I}}_{1,2,2} = \underbrace{\frac{a^2}{(1-a)}\int_0^1 \left(\frac{\xi}{((1-\xi)(a-\xi))^2}\right)^\varepsilon \frac{d\xi}{(a-\xi)}}_{\frac{a}{1-a}\tilde{\mathcal{I}}_{2,2,1}} - \underbrace{\frac{a}{(1-a)}\int_0^1 \left(\frac{\xi}{((1-\xi)(a-\xi))^2}\right)^\varepsilon \frac{d\xi}{(1-\xi)}}_{\tilde{I}_{II}} .$$
$$(6.4.42)$$

The first part can be identified as the already checked uniform weight function in the first MI, while in the second part $\tilde{I}_{II}$, the series expansion an integration can not be

interchanged, since the integral is not convergent at one. The integration with its full ε-dependence yields

$$\tilde{I}_{II} = (-a)^{-2\varepsilon}\Gamma(-2\varepsilon)\Gamma(\varepsilon+1)\,_2\tilde{F}_1\left(2\varepsilon, \varepsilon+1; 1-\varepsilon; \frac{1}{a}\right) , \qquad (6.4.43)$$

where $_2\tilde{F}_1\left(a, b; c; z\right) = \,_2F_1\left(a, b; c; z\right)/\Gamma(z)$ is the regularized Gauß hypergeometric function. This expression can be expanded with the help of the HypExp 2 package [58] and its first to orders read

$$\tilde{I}_{II} = -\frac{1}{2\varepsilon} + \left(\log\left(1-\frac{1}{a}\right) + \log(-a)\right)$$
$$+ \varepsilon\left(-2\mathrm{Li}_2\left(\frac{1}{a}\right) - 2\log^2\left(1-\frac{1}{a}\right) - \log^2(-a) - 2\log(-a)\log\left(1-\frac{1}{a}\right) - \frac{\pi^2}{6}\right) + \mathcal{O}\left(\varepsilon^2\right)$$
$$(6.4.44)$$

which is clearly a weight one function. The prefactor $C_{1,2,2}$ is two times $C_{2,2,1}$ and therefore as well of uniform weight.

The DEQ of the Sunrise with One Massive Propagator

From the explicit construction of the uniform weight integrals we read off a canonical basis as $\vec{I} = (I_1, I_2)^T = (\varepsilon^2 y I_{2,2,1}, \varepsilon^2\left(2I_{2,2,1} - (y-1)I_{2,2,1}\right))^T$ where $y = 1/a = t/m^2$ and we took into account that $C_{1,2,2} = 2C_{2,2,1}$ such that $I_1 \propto \mathcal{I}_{2,2,1}$ and $I_2 \propto \tilde{I}_{II}$. Furthermore we introduced the overall prefactor ε^2 ensuring, that the first non-vanishing Laurent coefficient is at order $\mathcal{O}(\varepsilon^j)$ with $j \geq 1$. The differential equation reads

$$\frac{\mathrm{d}}{\mathrm{d}y}\vec{I} = \varepsilon\left(\frac{1}{y}\begin{pmatrix} 1 & 0 \\ -4 & 0 \end{pmatrix} + \frac{1}{y-1}\begin{pmatrix} -2 & 1 \\ 4 & -2 \end{pmatrix}\right)\vec{I} \qquad (6.4.45)$$

and we see, that every term in the Laurent expansion can be integrated within the class of harmonic polylogarithms.

After this to explicit examples, let us summarize the three main takeaways of this chapter.

Firstly, a general class of functions, the hyperlogarithms, were introduced. These functions are defined as iterated integrals over certain one-forms but can be translated into nested sums, the multiple polylogarithms, which are suitable for numerical evaluations.

Secondly, by investigating the structure of Feynman integrals in the parametric representation we motivated that many of them can be computed within this class of functions.

Thirdly, this observation in addition to the method of differential equation led to the concept of a canonical basis of master integrals in which the solutions were manifest in the class of hyperlogarithms. The canonical basis could be found by investigating the

parameter representation of the integrals[19]. Once it was done and the alphabet identified, the solution of the MI's can be obtained to every order without further ado[20].

---

[19]Note that it is a special feature of banana-graphs which made the propagator power choice so suggestive. For them, the degree of the graph polynomial $\mathcal{F}$ is the same as the number of integrations. For more complicated graphs the methods described in [47–55, 81] have to be employed, whereby the investigation of the cuts seems to give the most obvious link to the properties of the diagram under consideration.

[20]Thereby, even solutions in terms of iterated integrals over dLog-forms of non-rational letters can be used. See e.g. [82, 83].

Chapter 7

Computing Feynman Integrals Beyond Hyperlogarithms

The previous chapter dealt with the computation of Feynman integrals, for which the system of differential equations could be decoupled at order ε. If we consider such a system of coupled differential equation for a given topology, there are some criteria from which it seems plausible to deduce that its Laurent coefficients can not be expressed in term of hyperlogarithms and therefore there does not exist a canonical basis of the MI's. A detailed review of the way this can be done is beyond the scope of this thesis since these are subject of current research. I will only outline the general ideas.

7.1 On Determining If Hyperlogarithms Will Not Be Enough

For many motivations in this thesis the parametric representation of Feynman integrals has been used. This is mainly due to the fact, that it seems in a way more directly related to the properties of the integrals than stating the "state of the art" algorithms, in which of course at the end these properties are manifest as well.

In that spirit, I will shortly comment on how observing that we leave the class of hyperlogarithms could might be motivated by the properties of the graph polynomials. By only investigating the linear reducibility of a given diagram, we could in principle deduce, if the method of hyperlogarithms will fail. But this method depends on the parametrization an we can not exclude, that there is a re-parametrization in which it becomes linearly reducible. The second viewpoint is far more general, but probably not feasible for practical, non-trivial considerations. It is based on the fact, that the coefficients in the Laurent expansion of Feynman integrals can be related to special numbers, called periods [84–86]. These numbers are defined as integrals over rational function ($\sim$ graph polynomials) over certain domains in $\mathbb{R}^n$ which are defined by polynomial in-equalities. By considering the periods associated to the polynomials, one could therefore deduce which class of functions is needed to compute the whole integral.

7.1.1 Outline On The Connection Between Cuts and Differential Equations

Another more recent way, which is easier and currently better understood for many examples (see e.g. [52, 77, 80, 87]) is based on the investigation of the maximal cut and its connection to the differential equation.

The physical interpretation of cutting an internal edge of a Feynman diagram is, broadly speaking, to force the corresponding particle in the diagram to be on-shell. These cuts can be used to study the discontinuity of Feynman integrals with respect to the kinematic invariants and to reconstruct the original integral from its imaginary part [88–91]. Thereby, a cut is treated within the framework of multivariate residues [92] and for propagators raised to power one, the cut propagator can simply be replaced by a δ-function[1].

In [52] it has been observed and illustrated, that the maximal cut (putting all propagators of a diagram on-shell) fulfils the same differential equation as the homogeneous solution of the integral under consideration. The main argument for that is the special form of the differential equation

$$\partial_x I_i = A_{i,j}(x,\varepsilon)I_j + \left(\sum_l k_l(x,\varepsilon)I_l \in (\text{sub-topologies})\right) , \qquad (7.1.1)$$

where $A_{i,j}$ are the coefficients of the homogeneous system. By applying the maximal cut to the rhs of the deq, all integrals of the sub-topologies vanish, since they have less propagators and therefore no support on the maximal cut of I_i[2] Therefore, one is left with the homogeneous system of differential equations

$$\partial_x \begin{pmatrix} Cut(I_1) \\ \vdots \\ Cut(I_k) \end{pmatrix} = A(x,\varepsilon) \begin{pmatrix} Cut(I_1) \\ \vdots \\ Cut(I_k) \end{pmatrix} \qquad (7.1.2)$$

where Cut denotes the maximal cut of the integral[3] where every integral I_j contains the full set of propagators. The main question is, if this homogeneous system can be decoupled at every order in ε.

The difficulty of computing the Laurent coefficients of a maximal cut is very much less than the computation of the full integrals and the obtained information can be related directly to the homogeneous system of differential equations. If the Laurent expansion of the maximal cut of every MI of the (sub)-topology evaluates into elementary functions or hyperlogarithms, there can likely be found a canonical basis for which the differential equation decouples [4].

If instead the Laurent coefficients of the maximal cut already evaluate to special functions[5] which fulfil a higher order differential equation[6], the system of first order

---

[1]For a prescription of higher propagator powers see e.g. [52, 92]

[2]They are holomorphic at the propagators they do not contain and therefore the residue vanishes.

[3]The cuts used do not have a restriction to positive energies and are therefore different to Cutkovsky-cuts.

[4]A similar observation can be found [47] where it was proposed to use the properties of general cuts (not only the maximal one) as an starting point for a construction of a canonical basis. See also [77, 80] for applications of cuts in Baikov-representation.

[5]Or integrals over special function (see e.g. [87])

[6]E.g. elliptic integrals or hypergeometric functions or more complicated objects

differential equations can not be decoupled at order ε and the integrals do not evaluate within the class of hyperlogarithms. Instead the system decouples as a n-*th* order system of differential equations.

7.2 A Reminder On Solving Linear Higher Order Differential Equations

For Feynman integrals beyond hyperlogarithms the system of first order differential equations can not be decoupled by a canonical basis. Instead, there will exist an inhomogeneous higher order differential equation[7] for the k-th Laurent coefficient. This differential equation can be transformed to a first order system by the usual replacement $x_1(t) := \mathcal{I}^{(k)}(t)$, $x_2(t) := \frac{\mathrm{d}}{\mathrm{d}t}\mathcal{I}^{(k)}(t)$, ..., $x_n = \frac{\mathrm{d}^{n-1}}{\mathrm{d}t^{n-1}}\mathcal{I}^{(k)}(t)$. We therefore deal with the first order system

$$\frac{\mathrm{d}}{\mathrm{d}t}\vec{x} = A(t)\vec{x} + \vec{b}^{(k)}(t) \tag{7.2.1}$$

with the boundary condition

$$\vec{x}(t_0) = \vec{\xi} \tag{7.2.2}$$

and the corresponding homogeneous system

$$\frac{\mathrm{d}}{\mathrm{d}t}\vec{x}^h = A(t)\vec{x}^h \ . \tag{7.2.3}$$

The solutions $\vec{x}_i^h$ are said to form a fundamental system $X(t_0, t)$, if $\det\left[\vec{x}_1^h(t), \ldots, \vec{x}_n^h(t)\right] = \det(X(t_0, t)) \neq 0$ for all t and it can be solved by the usual variation of constants

$$\vec{x}(t) = X(t_0, t)\vec{\xi} + \int_{t_0}^{t} X(t_0, s)\vec{b}^{(k)}(s)\mathrm{d}s \ . \tag{7.2.4}$$

It is important to highlight the fact that the fundamental system will be the same for every Laurent coefficient and only the inhomogeneous part changes. The solution of the k-th Laurent coefficient can therefore be written as a k-fold iterated integral and in this representation, the similarities to the approach with the canonical basis are manifest. In [87] it was shown for the 3-loop banana, that a basis transformation with specific elements of the fundamental system $X_i(t_0, t)$ for every of the three MIs I_1, I_2 and I_3 obtained by Laportas algorithm can be used to decouple the first order system of this MI choice at order ε.

If one chooses a fixed basis of MI's, the analogous discussion for the n-th order differential equation of the k-th Laurent coefficient reads

$$\frac{\mathrm{d}^n}{\mathrm{d}t^n}\mathcal{I}^{(k)}(t) + a_{n-1}(t)\frac{\mathrm{d}^{n-1}}{\mathrm{d}t^{n-1}}\mathcal{I}^{(k)}(t) + \ldots + a_0(t)\mathcal{I}^{(k)}(t) + b^{(k)}(t) = 0 \tag{7.2.5}$$

where the fundamental system is spanned by the n solutions y_h of the homogeneous deq (y_h to emphasize their independence on the order of expansion). Here, analogously, the fundamental system is a fundamental system, if the Wronskian determinant

$$W\left(y_1^h, y_2^h, \ldots, y_n^h\right) := \det \begin{bmatrix} y_1^h(t) & \cdots & y_n^h(t) \\ \frac{\mathrm{d}}{\mathrm{d}t}y_1^h(t) & \cdots & \frac{\mathrm{d}}{\mathrm{d}t}y_n^h(t) \\ \cdots & \cdots & \cdots \\ \frac{\mathrm{d}^{n-1}}{\mathrm{d}t^{n-1}}y_1^h(t) & \cdots & \frac{\mathrm{d}^{n-1}}{\mathrm{d}t^{n-1}}y_n^h(t) \end{bmatrix} \neq 0 \tag{7.2.6}$$

---

[7]Recent examples in that direction seem to hint, that the order of the system corresponds to the number of MI's which can not be decoupled at the first order differential equation [30, 80, 87, 93, 94]

for all t. The variation of the constant now yields the particular solution

$$\mathcal{I}_{\text{part}}^{(k)}(t) = \sum_{j=1}^{n} (-1)^{n+j} y_j^h(t) \int_{t_0}^{t} \frac{W\left(y_1^h, \ldots, y_{j-1}^h, y_{j+1}^h, \ldots, y_n^h\right)(s)}{W\left(y_1^h, \ldots, y_n^h\right)(s)} b^{(k)}(s) \mathrm{d}s \qquad (7.2.7)$$

where $W(y_1^h, \ldots, y_{j-1}^h, y_{j+1}^h, \ldots, y_n^h)$ denotes the Wronskian determinant with the *j-th* column and the *n-th* row removed. The general solution for the Laurent coefficient at order k is then the superposition of the homogeneous solutions and the particular solution, where the initial condition is obtained by the physical constraints.

Both the representations are of course equivalent and it is important to notice, that there is always the homogeneous solution in the kernel of integration and that the inhomogeneity will involve lower Laurent coefficients and their derivatives.

$$I_{\nu_1,\nu_2,\nu_3} = \qquad\qquad\qquad\qquad\qquad\qquad\qquad (7.3.1)$$

Figure 7.1: The equal mass sunrise topology.

7.3 The Equal Mass Sunrise Integral

The simplest example of a Feynman integral which does not evaluate within the class of hyperlogarithms is the equal mass sunrise integral depicted in fig. 7.1. It therefore received much interest and has been extensively studied in the literature [26, 93, 95–113].

7.3.1 Multivalued Functions and Elliptic Curves - An Informal Overview

But before I give a review on the solution of the sunrise with the methods used in [107,110] I will give a superficial, informal overview on elliptic curves and their periods. This addresses readers with small or no knowledge on these subjects, such that there is some intuition for the approaches of the following sections after this detour. We will achieve this by putting aside much of the mathematical rigour usually required to really understanding the subjects, since they are well covered in many mathematical textbooks.

On Multivalued Functions

Consider the complex valued function

$$z^{\frac{1}{n}} = |r|^{\frac{1}{n}} e^{\frac{i\varphi}{n}} \qquad\qquad\qquad\qquad (7.3.2)$$

in polar coordinates with $n \in \mathbb{Z}$. Obviously, after traversing a closed path in counterclockwise direction around the origin[8] $\varphi \to \varphi + 2\pi$ we have that

$$z^{\frac{1}{n}} \to z^{\frac{1}{n}} e^{\frac{2\pi i}{n}} = |r|^{\frac{1}{n}} e^{\frac{i\varphi}{n}} e^{\frac{2\pi i}{n}} \neq |r|^{\frac{1}{n}} e^{\frac{i\varphi}{n}} \ . \qquad\qquad (7.3.3)$$

That means by traversing a closed second loop we will get another value and so on, until we traversed n-loops and start at the beginning. Our function $z^{\frac{1}{n}}$ can take n-different values in $\mathbb{C}$ and is therefore multivalued. We may ask ourself, what happens if we make a closed loop around another point a in $\mathbb{C}$, with $|a| < |r|$. We therefore consider

$$|r|^{\frac{1}{n}} e^{\frac{i\varphi}{n}} (a(1 - e^{i\theta})). \qquad\qquad\qquad (7.3.4)$$

---

[8]Traversing the path $\gamma \in \mathbb{C}$ from a to b is done by starting with the holomorphic function $f = f_a$ defined in a disk D_a centered at a, such that the Taylor series of f is convergent at a. If γ can be covered by domains D_i, such that the function f_i and f_{i+1} agree in the intersection of D_i and D_{i+1}, we have an analytic continuation of f from a to b along γ.
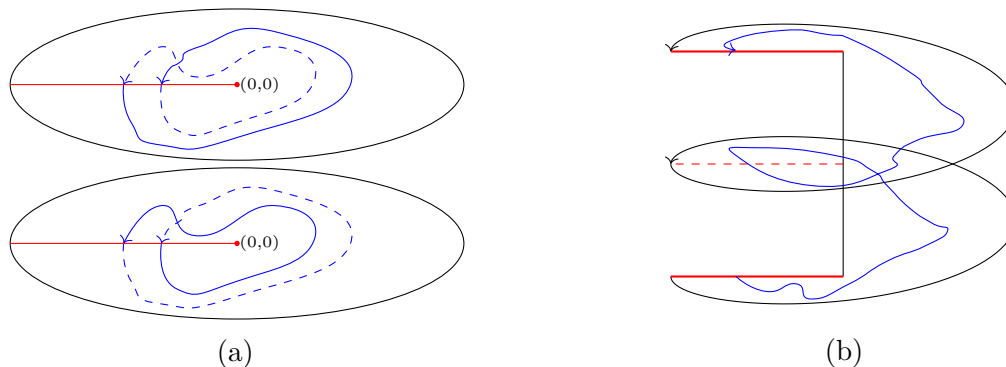
Figure 7.2: (a) Depiction of the two Riemann sheets of the root differing by a sign. Crossing the branch cut changes the sheet. Paths on one sheet are depicted as continuous lines, paths on the other sheet as dashed lines. (b) In between stage of the gluing process of the two sheets of the root. Gluing together the upper and lower cuts yields the Riemann surface of the square root shown in fig. 7.3.

and obviously, nothing changes after traversing the closed path with $\theta = 0 \to \theta = 2\pi$. Until now, the only special point is the origin. Lastly, we have to understand what happens at the point ∞. Therefore we consider the variable change $z \to \frac{1}{\xi}$, such that a closed loop around z at infinity corresponds to a closed loop of ξ around 0. The discussion of closed loops around ∞ is therefore the same as in (7.3.2) with $n \to -n$. The points 0 and ∞ are called *branch-points* of the function $z^{\frac{1}{n}}$ and if we want a single-valued in $\mathbb{C}$, we can not allow closed loops around either ∞ or zero.

This is "not allowing closed loops" is implemented by introducing a *branch-cut* which connects the point ∞ and zero. This can be done by any arbitrary straight, or waved but not self-intersecting line in $\mathbb{C}$, while the common choice is on the negative real axis. The function $z^{1/n}$ has now a single-valued determination on $\mathbb{C}$ minus the cut.

We know consider, what happens if we do cross a branch cut. Clearly, from the discussion above we know, that we pick up a term $e^{2\pi i/n}$. So we have to consider n-copies of the slit complex plane. On every of the this copies, the n-*th* root is single-valued and on the k-*th* copy defined as $|r|^{1/n}e^{i\varphi/n}e^{2i\pi k/n}$. For $n = \pm 2$, the two copies are depicted in fig. 7.2(a). They are referred to as *Riemann sheets*. Here, the solid line corresponds to the path on the Riemann sheet, while the dashed line presents the a path on the other. By crossing the branch-cut, we go from one sheet to the other and by going once counterclockwise over it and then clockwise back again, we did not pick up anything. By tracking a continuous path which crosses the branch cuts we avoided multivaluedness at the of defining multiple sheets on which we have single valued determinations. By gluing the boundaries of the sheets we obtain the *Riemann surface* (M) on which we have the single valued function $\tilde{f} : M \to \mathbb{C}$. The in-between stage of the gluing process is depicted in fig. 7.2(b) where the blue line corresponds to the lifted path $\tilde{\gamma}$. By gluing together the remaining upper and lower cuts we obtain the Riemann surface of the root shown in fig. 7.3, which corresponds to $\mathbb{C}\backslash 0$.

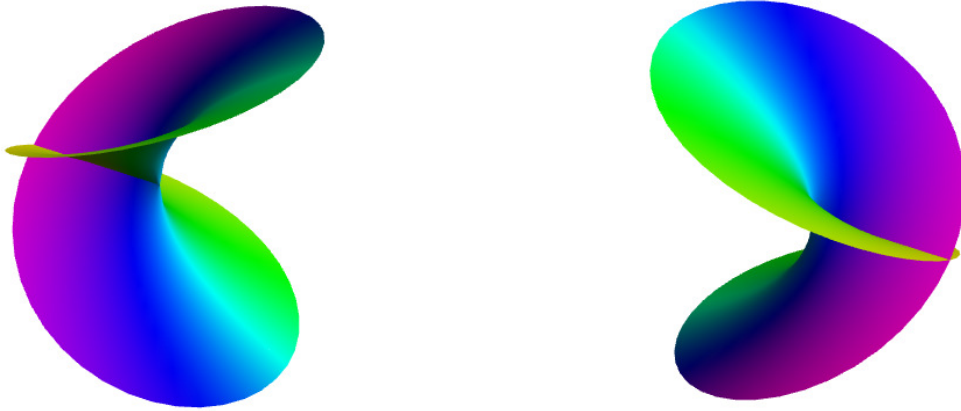Figure 7.3: Representation of the Riemann surface of the root function. The picture was created by usage of the presented Mathematica code in [114].

On Elliptic Curves

In the previous paragraph we sketched the notion of Riemann sheets and Riemann surfaces as possible options to define a single valued determination of multivalued functions in $\mathbb{C}$. The object of interest for the solution of the sunrise integral will be an elliptic curve [9]. An elliptic curve can be presented as a non-singular cubic[10] in $\mathbb{P}^2(\mathbb{C})$, which can be reduced to the form

$$Y^2 Z = 4X^3 - g_2 X Z^2 - g_3 Z^3 \ . \tag{7.3.5}$$

Indeed, every non-singular cubic in $\mathbb{P}^2(\mathbb{C})$ can be reduced to that form.[11] A dehomogenization to the chart $Z = 1$ yields the so-called Weierstraß form of the elliptic curve

$$y^2 = 4x^3 - g_2 x - g_3 \tag{7.3.6}$$

in the affine space. Factoring the polynomial yields

$$y^2 = (x - e_1)(x - e_2)(x - e_3) \tag{7.3.7}$$

in which the roots are manifest and furthermore $e_1 + e_2 + e_3 = 0$. By considering the Möbius transformation $M_{ij} : x \to x_{ij} = (x - e_i)/(e_j - e_i)$, which sends the root e_i to zero, the root e_j to one and e_k to $\lambda_{ijk} = (e_k - e_i)/(e_j - e_i)$ we get the Legendre form of the elliptic curve

$$y_{ij}^2 = x_{ij} \left(x_{ij} - 1 \right) \left(x_{ij} - \lambda_{ijk} \right) \tag{7.3.8}$$

---

[9]See e.g. [115] for an extensive overview on the here sketched subjects.

[10]three distinct roots

[11]One can use e.g. SageMath's [116] *WeierstrassForm* which brings any cubic in $\mathbb{P}^2(\mathbb{C})$ into Weierstraß form and gives the transformation into the weighted projective space $\mathbb{P}^2[2, 3, 1]$.

(a) two sheets

(b) glued together
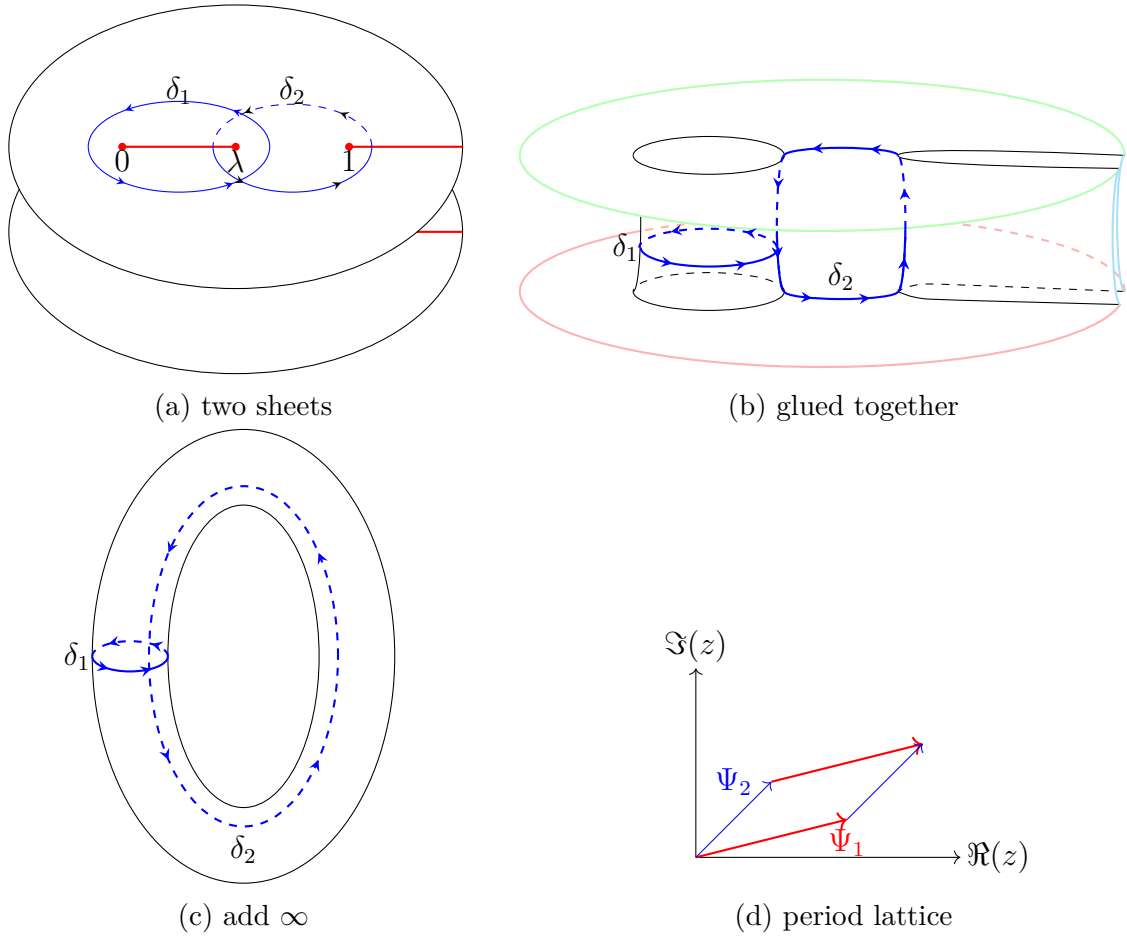
(c) add ∞

(d) period lattice

Figure 7.4: The gluing process of the function $y^2 = (x - e_1)(x - e_2)(x - e_3)$. Represented in (a), the two sheets with a branch-cut choice. The gluing of the branch-cut yields (b), where same colored boarders are identified by adding ∞. Gluing identified edges yields the torus depicted in (c). (d) shows a lattice of which identifying same colored periods yield a torus.

where $y_{ij} = y \, (a_j - a_i)^{-3/2}$. Starting from the Weierstraß form, there are six possible Legendre forms which can be obtained by different mappings of the roots.[12] The associated λ's are not independent[13] and one finds

$$\lambda_{jik} = 1 - \lambda_{ijk} \quad \lambda_{ikj} = \tfrac{1}{\lambda_{ijk}} \quad \lambda_{jki} = \tfrac{1}{1 - \lambda_{ijk}} \quad \lambda_{kij} = \tfrac{\lambda_{ijk} - 1}{\lambda_{ijk}} \quad \lambda_{kji} = \tfrac{\lambda_{ijk}}{\lambda_{ijk} - 1} \; . \qquad (7.3.9)$$

A third representation of elliptic curves is referred to as Jacobi form

$$\eta_{ij}^2 = (1 - \xi_{ij})(1 - \lambda_{ijk}\xi_{ij}^2) \; . \qquad (7.3.10)$$

This representation can be obtained e.g. from the Legendre form (7.3.8) by the transformation $x_{ij} = \xi_{ij}^{-2}$ and $\eta_{ij} = y_{ij}\xi_{ij}^{-3}$.

---

[12]This is just the action of the permutation group S_3 on e_i, e_j and e_k.

[13]That can be helpful if one wants to work e.g. with $0 < \lambda < 1$ and a branch-cut choice depicted in 7.4.

To study the Riemann surface associated to the elliptic curve in e.g. Legendre form (7.3.8) we have to consider the function

$$y = \sqrt{x\,(x-1)\,(x-\lambda)}\ . \tag{7.3.11}$$

This function is multivalued in $\mathbb{C}$ and, in analogy to the square root in the previous paragraph, we have to consider a two sheeted cover minus some cuts.[14] The branching points are 0, λ, 1 and ∞. A possible branch-cut choice is given by the line segments connecting 0, λ and 1, ∞ as depicted in fig. 7.4a, where the determination of y on the sheets differs by a sign. By opening the cuts, identifying the lips in which the root goes from one sheet to the other without a sign change and gluing them together we arrive at fig. 7.4b.[15] If the sheets of y are considered to be $\mathbb{C} \cup \{\infty\} \simeq \mathbb{P}^1(\mathbb{C})$[16], the same coloured boundaries have to be glued together. The resulting Riemann surface is the torus depicted in 7.4c minus four points associated to the roots e_i and ∞.

We may ask, if there is a map $f : \mathbb{C} \to \mathbb{P}^2(\mathbb{C})$ with $f(z) = (F_1(z), F_2(z), 1)$ which can be used to determine the parametrization of the cubic in $\mathbb{P}^2(\mathbb{C})$ such that the image of that map is a torus (our Riemann surface). Such a map exists and to visualize how it works, we consider the lattice depicted in fig. 7.4d. This lattice has two *periods* Ψ_1 and Ψ_2. If the function f is periodic with respect to the lattice, that means we identify all points $z + n_1\Psi_1 + n_2\Psi_2$ with $n_i \in \mathbb{Z}$, we obtain a torus. The function is then called *double periodic*. If it is furthermore meromorphic it is called *elliptic*. The mapping can be visualized by considering the *fundamental parallelogram* in fig. 7.4d. By identifying the blue coloured edges Ψ_2 and gluing them together one obtains a tube. Gluing together the boundary of the tube associated to the red coloured Ψ_1 yields a torus depicted in fig. 7.4c, where now δ_1 and δ_2 are "replaced" by Ψ_1 and Ψ_2. Another representation of the elliptic curve $\mathcal{E}$ is therefore $\mathcal{E} = \mathbb{C}/(\Psi_1\mathbb{Z} + \Psi_2\mathbb{Z}) \simeq \mathbb{C}/(\tau\mathbb{Z} + \mathbb{Z})$ with $\tau = \Psi_2/\Psi_1 \in \mathbb{H}$, where $\mathbb{H}$ denotes the upper half-plane.

One possible elliptic function with $f : \mathbb{C} \to \mathbb{P}^2(\mathbb{C})$ is the *Weierstraß $\wp$-function*

$$\wp(z; \Lambda) = \frac{1}{z^2} + \sum_{w \neq 0} \left(\frac{1}{(z-w)^2} - \frac{1}{w^2} \right)\ , \tag{7.3.12}$$

where the sum is over all non-zero lattice points in $\Lambda = \{n_1\Psi_1 + n_2\Psi_2 | n_1, n_2 \in \mathbb{Z}\}$. With respect to the fundamental parallelogram $\tilde{\Psi}_1 = 1$ and $\tilde{\Psi}_2 = \tau$ one has $\wp(z; \Psi_1, \Psi_2) = \frac{\wp(\frac{z}{\Psi_1}; \frac{\Psi_2}{\Psi_1} = \tau)}{\Psi_1^2}$. The parametrization of the elliptic curve in terms of the $\wp$-function is then

$$(\wp')^2 = 4\wp^2 - g_2\wp - g_3 \tag{7.3.13}$$

---

[14]For some notes on global, single-valued, continuous representatives of this particular case see paragraph 2 in [109].

[15]Notice that one of the sheets has to be rotated around the real axis to make the gluing from fig. 7.4a to fig. 7.4b without apparent "intersections" in three dimension.

[16]Consider for (7.3.5) the projection $p : \mathbb{P}^2(\mathbb{C})\backslash\{(0, 1, 0)\} \to \mathbb{P}^1(\mathbb{C})$, $(X, Y, Z) \mapsto (x, z)$. Then for $X - e_iZ \neq 0$, we have two solutions (points) in $\mathbb{P}^2(\mathbb{C})$ mapped to one point in $\mathbb{P}(\mathbb{C})$. For $\infty = (1, 0)$ there is only one solution of $X^3 = 0$ in $\mathbb{P}^2(\mathbb{C})$ namely $(0, 1, 0)$ and for $Z \neq 0$ and $Z/X = e_i$ we have the one solution $(X/Z = e_i, 0, 1)$. If from $\mathbb{P}^1(\mathbb{C})$ the points e_i and ∞ are excluded then all points in $\mathbb{P}^1(\mathbb{C})$ have to preimages in $\mathbb{P}^2(\mathbb{C})$. By considering the affine chart $Z = 1$ first, we have a projection of (7.3.5) on $\mathbb{P}^1(\mathbb{C})$ with $(x, y) \mapsto x$. In that sense, the figure 7.4b is to be understood as the two preimages of the curve (7.3.5) in $\mathbb{P}^1(\mathbb{C})$ lifted to $\mathbb{P}^2(\mathbb{C})$.

with

$$\wp'(z; \Lambda) = -2 \sum_w \frac{1}{(z - w)^3} \tag{7.3.14}$$

by setting $x = \wp(z)$ and $y = \wp'(z)$ for a suitable lattice. The sum in $\wp'$ is over all lattice points and it clearly is double-periodic as well. The map from the torus (Riemann surface) $f : \mathbb{C}/\Lambda \to \mathbb{P}^2(\mathbb{C})$ can be defined as (see e.g. [115] p. 37)

$$z \mapsto \begin{cases} (\wp(z), \wp'(z), 1) & z \neq 0 \\ (z^3 \wp(z), z^3 \wp'(z), z^3) = (0, 1, 0) & z = 0 \ . \end{cases} \tag{7.3.15}$$

The periods of the elliptic curve, which span the fundamental parallelogram depicted in 7.4d are the integrals of the holomorphic one-form $\eta = \mathrm{d}x/y$ along the contours δ_i depicted in fig. 7.4 and one finds

$$\Psi_i = \int_{\delta_i} \eta \ . \tag{7.3.16}$$

These contour integrals can be transformed into integrals proportional to complete elliptic integrals $K(k)$ and $K(k')$ with

$$K(k^2) = \int\limits_0^1 \frac{\mathrm{d}t}{\sqrt{1 - t^2}\sqrt{1 - k^2 t^2}} \tag{7.3.17}$$

and $k'^2 = 1 - k^2$ with

$$iK(k'^2) = \int\limits_1^{k^{-1}} \frac{\mathrm{d}t}{\sqrt{1 - t^2}\sqrt{1 - k^2 t^2}} = \frac{1}{i} \int\limits_1^{k^{-1}} \frac{\mathrm{d}t}{\sqrt{1 - t^2}\sqrt{1 - k'^2 t^2}} \ . \tag{7.3.18}$$

For the period Ψ_2 the mapping can be done directly by going from the Weierstraß- (7.3.6) to the Legendre- (7.3.8)[17] to the Jacobi-form (7.3.10) and identifying the resulting integral $\propto K(k')$ with $k'^2 = 1 - \lambda$. For the period Ψ_1 the first transformation is from Weierstraß- to Legendre-from. Then one can use, that the (e.g. clockwise) oriented integral along a contour encircling 0 and λ is the same as the (e.g. counter-clockwise) oriented integral encircling 1 and ∞[18]. Following with the translation[19] to line integrals and a transformation in the Jacobi-form (7.3.10) yields an integral $\propto K(k)$ with $k^2 = \lambda$. The advantage of working with $K(k)$ and $K(k')$ instead of the integrals along the contours δ_i is their implementation and fast numerical evaluation in established computer programs.

Given the periods Ψ_i obtained by evaluating the contour integrals, there is another representation of elliptic curves called the Jacobi uniformization. Here one considers

---

[17]Here, e.g. $\lambda = \lambda_{132}$ can be used for an root ordering with $e_1 < e_2 < e_3$.

[18]That is e.g. done by working in sheets $\mathbb{P}^1(\mathbb{C}) \simeq \mathrm{S}^1$ and deforming the contour "behind" the sphere with a continuously defined one-form $\propto \mathrm{d}x/(\sqrt{x}\sqrt{x - \lambda}\sqrt{x - 1})$ as e.g. defined in [109] and noticing, that it picks up an additional minus sign for $x > \lambda$.

[19]Notice that the one-form differs by a sign above and below the cuts (and on the different sheets for δ_2) and therefore $\int_\gamma \eta = 2 \int_{a_i}^{a_j} dx/y$ where a_i and a_j are branch-points.

the exponential map $z \mapsto e^{i\pi z} = w$ with $\mathbb{C} \to \mathbb{C} - \{0\} = \mathbb{C}^*$. The lattice $\Lambda = \mathbb{Z} + \mathbb{Z}\tau$ in $\mathbb{C}$ is mapped to $q^{2\mathbb{Z}}$ in $\mathbb{C}^*$, where the variable $q = e^{i\pi\tau}$ is called the *nome* and since $\tau = \Psi_2/\Psi_1 \in \mathbb{H}$ one has $|q| < 1$. Hence one has the isomorphism $\mathcal{E}_\tau = \mathbb{C}/\Lambda_\tau \to \mathbb{C}^*/q^{2\mathbb{Z}}$. The functions associated to this representation are the so-called four *Jacobi ϑ-functions*.[20]

To conclude this paragraph let us summarize its main takeaways:

- Defining a single valued determination of a complex valued function can be done by introducing branch-cuts or its Riemann-surface.

- An elliptic curve can be presented as a non-singular cubic $y^2 = ax^3 + bx + c$. Its Riemann surface is a torus.

- Therefore one can represent an elliptic curve as $\mathbb{C}/\Lambda$ or $\mathbb{C}^*/q^{2\mathbb{Z}}$

- The the periods of the elliptic curve $\Psi_i = \int_{\delta_i} \mathrm{d}x/y$ are associated to the lattice Λ. Associated to its Jacobi uniformization is the nome $q = e^{i\pi\Psi_1/\Psi_2}$.

7.3.2 The Solution of the Equal Mass Sunrise in Terms of Elliptic Polylogarithms in $D = 2 - 2\varepsilon$

The results of the previous section will be important for the sunrise topology (see fig. 7.1), which has two master integrals. For these two MI the first order system of differential equations of the Laurent coefficients can not be decoupled at order $\mathcal{O}(\varepsilon^k)$. Instead, there is a second order differential equation for the MI $I_{1,1,1}$. This second order differential equation has been obtained in [118] firstly by using the properties of the Feynman integral and reads in $D = 2 - 2\varepsilon$ and the Euclidean regime $p_\mu p^\mu < 0$

$$L_t^{\mathrm{homo}}\mathcal{I}_{1,1,1}^{(k)} = \underbrace{L_t^{(1)}\mathcal{I}_{1,1,1}^{(k-1)} + L_t^{(2)}\mathcal{I}_{1,1,1}^{(k-2)} + L_t^{\mathrm{tad}}\mathcal{I}_{1,1,0}^{(k-2)}}_{\text{inhomogeneous part}} \qquad (7.3.19)$$

with $t = p_\mu p^\mu/m^2$ and

$$L_t^{\mathrm{homo}} = \frac{\mathrm{d}^2}{\mathrm{d}t^2} + \left(\frac{1}{t} + \frac{1}{t-1} + \frac{1}{t-9}\right)\frac{\mathrm{d}}{\mathrm{d}t} + \left(-\frac{1}{3t} + \frac{1}{4(t-1)} + \frac{1}{12(t-9)}\right) \qquad (7.3.20)$$

$$L_t^{(1)} = \left(-\frac{2}{t-1} + \frac{1}{t} - \frac{2}{t-9}\right)\frac{\mathrm{d}}{\mathrm{d}t} + \left(-\frac{1}{4(t-1)} + \frac{5}{9t} - \frac{11}{36(t-9)}\right) \qquad (7.3.21)$$

$$L_t^{(2)} = \left(\frac{1}{2(t-1)} - \frac{2}{9t} - \frac{5}{18(t-9)}\right) \qquad (7.3.22)$$

$$L_t^{\mathrm{tad}} = \frac{\mu^2}{m^2}\left(-\frac{3}{4(t-1)} + \frac{2}{3t} + \frac{1}{12(t-9)}\right) . \qquad (7.3.23)$$

The equal mass sunrise is UV-finite in $D = 2 - 2\varepsilon$ and its expansion starts at order ε^0. The "squared" tadpole $I_{1,1,0}$ in $D = 2 - 2\varepsilon$ is $\propto \Gamma(\varepsilon)^2$ (see appendix (A.0.1)) and therefore

---

[20]For a review of these functions see e.g. [117] chap. 10.

starts at order $\mathcal{O}(\varepsilon^{-2})$. A suitable boundary value for the special solution is e.g. $t = 0$, since the result for the Laurent expansion of the vacuum sunrise $I_{1,1,1}(0)$ can be found in the literature [104, 119–121][21].

The Related Family of Elliptic Curves

An analytic solution of the differential equation (7.3.19) has been obtained already in [26] by relating the homogeneous deq to a known differential of special functions (elliptic integrals). By using a variation of the constant (7.2.7), the obtained solution is in terms of integrals over elliptic integrals.

Two more (similar) analytic solutions have been computed to order ε^0 in [110] and to "all-orders"[22] in [107]. Here, some key points of the solution in [107] are recalled.

The parametric representation of the sunrise integral in $D = 2 - 2\varepsilon$-dimensions is

$$I_{1,1,1} = \Gamma(1 + 2\varepsilon)(\frac{\mu^2}{m^2})^{1+2\varepsilon} \int_0^\infty \delta(1 - (x_1 + x_2 + x_3)) \frac{\mathcal{U}^{3\varepsilon}}{\mathcal{F}^{1+2\varepsilon}} \mathrm{d}x_1 \mathrm{d}x_2 \mathrm{d}x_3 \qquad (7.3.24)$$

with

$$\mathcal{U} = (x_1 x_2 + x_1 x_3 + x_2 x_3) \ , \qquad (7.3.25)$$
$$\mathcal{F} = (x_1 x_2 + x_1 x_3 + x_2 x_3)(x_1 + x_2 + x_3) - t x_1 x_2 x_3 \qquad (7.3.26)$$

and $t = p_\mu p^\mu / m^2$. Rewriting this integral as a projective integral[23] yields

$$I_{1,1,1} = \Gamma(1 + 2\varepsilon)(\frac{\mu^2}{m^2})^{1+2\varepsilon} \int_\sigma \frac{\mathcal{U}^{3\varepsilon}}{\mathcal{F}^{1+2\varepsilon}} \omega \qquad (7.3.27)$$

with

$$\omega = x_1 \mathrm{d}x_2 \wedge \mathrm{d}x_3 + x_2 \mathrm{d}x_3 \wedge \mathrm{d}x_1 + x_3 \mathrm{d}x_1 \wedge \mathrm{d}x_2 \qquad (7.3.28)$$

and the integration domain

$$\sigma = \left\{ [x_1 : x_2 : x_3] \in \mathbb{P}^2 | x_i > 0, i = 1, 2, 3 \right\} \ . \qquad (7.3.29)$$

We notice, that the graph polynomial $\mathcal{F}$ is a cubic in $\mathbb{P}^2(\mathbb{C})$, so that it's zero locus for a given t_0 defines an elliptic curve.[24]

The Weierstraß equation of the family of elliptic curves which varies with t is defined by $\mathcal{F} = 0$ and given as

$$\begin{aligned} y^2 &= 4x^3 - g_2(t)x - g_3(t) \\ &= 4(x - e_1(t))(x - e_2(t))(x - e_3(t)) \end{aligned} \qquad (7.3.30)$$

---

[21]The computation of this boundary is related to a connection between a massless one-loop three-point function and two-loop vacuum functions [119]. The results for the three point function can be found in [120, 121] and the explicit change of variables to the case at hand in [104].

[22]An algorithm for the analytic computation of an arbitrary Laurent coefficient has been obtained and the first three coefficients are explicitly given in the appendix therein.

[23]See comment 5 and references therein and eq's (7)-(10) in [107] for that particular case.

[24]A motivation for considering the zero locus of $\mathcal{F}$ can be found in [93] and [85].

with

$$g_2(t) = \frac{m^8}{12\mu^8} \left(3 - t\right) \left(3 - 3t + 9t^2 - t^3\right), \tag{7.3.31}$$

$$g_3(t) = \frac{m^{12}}{216\mu^{12}} \left(3 + 6t - t^2\right) \left(9 - 36t + 30t^2 - 12t^3 + t^4\right). \tag{7.3.32}$$

and

$$e_1(t) = \frac{m^4}{24\mu^4} \left(-t^2 + 6t + 3 + 3\left(1 - t\right)^{\frac{3}{2}} \left(9 - t\right)^{\frac{1}{2}}\right), \tag{7.3.33}$$

$$e_2(t) = \frac{m^4}{24\mu^4} \left(-t^2 + 6t + 3 - 3\left(1 - t\right)^{\frac{3}{2}} \left(9 - t\right)^{\frac{1}{2}}\right), \tag{7.3.34}$$

$$e_3(t) = \frac{m^4}{24\mu^4} \left(2t^2 - 12t - 6\right). \tag{7.3.35}$$

The transformation of the non-singular cubic to the Weierstraß form can be either found in appendix A in [105] or by the usage of SageMath [116]. Hereby the roots are real and ordered as $e_2 < e_3 < e_1$ in the Euclidean region.

The periods associated to the family of elliptic curves are given by

$$\Psi_1 = \int_{\delta_1} \frac{\mathrm{d}x}{y} = 2\int_{e_2}^{e_3} \frac{\mathrm{d}x}{y} = \frac{4\mu^2}{m^2(1 - t)^{\frac{3}{4}}(9 - t)^{\frac{1}{4}}} K(k^2) \tag{7.3.36}$$

and

$$\Psi_2 = \int_{\delta_2} \frac{\mathrm{d}x}{y} = 2\int_{e_1}^{e_3} \frac{\mathrm{d}x}{y} = \frac{4i\mu^2}{m^2(1 - t)^{\frac{3}{4}}(9 - t)^{\frac{1}{4}}} K(k'^2) \tag{7.3.37}$$

where $y = -2\sqrt{x - e_1(t)}\sqrt{x - e_2(t)}\sqrt{x - e_3(t)}$ and

$$k^2 = \lambda_{213} = \frac{e_3(t) - e_2(t)}{e_1(t) - e_2(t)}, \qquad k'^2 = 1 - k^2 = \frac{e_1(t) - e_3(t)}{e_1(t) - e_2(t)} \tag{7.3.38}$$

denote the parameter and the complementary parameter of the elliptic integral K of the first kind (7.3.17),(7.3.18). The integration cycle δ_i are chosen such that δ_1 encircles e_2 and e_3 counterclockwise and δ_2 goes around e_3 and e_1 in clockwise direction.

The two periods Ψ_i satisfy the differential equation

$$\left[\frac{\mathrm{d}^2}{\mathrm{d}t^2} + \left(\frac{1}{t} + \frac{1}{t - 1} + \frac{1}{t - 9}\right)\frac{\mathrm{d}}{\mathrm{d}t} + \left(-\frac{1}{3t} + \frac{1}{4(t - 1)} + \frac{1}{12(t - 9)}\right)\right]\Psi_i = L_t^{\mathrm{homo}}\Psi_i = 0 \tag{7.3.39}$$

and are therefore the two homogeneous solutions of the second order differential equation of the equal mass sunrise.[25] The same holds as well for the unequal mass case, as been used in [104].

---

[25] The periods of this particular family of elliptic curves have already been considered in the mathematical literature (see e.g. [122] [123]) and already known to mathematicians. In particular see [123] table 13, $N = 6$ (with $t \to t - 9$) for the Picard-Fuchs equation, table 9 with $N = 6$ for t as a modular form function of q and table 12, $N = 6$ for a homogeneous solution in terms of $_2F_1$.

By using (7.2.7) we may write the solution of the sunrise in the general form

$$I_{1,1,1}^{(k)}(t) = c_1\Psi_1(t) + c_2\Psi_2(t) + \int\limits_{t_0}^{t} \frac{\Psi_1(s)\Psi_2(t) - \Psi_1(t)\Psi_2(s)}{W(\Psi_1(s),\Psi_2(s))} b^{(k)}(s)\mathrm{d}s \qquad (7.3.40)$$

where the constants c_1, c_2 might be obtained by the comparison with the vacuum sunrise at $t_0 = 0$ and $b^{(k)}(s)$ is the r.h.s. from (7.3.19) for the k-th Laurent coefficient.

The Wronskian of the fundamental system can be easily obtained as [26]

$$W(\Psi_1(t),\Psi_2(t)) = \Psi_1(t)\frac{\mathrm{d}}{\mathrm{d}t}\Psi_2(t) - \Psi_2(t)\frac{\mathrm{d}}{\mathrm{d}t}\Psi_1(t) = -\frac{12i\pi\mu^4}{m^4}\frac{1}{t(t-1)(t-9)} \ . \qquad (7.3.43)$$

In the representation of the solution of the sunrise in (7.3.40) it is obvious, that a solution might be written as iterated integral over elliptic integrals of the first kind, since the integrand involves the homogeneous solutions Ψ_i.

7.3.3 Upshot of the Integration Algorithm by Adams, Bogner, Weinzierl

The approach by Adams, Bogner and Weinzierl [107] however has three mayor points, which simplify the solution drastically. They can be summarized as follows:[27]

1. There exists a basis transformation, such that the inhomogeneity $L_t^{(1)}\mathcal{I}_{1,1,1}^{(k-1)}$ in (7.3.19) can be removed without changing the homogeneous part.

2. The integration should not be performed with respect to the kinematic invariant t, but with respect to the nome q of the elliptic curve associated to the sunrise by $\mathcal{F} = 0$.

3. There exists a certain type of q-series in which a complete solution of the sunrise at arbitrary order can be expressed.

The Basis Transformation

The basis transformation used in [107] in $D = 2 - 2\varepsilon$ reads

$$I_{1,1,1}(t,\varepsilon) = \Gamma(\varepsilon+1)^2 \left(\frac{\mu^2}{m^2}\right)^\varepsilon \left(\frac{3\sqrt{y}}{(y-1)(y-9)}\right)^\varepsilon \tilde{I}_{1,1,1}(t,\varepsilon) \ . \qquad (7.3.44)$$

---

[26] By using

$$\frac{\mathrm{d}}{\mathrm{d}t}K(\lambda(t)) = \frac{\lambda'(t)(E(\lambda(t)) - (1-\lambda(t))K(\lambda(t)))}{2(1-\lambda(t))\lambda(t)} \qquad (7.3.41)$$

and the Legendre relation

$$K(1-\lambda)E(\lambda) + K(\lambda)E(1-\lambda) - K(\lambda)K(1-\lambda) = \frac{\pi}{2} \qquad (7.3.42)$$

where E denotes the complete elliptic integral of the second kind and λ the parameter.

[27]The point 2.) and 3.) have been treated similarly already in [110].

65

The second order differential equation fulfilled by $\tilde{I}_{1,1,1}$[28] is

$$L_t^{\text{homo}}\tilde{I}_{1,1,1}(t,\varepsilon) = \varepsilon^2 \tilde{L}_t^{(2)}\tilde{I}_{1,1,1}(t,\varepsilon) + \tilde{b}_{t,\varepsilon}^{\text{tad}} \tag{7.3.45}$$

where L_t^{homo} is given in (7.3.20),

$$\tilde{L}_t^{(2)} = -\left(\frac{m^2}{\mu^2}\right)^4 \frac{(t+3)^4}{576\pi^2} W^2\left(\Psi_1(t),\Psi_2(t)\right) \tag{7.3.46}$$

$$\tilde{b}_{t,\varepsilon}^{\text{tad}} = \frac{i}{2\pi}\frac{m^2}{\mu^2}\left(\frac{m^2}{\mu^2}\frac{3\sqrt{t}}{(t-9)(t-1)}\right)^{-\varepsilon} W\left(\Psi_1(t),\Psi_2(t)\right) \tag{7.3.47}$$

and $W\left(\Psi_1(t),\Psi_2(t)\right)$ denotes the Wronskian (7.3.43), which remains the same, since the fundamental system has not changed. Furthermore, in (7.3.45) the explicit result of the tadpole squared (A.0.1)

$$I_{1,1,0} = \Gamma(\varepsilon)^2 \left(\frac{\mu^2}{m^2}\right)^{2\varepsilon} \tag{7.3.48}$$

has been inserted.

The differential equation for the *k-th* Laurent coefficient is

$$L_t^{\text{homo}}\tilde{\mathcal{I}}_{1,1,1}^{(k)} = \tilde{L}_t^{(2)}\left(\sum_{i=1,2}\Psi_i(t)E_i^{(k-2)}(t)\right) + \frac{i}{2\pi}\frac{m^2}{\mu^2}W\left(\Psi_1(t),\Psi_2(t)\right)\frac{\log^k\left(\frac{\mu^2}{m^2}\frac{(t-9)(t-1)}{3\sqrt{t}}\right)}{k!} \tag{7.3.49}$$

where we used, that the periods are prefactors in the lower order coefficients due to (7.3.40). The general solution might be written as

$$\tilde{\mathcal{I}}_{1,1,1}^{(k)} = \tilde{c}_1\Psi_1(t) + \tilde{c}_2\Psi_2(t) + \sum_{i=1,2}(-1)^{i+1}\Psi_i(t)\left(\int_{t_0}^t \frac{\Psi_{k\neq i}(s)}{W\left(\Psi_1(s),\Psi_2(s)\right)}\tilde{L}_s^{(2)}\left(\sum_{j=1,2}\Psi_j(s)E_j^{(k-2)}(s)\right)\mathrm{d}s\right.$$

$$+ \frac{i}{2\pi}\frac{m^2}{\mu^2}\int_{t_0}^t \frac{\Psi_{k\neq i}(s)}{W\left(\Psi_1(s),\Psi_2(s)\right)}W\left(\Psi_1(s),\Psi_2(s)\right)\frac{\log^k\left(\frac{\mu^2}{m^2}\frac{(s-9)(s-1)}{3\sqrt{s}}\right)}{k!}\mathrm{d}s\Bigg)$$

$$= \tilde{c}_1\Psi_1(t) + \tilde{c}_2\Psi_2(t)$$

$$- \sum_{i=1,2}(-1)^{i+1}\Psi_i(t)\left(\left(\frac{m^2}{\mu^2}\right)^4\int_{t_0}^t \frac{\Psi_{k\neq i}(s)(s+3)^4}{576\pi^2}W\left(\Psi_1(s),\Psi_2(s)\right)\left(\sum_{j=1,2}\Psi_j(s)E_j^{(k-2)}(s)\right)\mathrm{d}s\right.$$

$$- \frac{i}{2\pi}\frac{m^2}{\mu^2}\int_{t_0}^t \Psi_{k\neq i}(s)\frac{\log^k\left(\frac{\mu^2}{m^2}\frac{(s-9)(s-1)}{3\sqrt{s}}\right)}{k!}\mathrm{d}s\Bigg) \ . \tag{7.3.50}$$

---

[28]Notice that $\tilde{I}_{1,1,1}$ has a logarithmic singularity at the boundary point $t = 0$. Since we will not compute it here however, for the treatment of this singularity and the boundary conditions is referred to [107].

The Class of Functions - Elliptic Generalization of Polylogarithms

In (7.3.50) the solution is given in terms of the kinematic invariant. With respect to the family of the elliptic curve, this is the parameter in which it varies. By solving the integral with respect to this parameter the variation will still be manifest but we neglect in a way the additional knowledge about the structure of the result. The solution should inherit directly the properties of the elliptic curve describing its homogeneous part. Therefore it is natural to ask, if the result can be formulated in terms of the period ratio $\tau = \Psi_2/\Psi_1 \in \mathbb{H}$ associated to the representation $\mathcal{E}_t = \mathbb{C}/\lambda_t$ or in terms of the nome $q = e^{i\pi\tau}$ associated to the Jacobi uniformization $\mathcal{E}_t = \mathbb{C}^*/q_t^{2\mathbb{Z}}$. Hereby the advantage of a formulation in terms of the nome is that it gives rise to a formulation in terms of power series, since $|q| < 1$. That approach has first been pursued in [110], where the first order of the massive sunrise in $D = 2 - 2\varepsilon$ has been solved in terms of *elliptic dilogarithms*, a generalization of the dilogarithm associated to the power series representation (6.2.25) in section 6.2.2. In the work [104–107, 124] this approach has been generalized and was used to compute the sunrise with arbitrary masses, the equal mass sunrise and the kite integral (the latter two to all orders). In the following the two points of interest are:

1. What is a suitable class of functions?

2. Can every integration of the sunrise be performed in this class of functions?

The Building Block $\mathrm{ELi}_{n;m}(x;y;q)$ and Its Properties

Adams et al defined the following series

$$\mathrm{ELi}_{n;m}(x;y;q) = \sum_{j=1}^{\infty} \sum_{k=1}^{\infty} \frac{x^j}{j^n} \frac{y^k}{j^k} q^{jk} \qquad \text{with } n, m \in \mathbb{Z}; \ x, y, q \in \mathbb{C}; \ |q| < 1 \ . \qquad (7.3.51)$$

Recalling the classical polylogarithm

$$\mathrm{Li}_n(x) = \sum_{j=1}^{\infty} \frac{x^j}{j^n} \ , \qquad (7.3.52)$$

we see, that the ELi-series corresponds to a product of classical polylogarithms "coupled" by a third variable which will later be associated to the nome q of an elliptic curve. This series has the property that the integral

$$\int_0^q \mathrm{ELi}_{n;m}(x;y;q') \frac{\mathrm{d}q'}{q'} = \mathrm{ELi}_{n+1;m+1}(x;y;q) \qquad (7.3.53)$$

will stay in this class of functions, analogously to the iterated integration of the classical polylogarithm with the one form $\mathrm{d}x/x$. By investigation of the sum one furthermore finds [105] the reflection formula

$$\mathrm{ELi}_{n;m}(x;y;-q) =$$
$$\frac{1}{2}\left(\mathrm{ELi}_{n;m}(x;y;q) + \mathrm{ELi}_{n;m}(x;-y;q) + \mathrm{ELi}_{n;m}(-x;y;q) - \mathrm{ELi}_{n;m}(-x;-y;q)\right) \ .$$
$$(7.3.54)$$

67

The Generalization $\mathrm{ELi}_{\vec{n};\vec{m};2\vec{o}}(\vec{x};\vec{y};q)$ and Its Properties

The generalization of this series is based on the consideration of the integral

$$\int\limits_0^q \mathrm{ELi}_{n_1;m_1}(x_1;y_1;q')\,\mathrm{ELi}_{n_2;m_2}(x_2;y_2;q')\,\frac{\mathrm{d}q'}{q'} = \int\limits_0^q \sum_{j_1,j_2,k_1,k_2>0} \frac{x_1^{j_1}}{j_1^{n_1}}\frac{x_2^{j_2}}{j_2^{n_2}}\frac{y_1^{k_1}}{k_1^{m_1}}\frac{y_2^{k_2}}{k_2^{m_2}}q'^{j_1k_1+j_2k_2}\frac{\mathrm{d}q'}{q'}$$

$$= \sum_{j_1,j_2,k_1,k_2>0} \frac{x_1^{j_1}}{j_1^{n_1}}\frac{x_2^{j_2}}{j_2^{n_2}}\frac{y_1^{k_1}}{k_1^{m_1}}\frac{y_2^{k_2}}{k_2^{m_2}}\frac{q^{j_1k_1+j_2k_2}}{(j_1k_1+j_2k_2)}$$

$$(7.3.55)$$

which is not in the class of $\mathrm{ELi}_{n,m}$-series.

Therefore one defines functions of $(2l+1)$ variables $x_1,\ \ldots,\ x_l,\ y_1,\ \ldots,\ y_l,\ q$ as follows:
For $l=1$ one has:

$$\mathrm{ELi}_{n;m}(x;y;q) = \sum_{j=1}^{\infty}\sum_{k=1}^{\infty}\frac{x^j}{j^n}\frac{y^k}{k^m}q^{jk}. \qquad (7.3.56)$$

For $l>1$ one defines:

$$\mathrm{ELi}_{n_1,\ldots,n_l;m_1,\ldots,m_l;2o_1,\ldots,2o_{l-1}}(x_1,\ldots,x_l;y_1,\ldots,y_l;q) =$$

$$= \sum_{j_1=1}^{\infty}\cdots\sum_{j_l=1}^{\infty}\sum_{k_1=1}^{\infty}\cdots\sum_{k_l=1}^{\infty}\frac{x_1^{j_1}}{j_1^{n_1}}\cdots\frac{x_l^{j_l}}{j_l^{n_l}}\frac{y_1^{k_1}}{k_1^{m_1}}\cdots\frac{y_l^{k_l}}{k_l^{m_l}}\frac{q^{j_1k_1+\ldots+j_lk_l}}{\prod\limits_{i=1}^{l-1}\left(\sum\limits_i^l j_ik_i\right)^{o_i}}. \qquad (7.3.57)$$

The multiplication is then given as

$$\mathrm{ELi}_{n_1;m_1}(x_1;y_1;q)\mathrm{ELi}_{n_2,\ldots,n_l;m_2,\ldots,m_l;2o_2,\ldots,2o_{l-1}}(x_2,\ldots,x_l;y_2,\ldots,y_l;q) =$$

$$\mathrm{ELi}_{n_1,n_2,\ldots,n_l;m_1,m_2,\ldots,m_l;0,2o_2,\ldots,2o_{l-1}}(x_1,x_2,\ldots,x_l;y_1,y_2,\ldots,y_l;q)$$

$$(7.3.58)$$

and the integration becomes

$$\int\limits_0^q \frac{dq'}{q'}\mathrm{ELi}_{n_1,\ldots,n_l;m_1,\ldots,m_l;2o_1,2o_2,\ldots,2o_{l-1}}(x_1,\ldots,x_l;y_1,\ldots,y_l;q') =$$

$$\mathrm{ELi}_{n_1,\ldots,n_l;m_1,\ldots,m_l;2(o_1+1),2o_2,\ldots,2o_{l-1}}(x_1,\ldots,x_l;y_1,\ldots,y_l;q). \qquad (7.3.59)$$

Therefore one can multiply arbitrary ELi-functions by using partial integration.
All results computed in terms of this q-series can be expressed using a alternative representation [124]. Therefore one defines a prefactor c_n and a sign s_n, both depending on an index n by

$$c_n = \begin{cases} 1, & n \text{ even,} \\ i, & n \text{ odd,} \end{cases} \qquad\qquad s_n = \begin{cases} 1, & n \text{ even,} \\ -1, & n \text{ odd.} \end{cases} \qquad (7.3.60)$$

and at depth 1 linear combinations

$$\overline{\mathrm{E}}_{n;m}(x;y;q) = \frac{c_{n+m}}{i}\left[\mathrm{ELi}_{n;m}(x;y;q) - s_{n+m}\mathrm{ELi}_{n;m}(x^{-1};y^{-1};q)\right]. \qquad (7.3.61)$$

More explicitly, one has

$$\overline{\mathrm{E}}_{n;m}\left(x;y;q\right) = \begin{cases} \frac{1}{i}\left[\mathrm{ELi}_{n;m}\left(x;y;q\right) - \mathrm{ELi}_{n;m}\left(x^{-1};y^{-1};q\right)\right], & n+m \text{ even}, \\[2mm] \mathrm{ELi}_{n;m}\left(x;y;q\right) + \mathrm{ELi}_{n;m}\left(x^{-1};y^{-1};q\right), & n+m \text{ odd}. \end{cases} \tag{7.3.62}$$

At higher depth the functions

$$\overline{\mathrm{E}}_{n_1,\dots,n_l;m_1,\dots,m_l;2o_1,\dots,2o_{l-1}}\left(x_1,\dots,x_l;y_1,\dots,y_l;q\right) \tag{7.3.63}$$

are defined in analogy to the ELi-function as follows:
For $o_1 = 0$ we set

$$\overline{\mathrm{E}}_{n_1,\dots,n_l;m_1,\dots,m_l;0,2o_2,\dots,2o_{l-1}}\left(x_1,\dots,x_l;y_1,\dots,y_l;q\right) =$$
$$\overline{\mathrm{E}}_{n_1;m_1}\left(x_1;y_1;q\right)\overline{\mathrm{E}}_{n_2,\dots,n_l;m_2,\dots,m_l;2o_2,\dots,2o_{l-1}}\left(x_2,\dots,x_l;y_2,\dots,y_l;q\right). \tag{7.3.64}$$

For $o_1 > 0$ one has

$$\overline{\mathrm{E}}_{n_1,\dots,n_l;m_1,\dots,m_l;2(o_1+1),2o_2,\dots,2o_{l-1}}\left(x_1,\dots,x_l;y_1,\dots,y_l;q\right) =$$
$$\int_0^q \frac{dq'}{q'}\overline{\mathrm{E}}_{n_1,\dots,n_l;m_1,\dots,m_l;2o_1,2o_2,\dots,2o_{l-1}}\left(x_1,\dots,x_l;y_1,\dots,y_l;q'\right). \tag{7.3.65}$$

The eq. (7.3.64) corresponds to (7.3.58) such that the multiplication of $\overline{\mathrm{E}}$ at any depth can be obtained by partial integration. (7.3.65) corresponds to (7.3.59) and the sign reflection formula (7.3.54) holds for $\overline{\mathrm{E}}$ as well.

The $\overline{\mathrm{E}}$-functions are linear combinations of their building blocks, the ELi-functions, with the same indices. One can show [124] that an $\overline{\mathrm{E}}$-function of depth l can be expressed as a linear combination of 2^l ELi-functions by using

$$\overline{\mathrm{E}}_{n_1,\dots,n_l;m_1,\dots,m_l;2o_1,\dots,2o_{l-1}}\left(x_1,\dots,x_l;y_1,\dots,y_l;q\right) =$$
$$\sum_{t_1=0}^{1}\cdots\sum_{t_l=0}^{1}\left[\prod_{j=1}^{l}\frac{c_{n_j+m_j}}{i}\left(-s_{n_j+m_j}\right)^{t_j}\right]\mathrm{ELi}_{n_1,\dots,n_l;m_1,\dots,m_l;2o_1,\dots,2o_{l-1}}\left(x_1^{s_{t_1}},\dots,x_l^{s_{t_l}};y_1^{s_{t_1}},\dots,y_l^{s_{t_l}};q\right). \tag{7.3.66}$$

This class of functions has now the properties, that they are closed under multiplication, differentiation with respect to $q\mathrm{d}/\mathrm{d}q$ and integration with the one form $\mathrm{d}q/q$. They are therefore suited to describe iterated solution of certain Feynman integrals.

The Iterated Structure of the Sunrise

The $\overline{\mathrm{E}}$-functions will be the suitable class of generalized functions to express the sunrise to all orders and the nome of the underlying elliptic curve is a suitable variable. The transformation of the kinematic invariant to the nome, however, is rather technical. The same holds for the derivation of the integration kernels of (7.3.50) in terms of $\overline{\mathrm{E}}$. Since

they are crucial for the results of this thesis and not well covered in the literature I devoted the appendix B to their detailed, ab initio derivation. Every relation stated in the following will be explicitly computed therein, such that these approaches may be of use for future computations.

Taking the special solution of (7.3.50) we observe, that the whole solution at every order boils down to solving the two integrals

$$
I_1^{(k)} = \sum_{i=1,2} \int_{t_0}^{t} \Psi_{k \neq i}(s) \frac{\log^k \left(\frac{(s-9)(s-1)}{s} \right)}{k!} \, \mathrm{d}s \ , \tag{7.3.67}
$$

$$
I_2^{(k)} = \sum_{i=1,2} \int_{t_0}^{t} \Psi_{k \neq i}(s)(s+3)^4 W\left(\Psi_1(s), \Psi_2(s)\right) \left(\sum_{j=1,2} \Psi_j(s) E_j^{(k-2)}(s) \right) \mathrm{d}s \tag{7.3.68}
$$

since they are the non-trivial part of the special solution. Thereby we have $I_2^{(0)} = I_2^{(1)} = 0$, since there is no $1/\varepsilon$ coefficient in $D = 2 - 2\varepsilon$ and the integral $I_1^{(0)}$ is just an integral over the periods.

For a transformation to the nome, we need that the measure changes according to (see app. B.1.1)

$$
\mathrm{d}t = \frac{1}{i\pi} \frac{\Psi_{1,q}^2}{W_q(\Psi_1, \Psi_2)} \frac{\mathrm{d}q}{q} \ . \tag{7.3.69}
$$

Notice that further integrations will be performed with $\mathrm{d}q/q$, the one-form associated with iterated integration of $\overline{\mathrm{E}}$-functions. From now on the subscript q will denote, that the function should be considered as a function of q rather than the kinematic invariant. The second important detail is, that by expressing the periods as q-series (see app. B.1.3) one gets the relation

$$
\Psi_{2,q} \propto \log(q)\Psi_{1,q} \tag{7.3.70}
$$

which is inherited from a known transformation of the complete elliptic integrals. This singularity corresponds to a singularity of $\Psi_{2,t}$ at $t = 0$. Since we are only interested in the structure of the result we can assume that we perform a partial integration to remove the logarithm whenever needed, such that we only consider $\Psi_{1,q} =: \Psi_q$ in the following.[29] We therefore have to show, that the integrals

$$
\tilde{I}_1^{(k)}(q) = \int_{q_0}^{q} \frac{\Psi_{q'}^3}{W_{q'}(\Psi_1, \Psi_2)} \frac{\log^k \left(\frac{(s_{q'}-9)(s_{q'}-1)}{s_{q'}} \right)}{k!} \frac{\mathrm{d}q'}{q'} \tag{7.3.71}
$$

$$
\tilde{I}_2^{(k)}(q) = \int_{q_0}^{q} \Psi_{q'}^4 (s_{q'}+3)^4 E_j^{(k-2)}(q') \frac{\mathrm{d}q'}{q'} \tag{7.3.72}
$$

---

[29]The same approach holds for actual computations as well, but one has to consider e.g. boundary terms (see [105]) which, however, often do not matter since $\lim_{q \to 0} \log(q) \overline{\mathrm{E}}_{\vec{n},\vec{m},2\vec{\sigma}}(\vec{x}, \vec{y}, q) = 0$ because every $\overline{\mathrm{E}}$ series starts at order q.

always stay in the class of $\overline{\text{E}}$-functions. The first step to show this, is to obtain a q-series representation t_q for the kinematic invariant t. One finds (see appendix B.1.2 for a derivation)

$$t_q = -\frac{9q\left((q^3; -q^3)_\infty\right)^4 \left((q^6; q^6)_\infty\right)^4}{\left((q; -q)_\infty\right)^4 \left((q^2; q^2)_\infty\right)^4} \tag{7.3.73}$$

where

$$(a; q)_\infty = \prod_{k=0}^{\infty}(1 - aq^k) \tag{7.3.74}$$

denotes the q-Pochammer symbol. This representation holds for the complete Euclidian regime, where the periods are defined. One can write t_q in terms of Dedekind-η functions by using

$$\eta(\tau) = e^{\frac{i\pi\tau}{12}} \prod_{n=1}^{\infty}\left(1 - e^{2i\pi n\tau}\right) = q^{\frac{1}{12}} \prod_{n=1}^{\infty}\left(1 - q^{2n}\right) = q^{\frac{1}{12}}\left(q^2; q^2\right)_\infty . \tag{7.3.75}$$

to obtain the expression given in [107]. Starting from this expression one can derive all q-series representations of the integration kernels of the integrals (7.3.71) and (7.3.72). At order ε^0 one has to integrate

$$\tilde{I}_1^{(0)}(q) = \int_{q_0}^{q} \frac{\Psi_{q'}^3}{W_{q'}(\Psi_1, \Psi_2)} \frac{\mathrm{d}q'}{q'} . \tag{7.3.76}$$

Therefore one has to express the kernel in terms of $\overline{\text{E}}$-functions. The result (for a derivation see appendix B.1.4) is given by

$$\frac{\Psi_1^3}{W(\Psi_1, \Psi_2)} = -6i\pi^2 \frac{\mu^2}{m^2}\overline{\text{E}}_{-2,0}(-1, r_3, -q) , \tag{7.3.77}$$

where r_3 denotes the third root of unity. The integration of this kernel will yield an $\overline{\text{E}}$-function as well.

At order ε and every higher order we have to integrate the logarithms $\log(t_q)$, $\log(1 - t_q)$ and $\log(9 - t_q)$ in terms of $\overline{\text{E}}$-functions. We find (for a derivation see appendix B.1.7)

$$\log(t_q) = -4\overline{\text{E}}_{1;0}\left(r_3; -1; -q\right) + \log(-9q) \tag{7.3.78}$$

$$\log(1 - t_q) = 3(\overline{\text{E}}_{1;0}\left(-1; 1; -q\right) - \overline{\text{E}}_{1;0}\left(r_6; 1; -q\right)) \tag{7.3.79}$$

$$\log\left(1 - \frac{t_q}{9}\right) = 3\overline{\text{E}}_{1;0}\left(-1; 1; -q\right) + \overline{\text{E}}_{1;0}\left(r_6; 1; -q\right) - 4\overline{\text{E}}_{1;0}\left(r_3; 1; -q\right) \tag{7.3.80}$$

where r_6 denotes the sixth root of unity. The logarithmic singularity on the r.h.s. of (7.3.78) corresponds to the point $t = q = 0$. Since every of the logarithms can be expressed in terms of $\overline{\text{E}}$-functions every product of them is as well an $\overline{\text{E}}$-function. From that it follows, that the complete integration (7.3.71) can be performed in terms of $\overline{\text{E}}$-functions at every order in ε.

The second integral involves the lower order coefficients of the sunrise. The first enters the inhomogeneity at order ε^2. But from the discussion of the integral $\tilde{I}_1(q)$ we know that $E_q^{(0)}$ will be in the class of $\overline{\mathrm{E}}$-functions[30]. The only thing to show is, that the kernel $\Psi_q(t_q + 3)$ is an $\overline{\mathrm{E}}$-function. That this is the case is derived in appendix B.1.5 and one finds

$$\Psi_q(t_q + 3) = \frac{6\pi\mu^2}{m^2}\left(\frac{1}{\sqrt{3}} + 2\overline{\mathrm{E}}_{0,0}\left(1, r_3, -q\right)\right) \ . \tag{7.3.81}$$

From that fact it follows, that $E_q^{(2)}$ will be in the class of $\overline{\mathrm{E}}$-functions an therefore $E_q^{(k)}$ as well.

In the end, the *k-th* Laurent coefficient of the sunrise in $D = 2 - 2\varepsilon$ will have the form

$$S_{111}^{(k)} \propto \Psi_1 \times \left(\overline{\mathrm{E}} - functions\right) \ , \tag{7.3.82}$$

since it is finite at $t = 0$ and the period Ψ_2 is not. The explicit result may be taken from [107].

To summarize the results of this section we conclude firstly, that the sunrise is not expressible in terms of hyperlogarithms. Secondly it was demonstrated, that the "right" variable to consider for a solution of the sunrise is the nome q associated with the family of elliptic curves $\mathcal{E}_t$ defined by $\mathcal{F} = 0$ in Jacobi uniformization and not the kinematic invariant. The third important result is, that the equal mass sunrise integral can be computed to all orders in elliptic generalizations of polylogarithms, depending on the variable q.

---

[30]Keep in mind, that we factored the periods out.

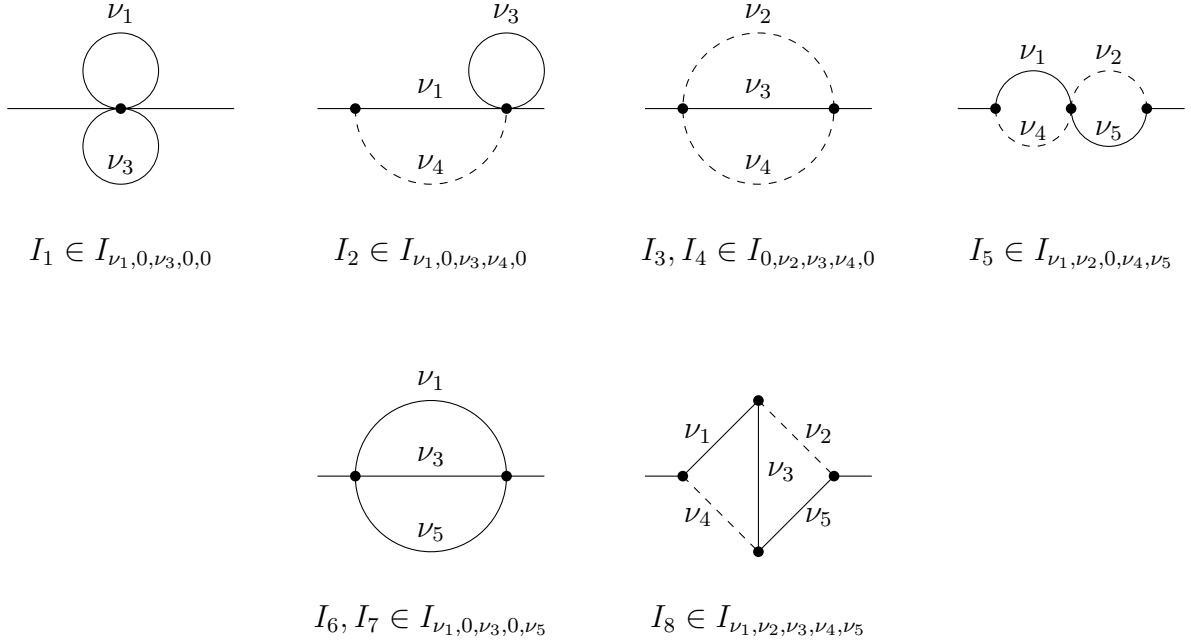## 7.4 The Iterated Solution of the Kite Integral in $D = 4 - 2\varepsilon$

Figure 7.5: The topologies contributing to the differential equation of the kite integral. The topologies in the upper row can be computed in a canonical basis, the ones in the lower row can not.

The class of elliptic generalizations of polylogarithms defined in the previous section were enough to compute the sunrise integral where one has otherwise a solution in terms of iterated integrals over elliptic integrals. The natural question is now, if the same class of functions and the same kind of variable change can be applied to other integrals as well. We addressed this question in a joint work with Luise Adams, Christian Bogner and Stefan Weinzierl [124] by computing the kite integral for which an analytical solution in terms of integrals over complete elliptic integrals was previously known due to [113]. This integral is closely related[31] to the two-loop contribution to the electron self-energy and has been studied in already [45, 95, 96, 125–127].

Instead of presenting the complete solution obtained in [124] I will focus on its main points, which reveal the structure of the result at every order in ε.

The kite topology in D dimensions, with the mass m and the external momentum p is given by all integrals

$$I_{\nu_1\nu_2\nu_3\nu_4\nu_5}\left(D, p^2, m^2, \mu^2\right) = (-1)^{\nu_{12345}} \left(\mu^2\right)^{\nu_{12345}-D} \int \frac{\mathrm{d}^D k_1}{i\pi^{\frac{D}{2}}} \frac{\mathrm{d}^D k_2}{i\pi^{\frac{D}{2}}} \frac{1}{D_1^{\nu_1} D_2^{\nu_2} D_3^{\nu_3} D_4^{\nu_4} D_5^{\nu_5}},$$
(7.4.1)

---

[31]Up to a prefactor involving the kinematic invariant.

with the propagators

$$D_1 = k_1^2 - m^2, \quad D_2 = k_2^2, \quad D_3 = (k_1 - k_2)^2 - m^2, \quad D_4 = (k_1 - p)^2, \quad D_5 = (k_2 - p)^2 - m^2 \tag{7.4.2}$$

and $\nu_{12345} = \sum_{i=1}^{5} \nu_i$. Furthermore we will work with the dimensionless kinematic invariant $t = p^2/m^2$ and suppress the dependence of D and t in the following.

The kite topology and the sub-topologies which contribute to the differential equation of its MI I_8 are depicted in fig. 7.5. Since there is only one MI where all propagator powers are non-zero we see that the elliptic contributions enter only through the sunrise sub-topology $I_{\nu_1,0,\nu_3,0,\nu_5}$ with its two MI's I_6 and I_7. In the upper row we have topologies for which a canonical basis can be found. Therefore, from these sub-topologies we will as well have no elliptic contributions. That means the elliptic part of the kite will be governed by the elliptic properties of the sunrise.

7.4.1 The Solution of the Canonical 5×5-Subsystem in Terms of $\overline{\mathrm{E}}$-Functions

In the section 6.4 on solving differential equations by using a canonical basis we considered two detailed examples, the bubble and the tadpole in section 6.4.3 as well as the sunrise with one massive propagator in section 6.4.4. Looking at the first row of fig. 7.5 we see the leftmost topology is just the tadpole squared and we therefore take

$$I_1(D) = (D - 4)^2 I_{2,0,2,0,0} \tag{7.4.3}$$

as an element of the canonical basis since we know that the tadpole with a squared propagator is of uniform weight. The second to left topology is just the bubble with one massive propagator times the tadpole. We therefore take

$$I_2(D, t) = (D - 4)^2 \frac{m^2}{\mu^2} t I_{2,0,2,1,0} \tag{7.4.4}$$

since we know from the discussion in section 6.4.3 a canonical basis element of the bubble-topology. For the two MI's of the sunrise topology with one massive propagator we derived a canonical basis in section 6.4.4 and we can take the results directly from there. We have

$$I_3 = (D - 4)^2 \frac{m^2}{\mu^2} t I_{0,2,2,1,0} \ , \tag{7.4.5}$$

$$I_4 = (D - 4)^2 \frac{m^2}{\mu^2} \left[2 I_{0,2,2,1,0} - (t - 1) I_{0,2,1,2,0} \right] \ . \tag{7.4.6}$$

The last MI of the canonical system is just the bubble "squared" and using the results from section 6.4.3 we have

$$I_5(D, t) = (D - 4)^2 \left(\frac{m^2}{\mu^2} \right)^2 t^2 I_{2,1,0,1,2} \ . \tag{7.4.7}$$

Taking the derivative with respect to t yields in $D = 4 - 2\varepsilon$ the differential equation in canonical form

$$\frac{\mathrm{d}}{\mathrm{d}t}\vec{I}_{sub} = \varepsilon \left(\frac{1}{t}A_0 + \frac{1}{t-1}A_1\right)\vec{I}_{sub} \tag{7.4.8}$$

where

$$A_0 = \begin{pmatrix} 0 & 0 & 0 & 0 & 0 \\ 0 & 1 & 0 & 0 & 0 \\ 0 & 0 & 1 & 0 & 0 \\ 0 & 0 & -4 & 0 & 0 \\ 0 & 0 & 0 & 0 & 2 \end{pmatrix}, \qquad A_1 = \begin{pmatrix} 0 & 0 & 0 & 0 & 0 \\ -1 & -2 & 0 & 0 & 0 \\ 0 & 0 & -2 & 1 & 0 \\ 0 & 0 & 4 & -2 & 0 \\ 0 & -2 & 0 & 0 & -4 \end{pmatrix}, \tag{7.4.9}$$

and $\vec{I}_{sub} = (I_1, I_2, I_3, I_4, I_5)^T$.

To obtain the boundary values of this subsystem we use the point $t = 0$ since we have

$$I_2(0) = I_3(0) = I_5(0) = 0 \tag{7.4.10}$$

due to the normalization. The non-vanishing boundaries are therefore given only by I_1 and I_4 and read [124]

$$I_1(0) = 4\left(\frac{m^2}{\mu^2}\right)^{-2\varepsilon}\Gamma(1+\varepsilon)^2 , \tag{7.4.11}$$

$$I_4(0) = 4\left(\frac{m^2}{\mu^2}\right)^{-2\varepsilon}\Gamma(1+\varepsilon)\Gamma(1+2\varepsilon)\Gamma(1-\varepsilon) . \tag{7.4.12}$$

Before writing down the iterated solution we notice that the first and the fourth column of A_0 are zero-columns. That means terms where A_0 is on the rightmost side of the matrix multiplication are identically zero since the hyperlogarithms are at most logarithmically singular at $t \to 0$ but the integrals I_2, I_3 and I_5 go to zero (at least) linear in t. Therefore the solution of the system[32] up to $\mathcal{O}(\varepsilon^3)$ reads

$$\vec{I}_{sub}(t) = \left(\mathbb{1} + \varepsilon\int_0^t \frac{A_1}{s-1}\mathrm{d}s + \varepsilon^2\int_0^t\int_0^{s_2}\left[\frac{A_0 A_1}{s_2(s_1-1)} + \frac{A_1 A_1}{(s_2-1)(s_1-1)}\right]\mathrm{d}s_1\mathrm{d}s_2\right.$$

$$+ \varepsilon^3\int_0^t\int_0^{s_3}\int_0^{s_2}\left[\frac{A_0 A_0 A_1}{s_3 s_2(s_1-1)} + \frac{A_1 A_0 A_1}{(s_3-1)s_2(s_1-1)} + \frac{A_0 A_1 A_1}{s_3(s_2-1)(s_1-1)}\right.$$

$$\left.\left. + \frac{A_1 A_1 A_1}{(s_3-1)(s_2-1)(s_1-1)}\right]\mathrm{d}s_1\mathrm{d}s_2\mathrm{d}s_3\right)\vec{I}_{sub}(0) \tag{7.4.13}$$

$$= \left(\mathbb{1} + \varepsilon A_1 G(1;t) + \varepsilon^2\left[A_0 A_1 G(0,1;t) + A_1 A_1 G(1,1;t)\right]\right.$$

$$+ \varepsilon^3\left[A_0 A_0 A_1 G(0,0,1;t) + A_1 A_0 A_1 G(1,0,1;t) + A_0 A_1 A_1 G(0,1,1;t)\right.$$

$$\left.\left. + A_1 A_1 A_1 G(1,1,1;t)\right]\right)\vec{I}_{sub}(0) .$$

---

[32]The explicit result can be taken from [124].

Since the kite integral involves the sunrise as a sub-topology we have to express both letters in terms of the nome q associated to the elliptic curve of the sunrise integral. We therefore consider the two one-forms

$$
\begin{aligned}
\frac{\mathrm{d}t}{t} = \mathrm{d}\log(t) &= \frac{\mathrm{d}\log(t_q)}{\mathrm{d}q}\mathrm{d}q \\
&= \frac{\mathrm{d}\left(\log(-9q) - 4\overline{\mathrm{E}}_{1;0}\left(r_3; -1; -q\right)\right)}{\mathrm{d}q}\mathrm{d}q \\
&= \left(1 - 4\overline{\mathrm{E}}_{0;-1}\left(r_3; -1; -q\right)\right)\frac{\mathrm{d}q}{q}
\end{aligned}
\tag{7.4.14}
$$

and

$$
\begin{aligned}
\frac{\mathrm{d}t}{t-1} = \mathrm{d}\log(1-t) &= \frac{\mathrm{d}\log(1-t_q)}{\mathrm{d}q}\mathrm{d}q \\
&= \frac{\mathrm{d}\left(3(\overline{\mathrm{E}}_{1;0}\left(-1; 1; -q\right) - \overline{\mathrm{E}}_{1;0}\left(r_6; 1; -q\right))\right)}{\mathrm{d}q}\mathrm{d}q \\
&= 3\left(\overline{\mathrm{E}}_{0;-1}\left(-1; 1; -q\right) - \overline{\mathrm{E}}_{0;-1}\left(r_6; 1; -q\right)\right)\frac{\mathrm{d}q}{q}
\end{aligned}
\tag{7.4.15}
$$

where we used the results already derived for the sunrise (see appendix B.1.7) and $r_3 = \exp(2i\pi/3)$, $r_6 = \exp(2i\pi/6)$ denote the third and sixth root of unity. Alternatively one can use the direct change of the measure (B.1.11) and find the $\overline{\mathrm{E}}$ representation with the methods described in appendix B.

We conclude that hyperlogarithms with the letters $(\mathrm{d}t/t, \mathrm{d}t/(t-1))$ and therefore every integral $I_1 \ldots I_5$ can be computed in terms of $\overline{\mathrm{E}}$-functions, since they are closed under multiplication and integration with $\mathrm{d}q/q$.

7.4.2   The Master Integrals I_6, I_7, I_8 and the Solution of the Kite

The lower row of fig. 7.5 shows the topologies which can not be computed in terms of hyperlogarithms. From a practical point of view, we want a basis for these topologies, which has the following properties[33]:

1. It should simplify the differential equation for basis integral I_8 of the kite topology.

2. The sunrise basis integrals I_6 and I_7 in $D = 4 - 2\varepsilon$ should be easily relatable to the case in $D = 2 - 2\varepsilon$ since the solution there is known [107].

---

[33]An algorithmic way of making such simplifications has been presented in [55] some month after the here discussed publication.

We choose the basis

$$I_6 = \frac{3(D-4)(D-5)t}{(t-1)(t-9)} \left[(3-t)I_{20200}\right.$$
$$+ (3D-8)(D-3)I_{10101} + 2(D-3)(t+3)I_{20101}\right] , \tag{7.4.16}$$

$$I_7 = \frac{2(D-4)t}{(t-1)^2(t-9)^2}$$
$$\left[(D-4)t^3 - (17D-71)t^2 + 3(9D-46)t - 27(D-5)I_{20200}\right.$$
$$+ (D-3)(3D-8)\frac{\mu^2}{m^2}\left((D-3)t^2 - 10t - 9(D-5)\right)I_{10101}$$
$$- (D-3)\left((D-4)t^3 - 6(6D-23)t^2 + 15(3D-8)t + 54(D-5)\right)I_{20101}\right] , \tag{7.4.17}$$

$$I_8 = (D-4)(D-5)\frac{m^2}{\mu^2}tI_{02210} + (D-3)(D-4)^2(D-5)\frac{m^2}{\mu^2}tI_{11111}. \tag{7.4.18}$$

This basis has two advantages. Firstly, the basis integral I_7 does not appear in the differential equation for I_8. Secondly we have

$$I_6(D,t) = (D-4)(D-5)\frac{m^2}{\mu^2}tI_{1,0,1,0,1}(D-2,t) , \tag{7.4.19}$$

$$I_7(D,t) = 2(D-4)\frac{m^4}{\mu^4}tI_{2,0,1,0,1}(D-2,t) , \tag{7.4.20}$$

which means that the differential equation for I_8 in $D = 4 - 2\varepsilon$ will only involve the sunrise integral $I_{1,0,1,0,1}$ in $D = 2 - 2\varepsilon$ dimensions. From a practical point of view these are great simplifications.

The differential equation of the basis integral I_8 in $D = 4 - 2\varepsilon$ reads [124]

$$\frac{dI_8}{dt} = \varepsilon\left(\frac{I_8 - 2I_5}{t} + \frac{I_1 - 2I_3 - 2I_8}{t-1}\right) + \left(\frac{8}{3(t-1)} - \frac{3}{t}\right)\varepsilon I_6 + \frac{1}{t-1}\left(\frac{I_1}{2} - I_3\right) - \frac{I_5}{t} , \tag{7.4.21}$$

where a suitable boundary point is $I_8(t=0) = 0$. We know from the previous section and [107], that the k-th Laurent coefficient of the sunrise integral in $D = 2 - 2\varepsilon$ can be written as $S_{111}^{(k)}(2-2\varepsilon) = \Psi_1/\pi\tilde{E}^{(k)}$ where $\tilde{E}^{(k)}$ is given in terms of $\overline{E}$-functions.[34] Using the definition of the basis integral

$$I_6(4-2\varepsilon) = 2\varepsilon(1+2\varepsilon)\frac{m^2}{\mu^2}tI_{1,0,1,0,1}(2-2\varepsilon) \tag{7.4.22}$$

we have for its k-th Laurent coefficient

$$I_6^{(k)}(D=4) = 2\frac{m^2}{\mu^2}t\left(I_{1,0,1,0,1}^{(k-1)}(D=2) + 2I_{1,0,1,0,1}^{(k-2)}(D=2)\right)$$
$$= 2\frac{m^2}{\mu^2}t\frac{\Psi_1}{\pi}\left(\tilde{E}^{(k-1)} + 2\tilde{E}^{(k-2)}\right) . \tag{7.4.23}$$

---

[34] Notice, there is a slight difference in the notation with respect to [124] mainly due to the overall factor $e^{-2\gamma_E\varepsilon}$ used there for a more compact Laurent expansion.

The differential equation for the *k-th* Laurent coefficient of the basis integral I_8 can be read off directly from (7.4.21) to

$$
\begin{aligned}
\frac{\mathrm{d}I_8^{(k)}}{\mathrm{d}t} &= \left(\frac{I_8^{(k-1)} - 2I_5^{(k-1)}}{t} + \frac{I_1^{(k-1)} - 2I_3^{(k-1)} - 2I_8^{(k-1)}}{t-1} \right) + \frac{1}{t-1} \left(\frac{I_1^{(k)}}{2} - I_3^{(k)} \right) - \frac{I_5^{(k)}}{t} \\
&\quad + \left(\frac{8}{3(t-1)} - \frac{3}{t} \right) I_6^{(k-1)} \\
&= \left(\frac{I_8^{(k-1)} - 2I_5^{(k-1)}}{t} + \frac{I_1^{(k-1)} - 2I_3^{(k-1)} - 2I_8^{(k-1)}}{t-1} \right) + \frac{1}{t-1} \left(\frac{I_1^{(k)}}{2} - I_3^{(k)} \right) - \frac{I_5^{(k)}}{t} \\
&\quad + \frac{2}{3} \frac{m^2}{\mu^2} \left(\frac{8}{t-1} - 1 \right) \frac{\Psi_1}{\pi} \left(\tilde{E}^{(k-2)} + 2\tilde{E}^{(k-3)} \right)
\end{aligned}
\tag{7.4.24}
$$

where we inserted the solution of $I_6^{(k)}$ (7.4.23). Let us comment on this differential equation before we transform it further. The first thing to notice is, that due to our basis choice, the first non-vanishing Laurent coefficient of every of the integrals $I_1, \ldots, I_8$ is at ε^j with $j \geq 0$. Indeed, by solving the canonical system (7.4.13) one finds immediately that I_1 and I_4 start at order ε^0, I_2 and I_3 at order ε^1 and I_5 at order ε^2. For the sunrise in two dimension we know that its first non-vanishing Laurent coefficient $\propto \tilde{E}^{(k)}$ is at order ε^0 from the discussion of the sunrise in section 7.3. Therefore we can deduce the structure of the solution of the basis integral I_8. At order ε it will have a non-vanishing contribution $\propto G(1;t)$ due to the term $\propto I_1^{(0)}/(t-1)$ in the differential equation (7.4.24). At order ε^2 there is also a contribution from I_3 such that the result will consist of hyperlogarithms of weight one and two. At order ε^2 the elliptic contributions of the sunrise will enter the differential equation. But if we are interested in the integral $I_{1,1,1,1,1}$ we have to consider already the first three orders of I_8 for the ε^0 coefficient (see (7.4.18)). Therefore the MI $I_{1,1,1,1,1}$ of the kite topology will involve elliptic generalizations already at order ε^0. We conclude, that we have to re-write the deq in a suitable variable, the nome q associated to the sunrise, and a suitable class of functions, the $\overline{\mathrm{E}}$-functions.

That means, our differential equation is given by

$$
\frac{\mathrm{d}I_{8,q}^{(k)}}{\mathrm{d}q} = \left(-2I_{5,q}^{(n-1)} - I_{5,q}^{(n)} + I_{8,q}^{(n-1)} \right) \left(\frac{1}{t_q} \frac{\mathrm{d}t_q}{\mathrm{d}q} \right)
\tag{7.4.25}
$$

$$
+ \left(I_{1,q}^{(n-1)} + \frac{1}{2}I_1^{(n)} - 2I_{3,q}^{(n-1)} - 2I_{8,q}^{(n-1)} - I_{3,q}^{(n)} \right) \left(\frac{1}{t_q - 1} \frac{\mathrm{d}t_q}{\mathrm{d}q} \right)
\tag{7.4.26}
$$

$$
+ \frac{2}{3} \frac{m^2}{\mu^2} \left(8 \left(\frac{\Psi_{1,q}}{\pi(t_q - 1)} \frac{\mathrm{d}t_q}{\mathrm{d}q} \right) - \left(\frac{\Psi_{1,q}}{\pi} \frac{\mathrm{d}t_q}{\mathrm{d}q} \right) \right) \left(\tilde{E}^{(k-2)} + 2\tilde{E}^{(k-3)} \right) ,
\tag{7.4.27}
$$

which is integrable in terms of $\overline{\mathrm{E}}$ if every of its terms is. We used the subscript q to indicate, that the corresponding q-series representation should be considered.
For the first and the second line we recall that every integral of the canonical subsystem as well as the letters $(\mathrm{d}t_q/t_q, \mathrm{d}t_q/(t_q - 1))$ can be written in terms of $\overline{\mathrm{E}}$-functions (see sec. 7.4.1 and eq. (7.4.14),(7.4.15)).

78

In the last line we have to transform

$$\left(\frac{\Psi_{1,q}}{\pi}\frac{\mathrm{d}t_q}{\mathrm{d}q}\right) \overset{\text{B.1.1}}{=\!=\!=} \frac{1}{i\pi^2}\frac{\Psi_{1,q}^3}{W_q(\Psi_1,\Psi_2)}\frac{1}{q}$$
$$\overset{\text{B.1.4}}{=\!=\!=} -6\frac{\mu^2}{m^2}\overline{\mathrm{E}}_{-2,0}(-1,r_3,-q)\frac{1}{q}\ , \tag{7.4.28}$$

where $r_3 = \exp(2i\pi/3)$ denotes the third root of unity. Here we used, that this particular expression already appeared in the computation of the contribution $\tilde{I}_1^{(k)}(q)$ to the equal-mass sunrise in section 7.3.3. The expression is derived in appendix B.1.4.

The $\overline{\mathrm{E}}$ representation of the second term in front of the sunrise is given by

$$\left(\frac{\Psi_{1,q}}{\pi(t_q-1)}\frac{\mathrm{d}t_q}{\mathrm{d}q}\right) \overset{\text{B.1.1}}{=\!=\!=} \frac{1}{i\pi^2}\frac{\Psi_{1,q}^3}{(t_q-1)W_q(\Psi_1,\Psi_2)}\frac{1}{q}$$
$$\overset{\text{B.1.4}}{=\!=\!=} -\frac{6}{8}\frac{\mu^2}{m^2}\left(9\overline{\mathrm{E}}_{-2;0}\left(1;r_3;-q\right)+\overline{\mathrm{E}}_{-2;0}\left(-1;r_3;-q\right)\right)\frac{1}{q}\ . \tag{7.4.29}$$

This expression is derived in appendix B.1.6 and it follows that the factor in front of the $\tilde{E}$-functions simplifies to

$$\frac{2}{3}\frac{m^2}{\mu^2}\left(8\left(\frac{\Psi_{1,q}}{\pi(t_q-1)}\frac{\mathrm{d}t_q}{\mathrm{d}q}\right)-\left(\frac{\Psi_{1,q}}{\pi}\frac{\mathrm{d}t_q}{\mathrm{d}q}\right)\right) = -36\overline{\mathrm{E}}_{-2;0}\left(1;r_3;-q\right)\frac{1}{q}\ . \tag{7.4.30}$$

Inserting the kernels into (7.4.27) yields

$$q\frac{d}{dq}I_{8,q}^{(j)} = \left[1-4\overline{\mathrm{E}}_{0;-1}\left(r_3;-1;-q\right)\right]\left(-2I_{5,q}^{(j-1)}-I_{5,q}^{(j)}+I_{8,q}^{(j-1)}\right)$$

$$+3\left[\overline{\mathrm{E}}_{0;-1}\left(-1;1;-q\right)-\overline{\mathrm{E}}_{0;-1}\left(r_6;1;-q\right)\right]\left(I_{1,q}^{(j-1)}+\frac{1}{2}I_{1,q}^{(j)}-2I_{3,q}^{(j-1)}-I_{3,q}^{(j)}-2I_{8,q}^{(j-1)}\right)$$

$$-36\overline{\mathrm{E}}_{0;-2}\left(r_3;1;-q\right)\left(\tilde{E}^{(k-2)}+2\tilde{E}^{(k-3)}\right)\ . \tag{7.4.31}$$

To summarize this section let me emphasize on the resulting differential equation (7.4.31). With it we have, since all integrals $I_1,\ldots,I_6$ and all our kernels have a representation in $\overline{\mathrm{E}}$-functions depending solely on the nome q associated to the sunrise topology, the possibility to compute the basis integral $I_{8,q}$ and therefore $I_{1,1,1,1,1}(q(t))$ to all orders in ε. Even though the obtained explicit expressions (see [124]) become longish quickly, from are purely structural point of view that is a strikingly simple result.

7.5   The Analytic Continuation of the Equal Mass Sunrise and the Kite

Until now we discussed the sunrise and the kite integral in the Euclidian region, where the periods Ψ_i and therefore the nome were defined. In the end however, we are interested in evaluating the obtained solutions in the whole kinematic regime. For the case of multiple polylogarithms the analytical continuation and the monodromy is well understood.[35] For the Feynman integrals involving complete elliptic integrals one can use special function identities[36] to define well defined functions in all kinematic regimes. Demanding matching expansions in a vicinity around the thresholds will yield an analytic continuation[37]. This approach has been used e.g. in [87, 112, 113] to obtain the analytic continuation of the results of the sunrise, the kite and the 3-loop banana as integrals over complete elliptic integrals.

In a recent joint work with Christian Bogner and Stefan Weinzierl [109] we chose another approach which makes use of the fact that the results are obtained depending on the nome q only. The properties of the underlying elliptic curve however, are a well understood and widely covered subject in the mathematical literature. In the following, I will cover the main points of [109].

Before we start let us discuss a simpler example of a multivalued function, namely the square root. In section 7.3.1 we discussed the two branch-points of the square root at 0, ∞ and we concluded, that in order to get a single valued determination, we have to connect these points by a branch-cut such that closed loops around branch-points do cross it. In practice one uses some program for the evaluation of the results and two technical aspects become important. Firstly, where does the branch cut lie and secondly, how is the function $f(z)$ evaluated there?. While its position should be documented, the value taken on the branch-cut is by convention such that a function is continuous when coming around the finite endpoint of the cut in counterclockwise direction [129] on the principal sheet.

For the root it is common to place the branch-cut on the negative real axis. That means by convention the root is evaluated for $t \in \mathbb{R}$ according to

$$\sqrt{-t} = \begin{cases} i\sqrt{|t|} \,, & z > 0 \\ \sqrt{|t|} \,, & z \leq 0 \,. \end{cases} \tag{7.5.1}$$

On the other hand, for evaluation of Feynman integrals, we have the Feynman $+i0$-prescription for the kinematic invariant t. This prescription, stemming from the definition of the propagator, tells us to evaluate the real kinematic invariant according to $t \to t + i0$, where $+i0$ denotes an infinitesimal, positive imaginary part. For the physical kinematic invariant t we therefore have

$$\sqrt{-t} = \begin{cases} -i\sqrt{|t|} \,, & z > 0 \\ \sqrt{|t|} \,, & z \leq 0 \end{cases} \tag{7.5.2}$$

---

[35]See e.g. [128] and [35] for more recent treatments on this subject.

[36]Known from the analytic continuation of elliptic integrals, which are well understood.

[37]Note that this approach is used in appendix B.1.2 to determine that the q-series representation of t holds in the whole Euclidian regime.

overriding the standard conventions by taking the limit $+i0$ to zero. In the following we denote $t + i0$ by t, but the small added imaginary part should always be assumed.

7.5.1 The Family of Elliptic Curves $\mathcal{E}_t$ and Its Variation With t

In the following we work with $t = p_\mu p^\mu$ in accordance to [109] and we recall from section 7.3.2, that the elliptic curve associated to the zero set of the second Symanzik polynomial $\mathcal{F}$ is given by

$$y^2 = 4 \left(x - e_1 \right) \left(x - e_2 \right) \left(x - e_3 \right) \tag{7.5.3}$$

with

$$
\begin{aligned}
e_1 &= \frac{1}{24\mu^4} \left(-t^2 + 6m^2 t + 3m^4 + 3 \left(m^2 - t \right)^{\frac{3}{2}} \left(9m^2 - t \right)^{\frac{1}{2}} \right), \\
e_2 &= \frac{1}{24\mu^4} \left(-t^2 + 6m^2 t + 3m^4 - 3 \left(m^2 - t \right)^{\frac{3}{2}} \left(9m^2 - t \right)^{\frac{1}{2}} \right), \\
e_3 &= \frac{1}{24\mu^4} \left(2t^2 - 12m^2 t - 6m^4 \right) .
\end{aligned}
\tag{7.5.4}
$$

In the Euclidian region $t < 0$ the periods of this family coming from an evaluation of the contour integrals depicted in fig. 7.4a are computed to

$$\Psi_1 = 2 \int_{e_2}^{e_3} \frac{dx}{y} = \frac{4\mu^2}{\left(m^2 - t \right)^{\frac{3}{4}} \left(9m^2 - t \right)^{\frac{1}{4}}} K \left(k^2 \right), \tag{7.5.5}$$

$$\Psi_2 = 2 \int_{e_1}^{e_3} \frac{dx}{y} = \frac{4i\mu^2}{\left(m^2 - t \right)^{\frac{3}{4}} \left(9m^2 - t \right)^{\frac{1}{4}}} K \left(k'^2 \right), \tag{7.5.6}$$

where

$$y = -2\sqrt{x - e_1}\sqrt{x - e_2}\sqrt{x - e_3} \tag{7.5.7}$$

and

$$k^2 = \frac{e_3 - e_2}{e_1 - e_2}, \qquad k'^2 = 1 - k^2 = \frac{e_1 - e_3}{e_1 - e_2}. \tag{7.5.8}$$

The result of all sub-topologies of the kite integral is given in terms of $\overline{\mathrm{E}}(x, y, -q)$ with $|x| = |y| = 1$ and $\sum_i n_i + m_i > 0$ which are convergent since $|q| < 1$ in the Euclidian regime[38]. But since the underlying structure is a family of elliptic curves, $|q|$ will stay smaller than 1 except for points, where the family degenerates. These points are given by values of t for which two of the roots e_i coincide and the elliptic curve degenerates to the nodal curve

$$y^2 = (x - e_i)^2 (x - e_j) = \tilde{x}^2 (\tilde{x} + e_i - e_j) = \tilde{x}^2 (\tilde{x} - 1) . \tag{7.5.9}$$

---

[38] In [130] an analytic continuation for special cases of ELi-functions is discussed.

For the integration contours δ_i in fig. 7.4a encircling two roots this results in the shrinking of one contour to a point. The Riemann surface of the family of elliptic curves fig. 7.4c will degenerate to a pinched torus. This degeneration happens for the family associated to the sunrise at the (pseudo) thresholds $t = 0$, where $e_2 = e_3$, at $t = m^2$ and $t = 9m^2$, where $e_1 = e_2$ and at $t = \pm\infty$ where e_1 and e_3 coincide. These are the branch-points of the elliptic curve as discussed in section 7.3.1 which we had to exclude from the two-sheeted cover and the torus to get a well defined expression.

To summarize the main ideas: When we vary t in the complex plain the roots and therefore periods and the nome will vary. However, up to the singular points, the ratio of the periods $\tau = \Psi_2/\Psi_1$ will be in the upper half plain and therefore $|q| < 1$. But as in the discussion of the simple root in section 7.3.1 the periods are multivalued functions due to the one-form $\mathrm{d}x/y$ and therefore depend on whether the path did or did not cross the branch-cut. So, instead of asking for the analytic continuation of the $\overline{\mathrm{E}}$-function, we have to determine whether or not the periods pick-up monodromy due to the path they are continued on if we vary t from the Euclidian to the physical regime.
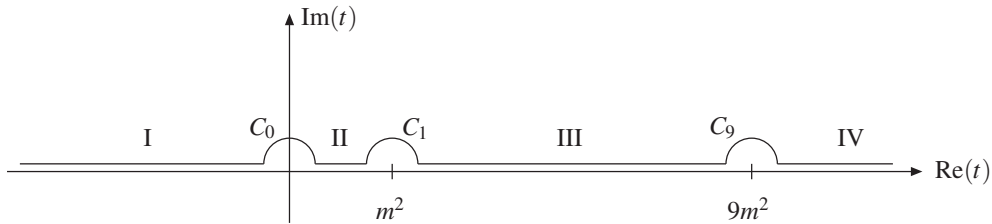

Figure 7.6: Representation of the variation of t in the complex plain taking into account Feynman's $+i0$ prescription. Figure taken from [109].

The path we have to consider for the variable t with respect to Feynman's $+i0$ prescription is depicted in fig. 7.6. The path is divided in into seven concatenated sub-paths where the straight line segments govern the regions:

$$
\begin{aligned}
\text{Region I}: &\quad -\infty \;<\; \mathrm{Re}(t) \;<\; 0 \,, \\
\text{Region II}: &\quad 0 \;<\; \mathrm{Re}(t) \;<\; m^2 \,, \\
\text{Region III}: &\quad m^2 \;<\; \mathrm{Re}(t) \;<\; 9m^2 \,, \\
\text{Region IV}: &\quad 9m^2 \;<\; \mathrm{Re}(t) \;<\; \infty \,.
\end{aligned}
\tag{7.5.10}
$$

The three semicircles C_i around the (pseudo)-thresholds determine the variation of the roots, which do not coincide anymore.

Instead of tracking the variation of the roots e_i in Weierstraß form it is easier to consider the Legendre- or Jacobi-form (see 7.3.1), since there only $\lambda = k^2$ ($k'^2 = 1 - k'^2$ respectively) will vary. Since the complete elliptic integrals[39] are used for the evaluation, we consider the variation of the (complementary) modulus $((1 - k^2))\, k^2$.

The variation of the parameter k^2 is shown in fig. 7.7. In the regions I, II, IV the path is an infinitesimal distance below the real axis. That means we evaluate the elliptic integral according to the standard conventions, since we approach the cut from counterclockwise direction from its finite endpoint in region IV. In the region III we have $\mathrm{Re}(k^2) = 1/2$. The

---

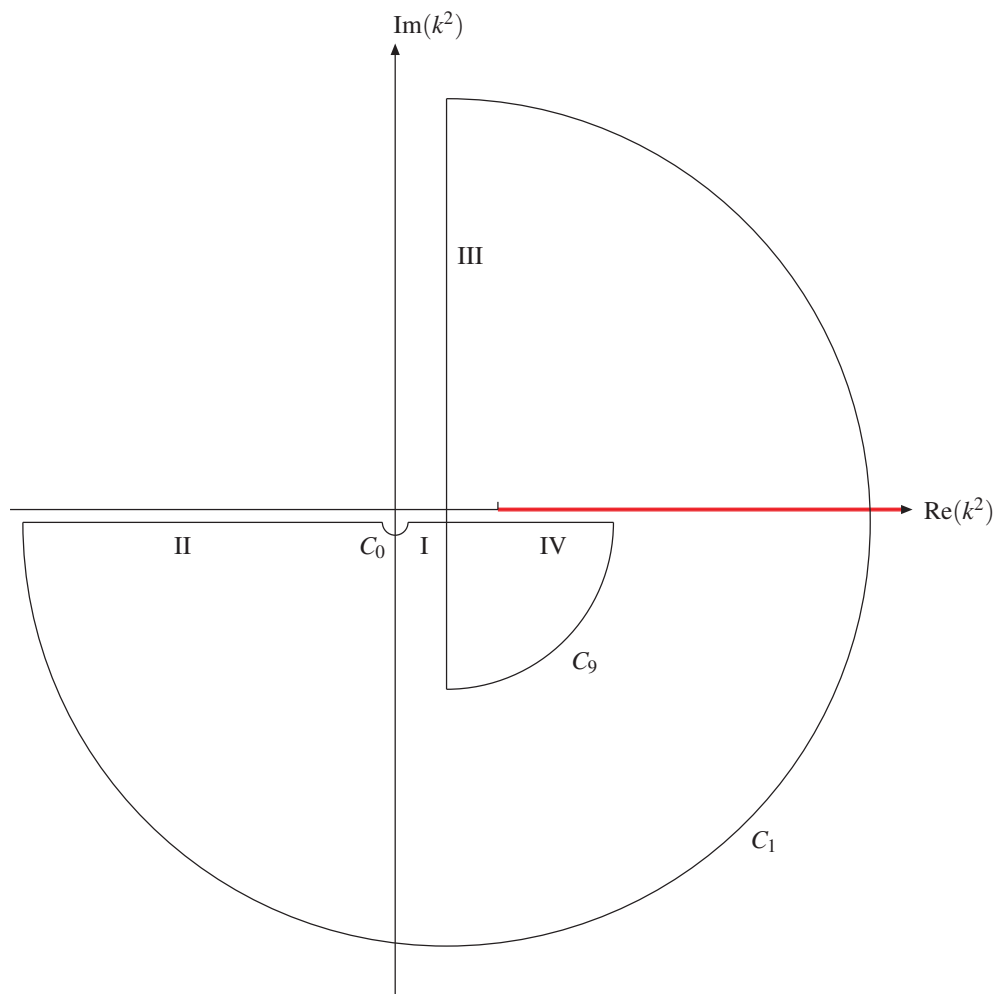[39]Corresponding to the Jacobi-representation of the elliptic curve.

Figure 7.7: The path of the parameter k^2 while t varies along the path depicted in 7.6. k^2 crosses the branch cut $[1, \infty[$ while t goes in the semicircle C_1 around $t = m^2$. Figure taken from [109].
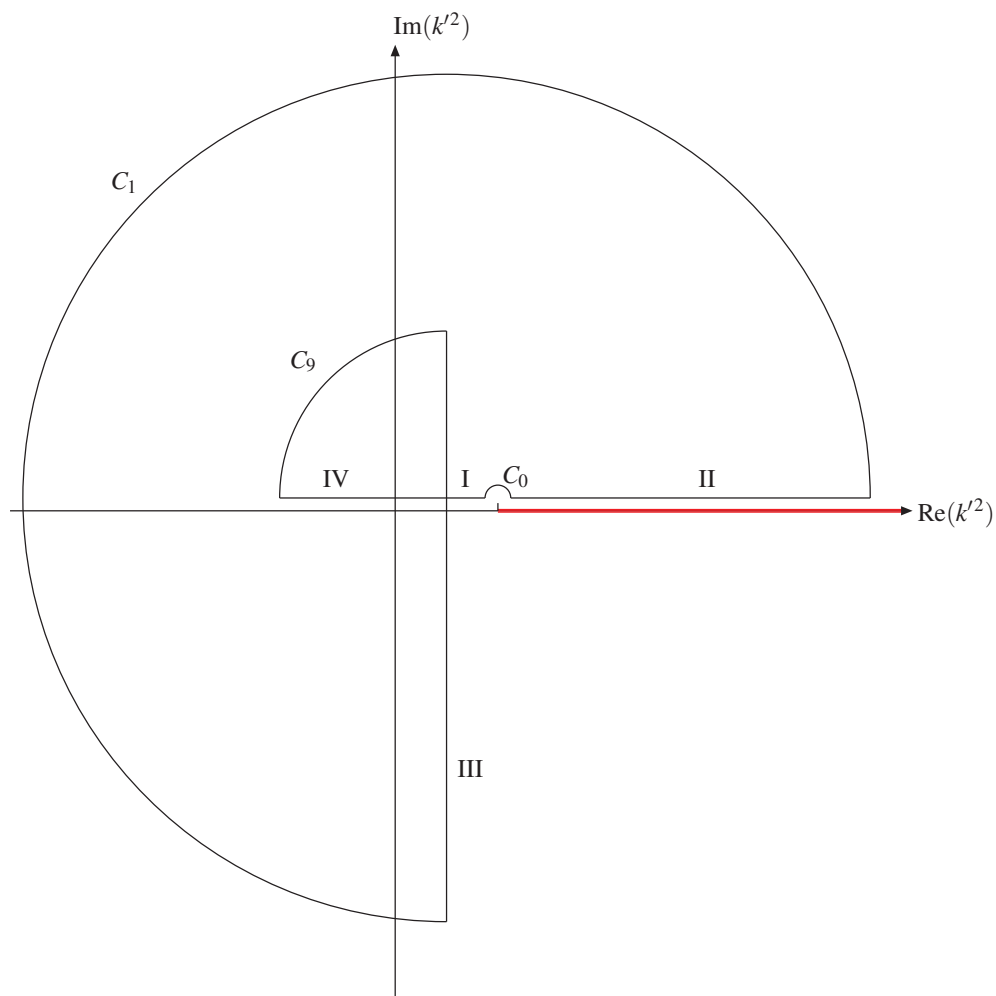
Figure 7.8: The path of the complementary parameter $k'^2 = 1 - k^2$ while t varies along the path depicted in 7.6. k'^2 does not cross the branch cut $[1, \infty[$. Figure taken from [109].

paths corresponding to the semicircles C_0 and C_9 show, that an evaluation for real t in the transition from one region to another might jump (C_9[40]), but both paths do not cross the branch-cut. On the other hand we see, that the path corresponding to the variation of t along the path C_1 around $t = m^2$ does cross the branch-cut $[1, \infty[$ of the complete elliptic integral. That means in the regions III and IV we have to consider (with respect to the period Ψ_1 in (7.5.5)) the additional part from stemming from the monodromy.[41]

The path of the complementary modulus is depicted in fig. 7.8. This path does not cross the branch-cut and therefore the definition of Ψ_2 (7.5.6) holds for all t along the path shown in fig. 7.6. Since in the end we will be interested in the evaluation for $t \in \mathbb{R}$ we point out, that in the region II the branch-cut is approached from above. Therefore one has to override the standard conventions by considering the limit $+i0$ to zero[42] and compensate for the difference by hand. Alternatively one can use the identity [131]

$$K\left(k \pm i0\right) = \frac{1}{k}\left[K\left(\frac{1}{k}\right) \pm iK\left(\sqrt{1 - \frac{1}{k^2}}\right)\right] \tag{7.5.13}$$

to map the evaluation in a region without ambiguities.
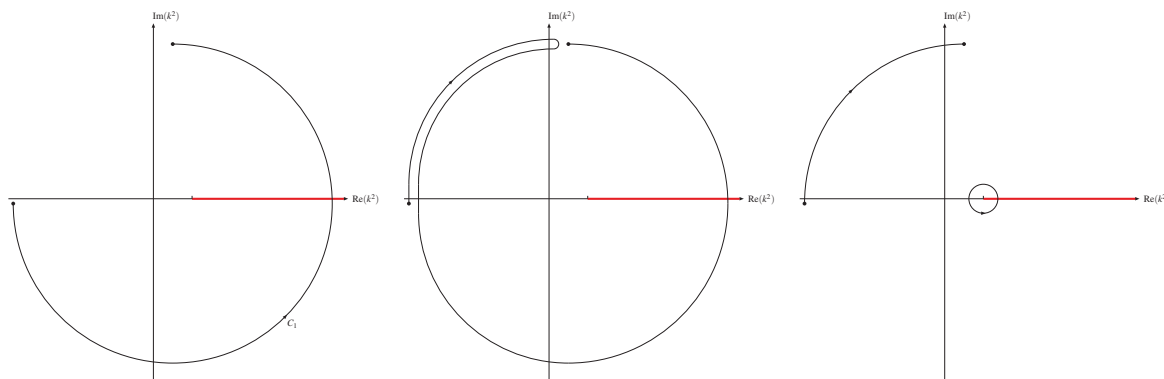
7.5.2 Computing the Monodromy

Figure 7.9: Deformation of the path in the k^2 space corresponding to the variation of t along C_1 shown in 7.6. The path is deformed into a quarter circle and a full counterclockwise oriented circle around the branch-point 1. Figure taken from [109].

In section 7.3.1 we studied the monodromy of the simple root by dragging it in a full circle around its branch-points. To make the connection to the variation of k^2 along the

---

[40]Due to a root in the modulus which picks up monodromy.

[41]Note that the prefactor in front of the elliptic integral as well as the (complementary) parameter has monodromy as well. But that is trivially given by considering the Feynman prescription directly for the evaluation of the roots.

[42]E.g. Mathematica uses

$$\begin{aligned}
&1.) && \lim_{\eta \to 0^-} K(x + i\eta) = K(x) && \text{with } x, \eta \in \mathbb{R} \text{ and } x > 1 && (7.5.11) \\
&2.) && \lim_{\eta \to 0^+} K(x + i\eta) = K(x) + 2iK(1 - x) && \text{with } x, \eta \in \mathbb{R} \text{ and } x > 1. && (7.5.12)
\end{aligned}$$

path depicted in fig. 7.7 we consider the deformation of the three quarter circle into a quarter circle and a full counterclockwise orientated circle. This deformation is depicted in 7.9. Our discussion follows closely chapter one in [132] since for the simple case at hand, the whole procedure can be depicted nicely. We note that the Picard-Lefschetz theorem as discussed in great detail in [133] could be used directly but it would require an introduction of new concepts not necessarily needed here.

We recall from section 7.3.2 that we can describe the elliptic curve in Legendre form

$$\mathcal{E}_\lambda: \qquad y^2 = x(x - \lambda)(x - 1) \tag{7.5.14}$$

as well as in Jacobi form and may use the representation

$$K(k^2 = \lambda) = \frac{1}{2} \int_0^\lambda \frac{1}{\sqrt{x}\sqrt{x - \lambda}\sqrt{x - 1}} dx \tag{7.5.15}$$

of the complete elliptic integral of the first kind. We now have to study what happens if λ moves around 1 in a full circle.

That task can be simplified by first studying the variation of the elliptic curve

$$\mathcal{E}_\varphi: \qquad y^2 = x(x - e_1(\varphi))(x - e_2(\varphi)) \tag{7.5.16}$$

with the roots

$$e_1(\varphi) = 1 - re^{i\varphi}, \qquad\qquad e_2(\varphi) = 1 + re^{i\varphi} \tag{7.5.17}$$

where $0 < r < 1$ and $\varphi \in [0, 2\pi]$. This family can be thought of as the Legendre form where we go locally in a "center-of-mass system" such that we have two roots e_i which encircle 1 as φ varies.[43] The periods associated to the family $\mathcal{E}_\varphi$ are given by

$$P_1(\varphi) = \int_{\delta_1} \frac{dx}{y} \ , \qquad\qquad P_2(\varphi) = \int_{\delta_2} \frac{dx}{y} \ , \tag{7.5.18}$$

with

$$y = -\sqrt{x}\sqrt{x - e_1(\varphi)}\sqrt{x - e_2(\varphi)} \ . \tag{7.5.19}$$

The orientation of the cycles δ_i is chosen as depicted in fig. 7.10 such that we have for $\varphi = 0$

$$P_1(0) = 2\int_0^{e_1(0)} \frac{dx}{y} = -2\int_{e_2(0)}^\infty \frac{dx}{y}, \qquad\qquad P_2(0) = 2\int_{e_2(0)}^{e_1(0)} \frac{dx}{y} \tag{7.5.20}$$

where the line integral is taken with an infinitesimal small negative imaginary part for x.

---

[43] Alternatively one can think of the Legendre form $y^2 = x(x - (1 - 2re^{i\varphi}))(x - 1)$ with $\lambda = (1 - 2re^{i\varphi})$ and sufficiently small and constant $r < 1/2$. Now we shift $x \to \tilde{x} - re^{i\varphi}$ and have $y^2 = (\tilde{x} - re^{i\varphi})(\tilde{x} - (1 - re^{i\varphi}))(\tilde{x} - (1 + re^{i\varphi}))$. That is a Weierstraß form where two roots encircle each other while the third just makes a small circle as φ varies. But that small circle does not matter and we might take r so small, that $\tilde{x} - re^{i\varphi} \approx \tilde{x}$. That means for the study of what happens as λ makes a small circle around 1 we have $\mathcal{E}_\lambda \sim \mathcal{E}_\varphi$.
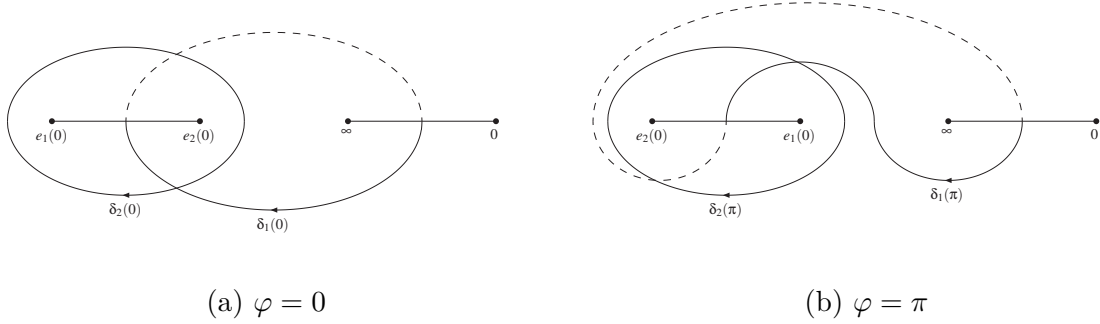
(a) $\varphi = 0$ (b) $\varphi = \pi$

Figure 7.10: Representation of the cycles δ_1, δ_2 for $\varphi = 0$ and $\varphi = \pi$. The cycle δ_1 is dragged along with the rotation. The dashed line represents the part of δ_1 lying on the other Riemann sheet. Figure taken from [109].

To study what happens to the periods while we vary φ we first note that the cubic describing $\mathcal{E}_\varphi$ is the same for $\varphi = 0$, $\varphi = \pi$ and $\varphi = 2\pi$ since we have

$$e_1(0) = e_2(\pi) = e_1(2\pi) \qquad\qquad e_2(0) = e_1(\pi) = e_2(2\pi) \;. \tag{7.5.21}$$

While we vary from $\varphi = 0$ to $\varphi = \pi$ the two roots e_1 and e_2 interchange their position. The deformation of the cycles is depicted in fig. 7.10 were δ_1 is dragged along during the rotation. We see that under a half turn $\delta_2(0) \to \delta_2(\pi) = \delta_2(0)$ but $\delta_1(0) \to \delta_1(\pi) \neq \delta_1(0)$. To express $\delta_1(\pi)$ in terms of $\delta_i(0)$ we consider the deformation depicted in 7.11. By going from fig. 7.11c to fig. 7.11d we use, that by changing the Riemann sheet we have to change orientation of a cycle since the one-form has the opposite global sign. Comparing the last picture 7.11e with the cycles at $\varphi = 0$ depicted in fig. 7.10a we see that we have

$$\delta_1(\pi) = \delta_1(0) - \delta_2(0) \;. \tag{7.5.22}$$

That means we can associate the matrix

$$T_\pi = \begin{pmatrix} 1 & -1 \\ 0 & 1 \end{pmatrix} \tag{7.5.23}$$

with a rotation of π and with respect to the basis $\{\delta_1(0), \delta_2(0)\}$. A complete rotation to $\varphi = 2\pi$ will therefore transform our periods according to

$$\begin{pmatrix} \Psi_1(2\pi) \\ \Psi_2(2\pi) \end{pmatrix} = T_\pi T_\pi \begin{pmatrix} \Psi_1(0) \\ \Psi_2(0) \end{pmatrix} \tag{7.5.24}$$

and the monodromy matrix is given by

$$M = T_\pi T_\pi = \begin{pmatrix} 1 & -2 \\ 0 & 1 \end{pmatrix} . \tag{7.5.25}$$

One could do the same analysis by considering the full turn in e.g. Legendre form without introducing the family $\mathcal{E}_\varphi$ locally (see footnote 43), but the "unravelling" of the cycle $\delta_1(2\pi)$ in analogy to fig. 7.11 would become a more tedious and sophisticated task.
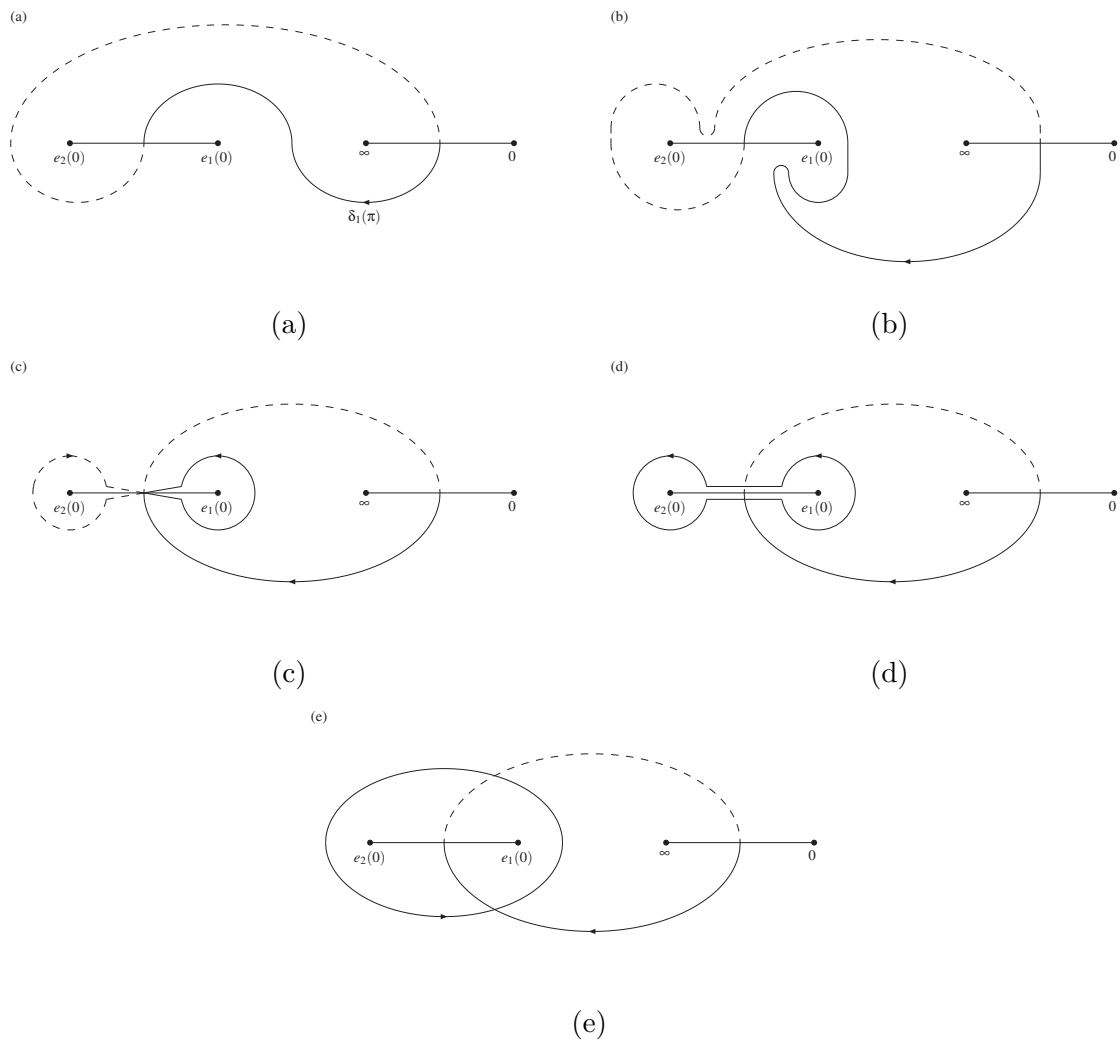
87

(a)

(b)

(c)

(d)

(e)

Figure 7.11: Deformation of the cycle $\delta_1(\pi)$ into the linear combination $\delta_1(\pi) = \delta_1(0) - \delta_2(0)$. Figure taken from [109].

To make the connection to the MI of the kite and its sub-topologies we can now use the derived monodromy matrix to analytically continue the results beyond $t = m^2$. We have the period vector

$$\begin{pmatrix} \Psi_1(t) \\ \Psi_2(t) \end{pmatrix} = \lim_{\eta \downarrow 0^+} \frac{4\mu^2}{(m^2 - t - i\eta)^{\frac{3}{4}}(9m^2 - t - i\eta)^{\frac{1}{4}}} M_t \begin{pmatrix} K\left(k^2(t + i\eta)\right) \\ K\left(k'^2(t + i\eta)\right) \end{pmatrix} \tag{7.5.26}$$

with $t \in \mathbb{R}$ and the monodromy matrix

$$M_t = \begin{cases} \begin{pmatrix} 1 & 0 \\ 0 & 1 \end{pmatrix} & t < m^2 \ , \\[2em] \begin{pmatrix} 1 & -2 \\ 0 & 1 \end{pmatrix} & t < m^2 \ . \end{cases} \tag{7.5.27}$$

The limit implements Feynman's $+i0$ prescription and tells us which values we should assign to the roots in the prefactors and how to approach the branch-cut of the elliptic integrals.

To summarize let us state the main result of this section. We computed the monodromy matrix of the periods Ψ_i by taking into account the variation of t according to Feynmans $+i0$ prescription. But due to the properties of the $\overline{\text{E}}$-functions as well as the variable choice this one monodromy matrix will be everything needed to evaluate the kite and all its sub-topologies in the complete kinematic regime.

7.6 Numerical Results

In this section I will consider the numerical evaluation of selected integrals from the kite and its sub-topologies. Some of the results are already published in [109].

For the numerical evaluation the $\overline{\mathrm{E}}$-functions are expanded to order $\mathcal{O}(q^{100})$ with a Mathematica [56] implementation of the algorithm described in appendix B.4 and evaluated with a 50-digit precision. For the numerical evaluation of the hyperlogarithms the HPL-Mathematica package by Maitre [66, 67] is used. The computation of the Feynman integrals by the method of sector decomposition [134–136] is done by using the program **SecDec** 3 [137–140]. In the following we will work with $\mu = m = 1$.

7.6.1 The Numerical Results for I_{02210}

The integral I_{02210} is one of the MI's of the sunrise topology where one massive and one massless propagator are raised to the power two. It can be obtained from the basis integral I_3 of the canonical 5×5-subsystem of the kite topology. The solution of I_3 can be obtained by expanding the boundary vector $\vec{I}_{sub}(0)$ in (7.4.13). One finds in $D = 2 - 2\varepsilon$

$$I_{02210} = \sum_{i=-1}^{\infty} \varepsilon^i \mathcal{I}_{02210}^{(i)} = \frac{1}{4t\varepsilon^2} I_3(4 - 2\varepsilon, t) \ , \tag{7.6.1}$$

with the first three Laurent coefficients

$$\mathcal{I}_{02210}^{(-1)}(t) = \frac{G(1;t)}{t} \tag{7.6.2}$$

$$\mathcal{I}_{02210}^{(0)}(t) = -\frac{2\gamma_E G(1;t) - G(0,1;t) + 4G(1,1;t)}{t} \tag{7.6.3}$$

$$\mathcal{I}_{02210}^{(1)}(t) = -\frac{1}{2t}\left[-\left(4\gamma_E^2 + \pi^2\right)G(1;t) + 2(-G(0,0,1;t) - 2\gamma_E(-G(0,1;t) + 4G(1,1;t))\right.$$
$$\left. + 6G(1,0,1;t) + 4G(0,1,1;t) - 16G(1,1,1;t))\right] \ . \tag{7.6.4}$$

But as discussed in section 7.4.1, we can express every of the hyperlogarithms (harmonic polylogarithms) in terms of $\overline{\mathrm{E}}$-functions. The explicit expressions can be found in appendix B.5.

In fig. 7.12 the results of the numerical evaluation of the imaginary and real part of the first three Laurent-coefficients in terms of $\overline{\mathrm{E}}$-functions in comparison with the results obtained by SecDec are shown. The plots show a perfect agreement in all kinematic regimes including the threshold.

To estimate the goodness of the approximation by a finite expansion order in q, the relative error with respect to an evaluation in terms of hyperlogarithms is shown in fig. 7.13 for an expansion order of q^{50} and q^{100}. In this figure same coloured plots correspond to the same expressions. Continuous lines are evaluations with order q^{100} while dashed lines correspond to order q^{50}. In this plot we see three important points.

The first and most important point is, that the error is due to a finite expansion in q only since it decreases by more than four orders of magnitude even in the worst regime near $t \approx 9m^2$ when the expansion order in q is increased from 50 to 100. Furthermore we see,

(a) $\mathcal{O}\left(\varepsilon^{-1}\right)$

(b) $\mathcal{O}\left(\varepsilon^{0}\right)$
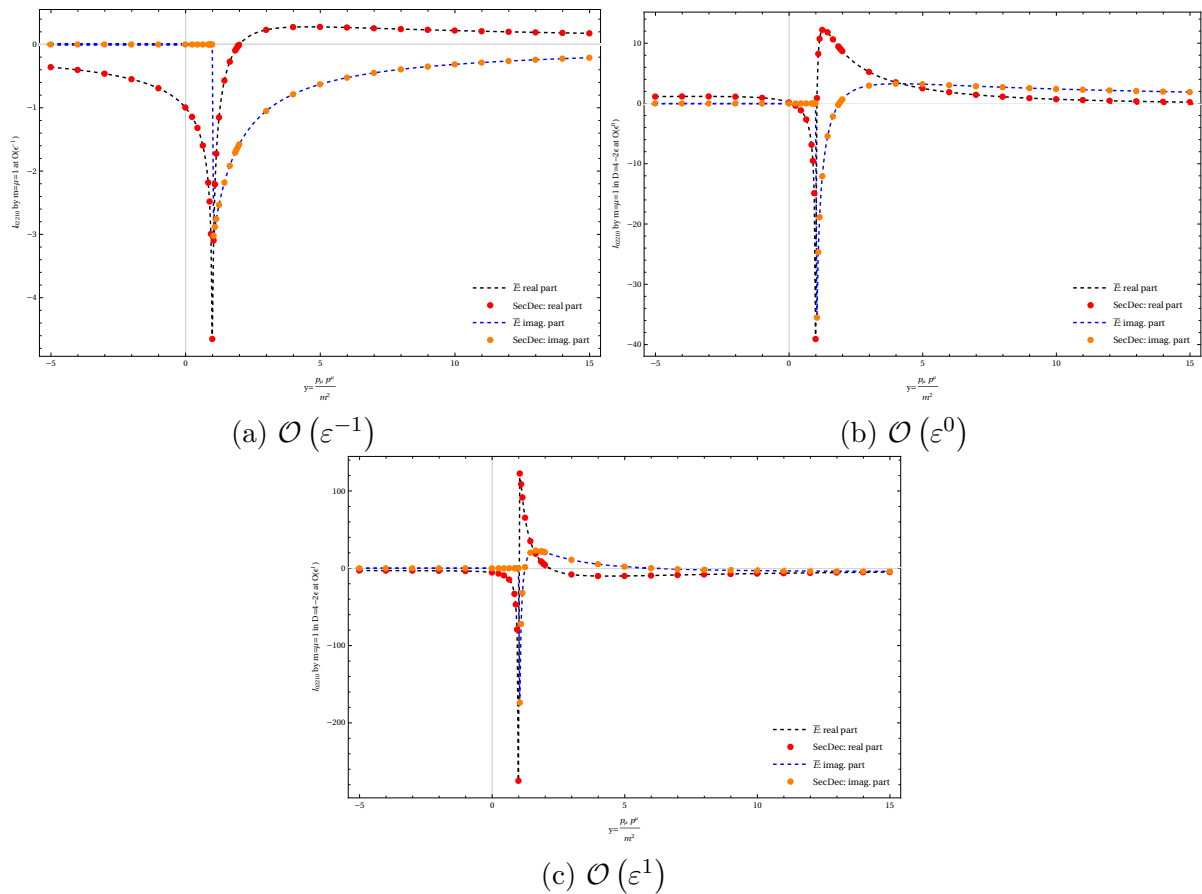
(c) $\mathcal{O}\left(\varepsilon^{1}\right)$

Figure 7.12: Comparison of the numerical evaluation of the real and the imaginary part of first three Laurent coefficients of I_{02210} in terms of $\overline{\mathrm{E}}$-functions with the SecDec results.
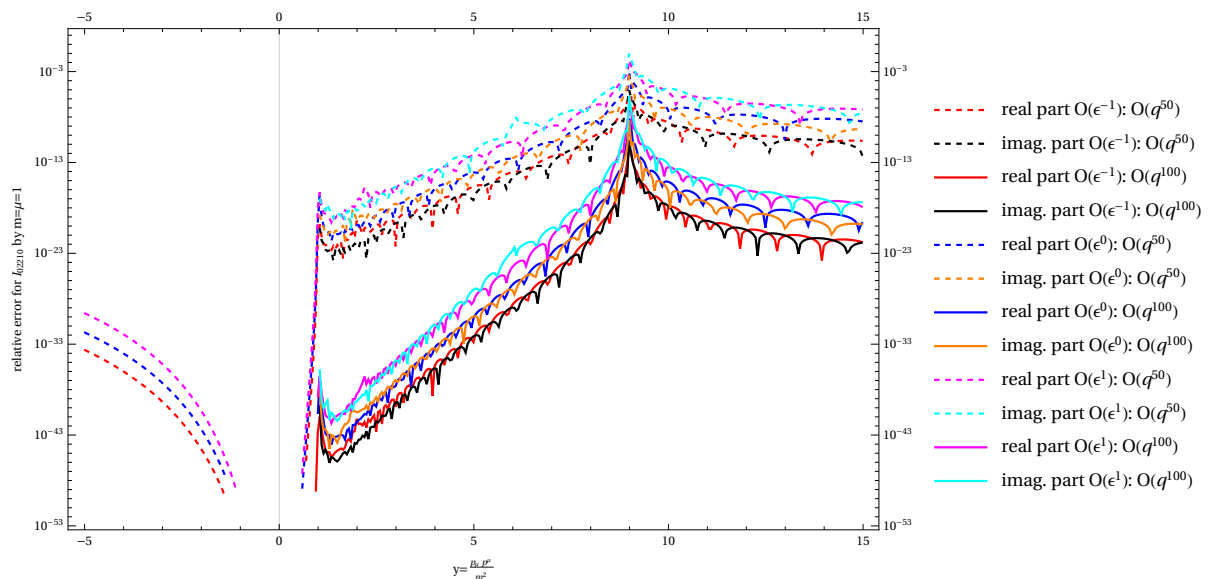

Figure 7.13: The relative error between an evaluation in terms of hyperlogarithms and $\overline{\mathrm{E}}$-functions for the real and imaginary part of the first three Laurent-coefficients of I_{02210}. Same coloured lines represent the same expressions while dashed lines correspond to an expansion of the $\overline{\mathrm{E}}$-functions to $\mathcal{O}\left(q^{50}\right)$ and continuous lines to $\mathcal{O}\left(q^{100}\right)$.
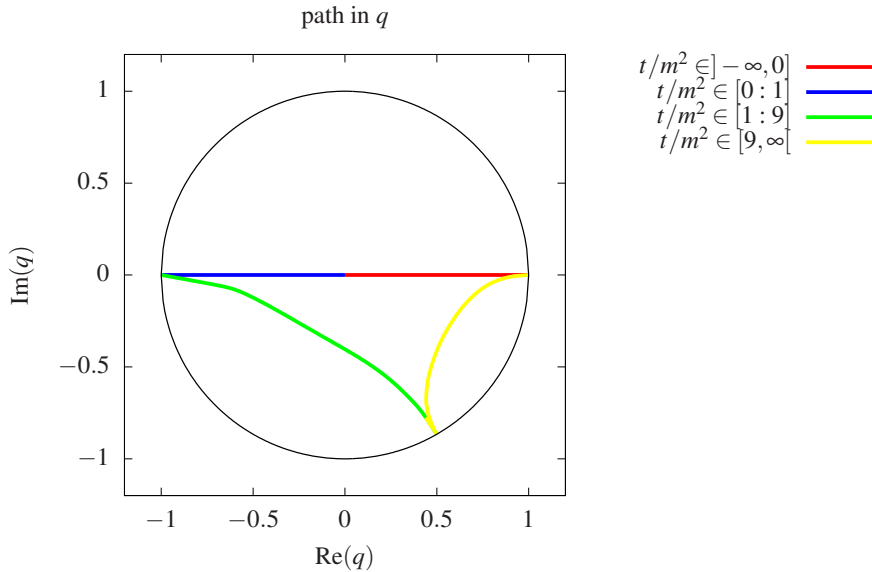
91

Figure 7.14: The path of the nome q in the complex plain while t varies along the path in fig. 7.6. At $t = 0$ we have $q = 0$, $t = m^2$ corresponds to $q = -1$ and $t = 9m^2$ to $q = r_6^* = e^{-2i\pi/6}$. In the limit $t \to -\infty$ we have $q \to 1$. Figure taken from [109].

that the relative error for real and imaginary parts is in the same order of magnitude and we have mostly errors $< 10^{-16}$ at an expansion order of q^{100}, which shows a really good agreement.

The second trend is, that the error increases for higher coefficients in the Laurent expansion. This can probably be explained by the rapidly growing number of higher depth $\overline{\text{E}}$-functions necessary to express higher weight harmonic polylogarithms (explicitly listed in appendix B.5). Since we expect an error for every finite q-expansion of an $\overline{\text{E}}$-function a possibly adding up of the errors would explain the overall increasing error for higher Laurent-coefficients.

The last thing all the real and imaginary parts of the Laurent-coefficients have in common is, that the error increases in the vicinity around $t = 9m^2$ drastically. This can be explained by the path on which q-varies as t increases as shown in fig. 7.14. There we see near the degeneration points $t = m^2$ and $t = 9m^2$ that the absolute values of q comes, as expected, close to the convergence radius. The same effect but far less pronounced can be seen in the vicinity around $t = m^2$. The reason why it is so much less pronounced near $t = m^2$ becomes clear by studying the absolute value of the nome in a close vicinity around m^2 and $9m^2$ as tabulated in table 7.1. We see, that we have to go extremely close ($\approx m^2 \pm 10^{-9}$) to m^2 to obtain a similar absolute value of the nome as in a relative large distance ($t = 9m^2 \pm 10^{-1}$) around $t = 9m^2$.

Table 7.1: The absolute value of the nome in a vicinity of m^2 and $9m^2$.

Δ	$|q(m^2 - \Delta)|$	$|q(m^2 + \Delta)|$	$|q(9m^2 - \Delta)|$	$|q(9m^2 + \Delta)|$
10^{-1}	0.22	0.37	0.72	0.74
10^{-5}	0.61	0.63	0.87	0.87
10^{-9}	0.75	0.75	0.92	0.92
10^{-13}	0.81	0.82	0.94	0.94

7.6.2 The Numerical Result for the Sunrise and the Kite

The first two terms of the sunrise in $D = 2 - 2\varepsilon$ with $m = \mu = 1$ are [107]

$$S_{111} = \frac{\Psi_1}{\pi} \left[E_{111}^{(0)}(q) + \varepsilon \left(E_{111}^{(1)}(q) - 2\gamma_E E_{111}^{(0)} \right) \right] \tag{7.6.5}$$

with

$$E_{111}^{(0)} = 3E_{2;0}(r_3; -1; -q) \tag{7.6.6}$$

$$E_{111}^{(1)} = 3E_{3;1}(r_3; -1; -q) + 18E_{0,1;-2,0;4}(r_3, -1; -1, 1; -q) + 3E_{0,1;-2,0;4}(r_3, r_3; -1, -1; -q)$$

$$- 9E_{0,1;-2,0;4}(r_3, r_3; -1, 1; -q) - \frac{3}{2}i \Big[2 \left(\mathrm{Li}_{2,1} \left(r_3^*, 1 \right) - \mathrm{Li}_{2,1}(r_3, 1) \right) + 2 \left(\mathrm{Li}_3 \left(r_3^* \right) - \mathrm{Li}_3(r_3) \right)$$

$$+ 6 \log(2) \left(\mathrm{Li}_2 \left(r_3^* \right) - \mathrm{Li}_2(r_3) \right) \Big] + L_{1;0} E_{111}^{(0)} \tag{7.6.7}$$

$$L_{1;0} = -E_{1;0}(r_3; -1; -q) + 3E_{1;0}(r_3; 1; -q) - 6E_{1;0}(-1; 1; -q) . \tag{7.6.8}$$

Hereby the E-functions introduced in [107] can be expressed by $\overline{\mathrm{E}}$-functions with the relation [124]

$$\mathrm{E}_{n_1,...,n_{l-1},n_l;m_1,...,m_{l-1},m_l;2o_1,...,2o_{l-2},2o_{l-1}} \left(x_1, ..., x_{l-1}, x_l; y_1, ..., y_{l-1}, y_l; q \right) =$$

$$\overline{\mathrm{E}}_{n_1,...,n_{l-1},n_l;m_1,...,m_{l-1},m_l;2o_1,...,2o_{l-2},2o_{l-1}} \left(x_1, ..., x_{l-1}, x_l; y_1, ..., y_{l-1}, y_l; q \right)$$

$$+ \frac{c_{n_l+m_l}}{2i} \left[\mathrm{Li}_{n_l} \left(x_l \right) - s_{n_l+m_l} \mathrm{Li}_{n_l} \left(x_l^{-1} \right) \right]$$

$$\times \begin{cases} \overline{\mathrm{E}}_{n_1,...,n_{l-2},n_{l-1}+o_{l-1};m_1,...,m_{l-2},m_{l-1}+o_{l-1};2o_1,...,2o_{l-2}} \left(x_1, ..., x_{l-1}; y_1, ..., y_{l-1}; q \right) & l > 1 \\ 1 & l = 1 \end{cases}$$

$$\tag{7.6.9}$$

where c and s are as in the definition of the $\overline{\mathrm{E}}$-functions (7.3.62). The explicit expressions of the here needed E-functions in terms of $\overline{\mathrm{E}}$-functions are listed in appendix B.5.

By evaluating the sunrise we are, due to the prefactor, explicitly sensitive of the analytic continuation of the period Ψ_1, since there is no exponential as in the nome. In fig. 7.15 the results in terms of $\overline{\mathrm{E}}$-functions are compared with SecDec. We see a perfect agreement in all kinematic regimes as well as close to the threshold.

Lastly we turn to the kite integral. The kite integral I_{11111} depends on the basis integral I_8 defined in section 7.4 by

$$I_{11111} = \frac{I_{02210}}{2\varepsilon} - \frac{I_8}{4\varepsilon^2 t} + \mathcal{O}(\varepsilon) . \tag{7.6.10}$$

(a) $\mathcal{O}\left(\varepsilon^0\right)$ (b) $\mathcal{O}\left(\varepsilon^1\right)$
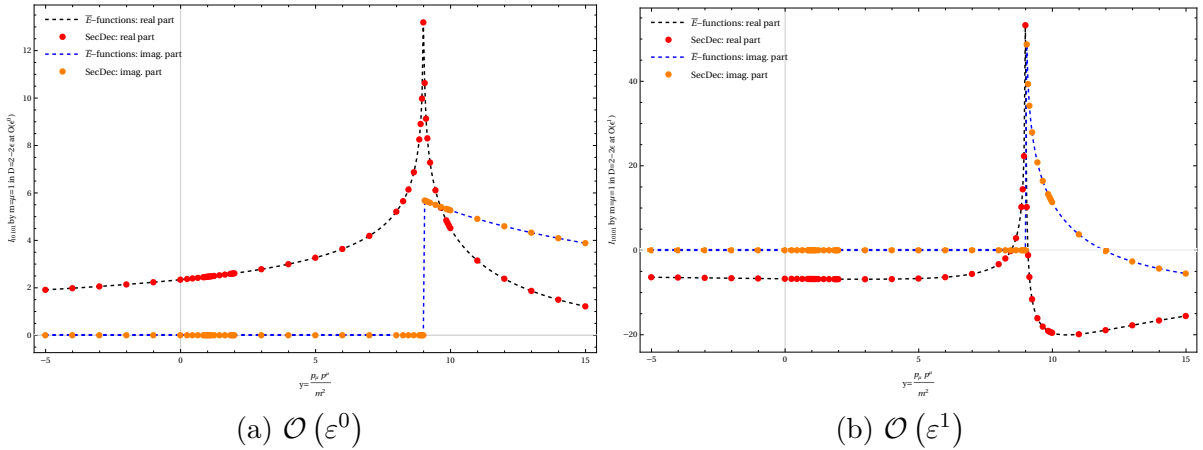
Figure 7.15: Comparison of the numerical evaluation of the real and the imaginary part of first two Laurent coefficients of the sunrise integral in $D = 2 - 2\varepsilon$ in terms of $\overline{\mathrm{E}}$-functions with the SecDec results.

We therefore need the first three orders of I_8 which can be taken from [124] and the first three orders of the integral I_{02210} listed above. The ε^{-2} and ε^{-1} contribution cancel and one finds the simple expression

$$\mathcal{I}_{11111}^{(0)} = \frac{1}{6t}\Bigg(81i\left(\mathrm{Li}_2\left(r_3^*\right) - \mathrm{Li}_2(r_3)\right)\overline{\mathrm{E}}_{1;-1}(r_3; 1; -q) + 162\overline{\mathrm{E}}_{0,2;-2,0;2}(r_3, r_3; 1, -1; -q)$$

$$+ \pi^2 G(1; t) - 6G(1, 0, 1; t) + 12G(0, 1, 1; t)\Bigg) .$$

$$(7.6.11)$$

for its first Laurent coefficient.

The numerical evaluation of the first Laurent coefficient and its comparison with SecDec is shown in fig. 7.16. We find good agreement in all kinematic regimes as well as on the thresholds. Since the kite develops an additional small imaginary part for $t = 9m^2$ which vanishes as t approaches $9m^2$ from above which might not be seen in fig. 7.16, we also compared numerically with the result from Remiddi and Tancredi [113]. We find that this additional imaginary part is well described by our analytical continuation, since we were able to obtain a smaller deviation from their result in terms of integrals over elliptic integrals than the change due to this additional small imaginary part. In our results this additional imaginary part can be seen in the discontinuity of the (complementary) parameter in the transition from region III to region IV shown in fig. (7.8) 7.7 (see also footnote 40).

I conclude this section by summarizing the results. Firstly we find, that all results obtained in [107, 109, 124] show already at low expansion orders in q very good agreement with the results obtained independently by SecDec and HPL obtained. We furthermore only have deviations which are explainable solely by the finite order of the expansion. By our analytic continuation of the periods, we completely governed all kinematic regimes and reproduce the correct monodromy of the hyperlogarithms in the letters $\{\frac{\mathrm{d}t}{t}, \frac{\mathrm{d}t}{t-1}\}$.
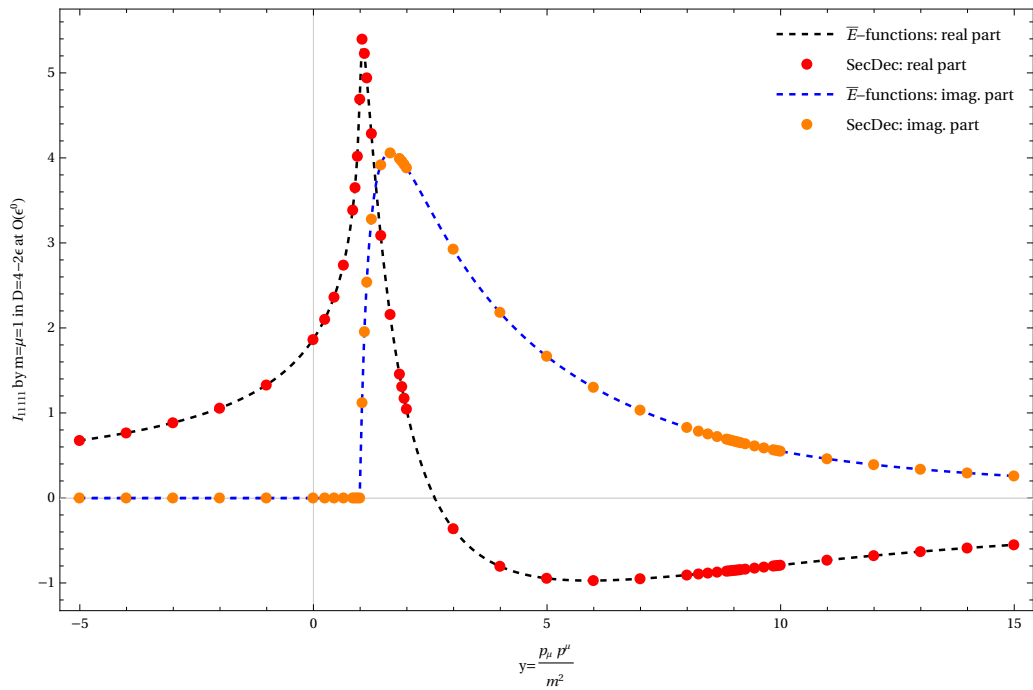
Figure 7.16: Comparison of the numerical evaluation of the real and the imaginary part of the first Laurent coefficient of the kite integral I_{11111} in $D = 4 - 2\varepsilon$ in terms of $\overline{\mathrm{E}}$-functions with the SecDec results.

Chapter 8

Conclusions and Outlook

In this chapter I will attempt to summarize the covered subjects of this thesis and to pin point their function therein. One can structure the content roughly into three main parts.

The first part includes the chapters 2, 3, 4 and 5 and can be seen as an introductory part. Its function is to establish some notions and recipes necessary during the later stages of this thesis. In these four chapters is outlined why we work in $D = 4 - 2\varepsilon$, what is meant by "families" or "topologies" and their master integrals and how to write down the parametric representation of Feynman integrals. Every of these sketched subjects is common in the computations of Feynman integrals but they are nonetheless objects of recent research and every of them would be worth a thesis in their own right since they are by no means exhausted. To give an example: During the later stage of this thesis another program for IBP-reductions has been introduced [31] and the here used one, Reduze 2 [28, 30], got a new update including many additional features.

The second main part is chapter 6. This part consists of two different approaches for a systematic computation of the Laurent-coefficients of Feynman integrals.

The main purpose of the introduction of parametric representation is threefold[1]. Firstly it should emphasize that already rather simple Feynman integrals give rise to a class of special functions, the hyperlogarithms, which are usually not encountered in the standard master studies in physics. Secondly it should introduce their properties as iterated integrals needed in the further proceeding of the thesis. Its third main purpose was to outline that by understanding the class of functions, their properties and application to Feynman integrals many at first different looking problems can be computed within the same framework.

The second presented approach was the method of differential equations. Here, the previously introduced hyperlogarithms were used to establish the concept of a canonical basis. I decided to introduce it by looking at the parametric representation for two reasons. The first one is, that there are currently only two approaches which make a direct connection to the properties of the Feynman integral. One is the parametric representation and one is the study of generalized unitary cuts [47]. While the latter one seems to be more universal it was at the time I started this thesis not as detailed covered[2] and the direct connection to the differential equations has been made explicitly

---

[1]I will refer here once again to the thesis of Panzer [35] since it is in my opinion the most complete and most detailed account on hyperlogarithms, their properties and application to Feynman integrals.

[2]That has changed recently due to e.g. [52, 77, 80, 87].

only recently [50]. The second one is, that by introducing the canonical basis within the parametric representation I could easily derive the basis of the canonical 5×5-subsystem needed in the computation of the kite [124]. Since the canonical basis approach turns the method of differential equations into the most powerful tool available for the computation of complete families of Feynman integrals its algorithmic construction has been gotten much attention in the last year [48, 53–55, 81].

The third part of this thesis is chapter 7. It can be seen as its main achievement, for which the other chapters lay out the foundations. To understand the approaches therein, one has to have a clear notion of which class of functions are currently used and how they contribute to the iterated structure of all order expansions of Feynman integrals. By understanding this it becomes clear, that one is interested in a similar approach for what can be described as mostly unknown territory currently. I decided to review the result of the equal mass sunrise [107] with an emphasis on its iterated structure since it is the first example of an expanded all order result of a Feynman integral beyond hyperlogarithms[3]. To obtain it a variable change to the nome associated with the family of elliptic curves defined by the zero locus of the second Symanzik polynomial has to be made. Furthermore a new class of functions, an elliptic generalization of polylogarithms, has to be introduced. Since both, the variable transform and the formulation of the integration kernels in terms of $\overline{\mathrm{E}}$-functions are highly non-trivial I devoted the appendix B to their derivation.

Understanding the equal mass sunrise and its iterated solution enabled us to compute the iterated all order result of the kite integral obtained in a joint work with Luise Adams, Christian Bogner and Stefan Weinzierl [124]. The kite integral is currently only the second Feynman integral beyond hyperlogarithms whose Laurent coefficients can be computed to all orders. I decided to present the result with emphasis on the structure rather than its explicit solution.

Lastly I discussed the analytic continuation into the physical regime as well as the numerical evaluation of the kite and all its sub-topologies. This results has been obtained in a joint work with Christian Bogner and Stefan Weinzierl [109]. The analytic continuation has its own striking beauty. Because rather than being a difficult computational task, as might be expected, it is simply a matter of understanding the underlying structure of the results and applying Feynman's $+i0$-prescription rigorously to it. From an aesthetic point of view that is quite satisfying. The numerical evaluation of our results and a comparison with the purely numerical evaluation by SecDec show perfect agreement in all kinematic regimes as well as close to the thresholds.

To me, the subjects covered in chapter 7 give rise to a number of new, but related questions. I will summarize some of them and attempt to give a short description of their origin.

The first known iterated all order solutions beyond hyperlogarithms for the sunrise was found by investigating the zero locus of the second Symanzik polynomial which is a nonssingular cubic in $\mathbb{P}^2$. But the sunrise only involves the trivial tadpole as an sub-topology. On the other hand we have the kite which has a far more complicated second Symanzik polynomial in $\mathbb{P}^4$. Furthermore, its differential equation involves non-trivial sub-topologies. We could compute it since we knew that the singular points of the differential equation of the kite are the same as the (pseudo-) thresholds of the sunrise. Therefore a transformation

---

[3]In a recent work it has been shown that it can as well be written as an iterated integral over modular forms [108].

into a differential equation in terms of the nome q of the sunrise could be obtained. That is a completely different approach compared to the study of an algebraic variety as in the sunrise case and, as shown in appendix B, expressing the singular points relies heavily on comparisons with **OEIS** . Resulting from that are two relevant questions.

Are Feynman integrals which involve the sunrise as the only elliptic sub-topology but for which the differential equation has different singular points computable in terms of $\overline{E}$-functions only?

Assuming they are computable in terms of $\overline{E}$-functions, what is their argument? The answer to these two questions will determine if we can compute e.g. the fully massive kite and its four-propagator sub-topology.

The second main question is related to the sunrise being the only elliptic integral having a second Symanzik polynomial in $\mathbb{P}^2$. With the knowledge from that polynomial the elliptic curve and its periods could be determined. The periods are hereby integrals along the cycles which generate the first homology group of the associated Riemann surface, the torus. The one-form in the period integrals is one element of the two dimensional first cohomology group.[4] We furthermore know that the periods fulfil the homogeneous part of the second order differential equation of the sunrise. On the other hand we know due to [52], that the maximal cut of a Feynman integral fulfils the homogeneous part of the differential equation as well. Furthermore, in Baikov-representation, the maximal cut can be directly computed as a contour integral determined by the vanishing of the Baikov polynomial and the cut Baikov variables [77,80]. Lastly, we have the connection between the dimension of the (co-) homology group and the number of master integrals made in [22]. Putting all these different approaches together hints at the questions:

Can we use the maximal cut to reconstruct the elliptic curve associated to our elliptic Feynman integral? If the connection between the contour-integrals obtained by the maximal-cut and the periods (integrals along the homology cycles) can be made, the parametrization of the Weierstraß-form of the associated elliptic curve can be reconstructed by using the Weierstraß $\wp$-function. The main advantage would be, that one would not have to use the zero locus of the second Symanzik polynomial, which will be in general a complicated high dimensional projective algebraic variety.

If one of the here formulated questions will have an positive answer will certainly determine the applicability of the discussed approach for the iterated all order solutions of Feynman integrals beyond hyperlogarithms.

---

[4]I did not use this terminology during the thesis since it would involve introducing new concepts.

Appendix A

Computation of the tadpole and the massless bubble

In the following, the tadpole-topology $\mathcal{I}_\nu$ is computed in Minkowskian-metric.

$$\mathcal{I}_n = (-1)^\nu \left(\mu^2\right)^{\nu-\frac{D}{2}} \int \frac{\mathrm{d}k^D}{i\pi^{\frac{D}{2}}} \frac{1}{(k^2-m^2)^\nu} \stackrel{\text{Wick-r.}}{=\!=\!=} \left(\mu^2\right)^{\nu-\frac{D}{2}} \left(\mu^2\right)^{\nu-\frac{D}{2}} \int \frac{\mathrm{d}K^D}{\pi^{\frac{D}{2}}} \frac{1}{(K^2+m^2)^\nu}$$

$$\stackrel{\text{sph. coor.}}{=\!=\!=} \left(\mu^2\right)^{\nu-\frac{D}{2}} \int_0^\infty \frac{K_e^{D-1}}{(K_e^2+m^2)^\nu} \frac{\mathrm{d}K_e}{\pi^{\frac{D}{2}}} \cdot \int \mathrm{d}\Omega_D = \left(\mu^2\right)^{\nu-\frac{D}{2}} \frac{2}{\Gamma(\frac{D}{2})(m^2)^\nu} \int_0^\infty \frac{K_e^{D-1}}{(\frac{K_e^2}{m^2}+1)^\nu} \mathrm{d}K_e$$

$$\stackrel{s=K_e^2/m^2}{=\!=\!=} \left(\frac{\mu^2}{m^2}\right)^{\nu-\frac{D}{2}} \frac{1}{\Gamma(\frac{D}{2})} \int_0^\infty \mathrm{d}s \frac{s^{\frac{D-2}{2}}}{(s+1)^\nu} \stackrel{\text{(A.0.2)}}{=\!=\!=} \left(\frac{\mu^2}{m^2}\right)^{\nu-\frac{D}{2}} \frac{\Gamma(\nu-\frac{D}{2})}{\Gamma(\nu)}$$

$$(\text{A.0.1})$$

where we used the definition of the Beta-function (see e.g. [141], S. 258)

$$B(z,w) = \int_0^\infty \mathrm{d}t \frac{t^{z-1}}{(t+1)^{z+w}} = \frac{\Gamma(z)\Gamma(w)}{\Gamma(z+w)} \qquad (\Re(z) > 0, \Re(w) > 0) \qquad (\text{A.0.2})$$

with $z = D/2$ und $w = n - D/2$ whereby $\Gamma(z)$ cancels the Gamma-function obtained by the integration of the D-sphere.

The result for the massless bubble can be easily computed from its parametric repre-

sentation:

$$
\begin{aligned}
I_{\nu_1,\nu_2} &= \left(\mu^2\right)^{\nu - \frac{D}{2}} \frac{\Gamma\left(\nu - \frac{D}{2}\right)}{\Gamma\left(\nu_1\right)\Gamma(\nu_2)} \int_0^\infty \int_0^\infty \mathrm{d}x_1 \mathrm{d}x_2 \delta(1 - (x_1 + x_2)) x_1^{\nu_1} x_2^{\nu_2} \frac{(x_1 + x_2)^{\nu - D}}{(-t x_1 x_2)^{\nu - \frac{D}{2}}} \\
&= \left(-\frac{\mu^2}{t}\right)^{\nu - \frac{D}{2}} \frac{\Gamma\left(\nu - \frac{D}{2}\right)}{\Gamma\left(\nu_1\right)\Gamma(\nu_2)} \int_0^\infty \mathrm{d}x \frac{x^{\nu_2 - 1}(1 + x)^{\nu - D}}{x^{\nu - \frac{D}{2}}} \\
&= \left(-\frac{\mu^2}{t}\right)^{\nu - \frac{D}{2}} \frac{\Gamma\left(\nu - \frac{D}{2}\right)}{\Gamma\left(\nu_1\right)\Gamma(\nu_2)} \int_0^\infty \mathrm{d}x \frac{x^{\nu_1 - 1 + \frac{D}{2}}}{(1 + x)^{\nu - D}} \\
&\stackrel{\text{(A.0.2)}}{=} \left(-\frac{\mu^2}{t}\right)^{\nu - \frac{D}{2}} \frac{\Gamma\left(\nu - \frac{D}{2}\right)}{\Gamma\left(\nu_1\right)\Gamma(\nu_2)} \frac{\Gamma\left(\frac{D}{2} - \nu_1\right)\Gamma\left(\frac{D}{2} - \nu_2\right)}{\Gamma(D - \nu_1 - \nu_2)} \; ,
\end{aligned}
\tag{A.0.3}
$$

where t denotes the momentum squared, $\nu = \nu_1 + \nu_2$ and the result is to be understood by means of an anlytic continuation of the Γ functions for higher propagator powers than $\nu_i = 2$.

Appendix B

Variable Transformations, Identities and Algorithms for $\overline{\text{E}}$-Functions

B.1 Changing the Kinematic Invariant to the Nome - The Sunrise and the Kite

The investigation of the iterated structure of the sunrise integral in section 7.3.2 makes intensive use of the change from the kinematic invariant $t = p_\mu p^\mu / m^2$ to the nome of the elliptic curve, associated with a representation of the elliptic curve in Jacobi uniformization. In this appendix some of the results presented e.g. in [105], which are used in section 7.1.1 will be derived[1] in a more explicit way.

Therefore we recall the two periods of the sunrise

$$\Psi_1 = \frac{4\mu^2}{m^2(1-t)^{\frac{3}{4}}(9-t)^{\frac{1}{4}}}K(m)$$

$$\Psi_2 = \frac{4i\mu^2}{m^2(1-t)^{\frac{3}{4}}(9-t)^{\frac{1}{4}}}K(m') \tag{B.1.1}$$

in terms of complete elliptic integrals of the first kind, where (m') m denotes the (complementary) parameter given as

$$m = \frac{e_3(t) - e_2(t)}{e_1(t) - e_2(t)}, \qquad\qquad m' = \frac{e_1(t) - e_3(t)}{e_1(t) - e_2(t)} \tag{B.1.2}$$

with

$$e_1(t) = \frac{m^4}{24\mu^4}\left(-t^2 + 6t + 3 + 3(1-t)^{\frac{3}{2}}(9-t)^{\frac{1}{2}}\right),$$

$$e_2(t) = \frac{m^4}{24\mu^4}\left(-t^2 + 6t + 3 - 3(1-t)^{\frac{3}{2}}(9-t)^{\frac{1}{2}}\right), \tag{B.1.3}$$

$$e_3(t) = \frac{m^4}{24\mu^4}\left(2t^2 - 12t - 6\right). \tag{B.1.4}$$

---

[1]Sometimes with different looking intermediate results which can all be transformed into the expression given in the literature.

The Wronskian of these to periods is given as

$$W\left(\Psi_1(t), \Psi_2(t)\right) = \Psi_1(t)\frac{\mathrm{d}}{\mathrm{d}t}\Psi_2(t) - \Psi_2(t)\frac{\mathrm{d}}{\mathrm{d}t}\Psi_1(t) = -\frac{12i\pi\mu^4}{m^4}\frac{1}{t(t-1)(t-9)} \; . \quad \text{(B.1.5)}$$

The nome is defined as

$$q = e^{i\pi\tau} \quad \text{(B.1.6)}$$

where

$$\tau = \frac{\Psi_2}{\Psi_1} \; . \quad \text{(B.1.7)}$$

B.1.1 Transformation of the Measure

The iterated integration obtained by varying the constant of the differential equation 7.3.49 is over the the kinematic invariant. The transformation of the measure reads

$$\mathrm{d}t = \frac{\mathrm{d}t}{\mathrm{d}\tau}\frac{\mathrm{d}\tau}{\mathrm{d}q}\mathrm{d}q \quad \text{(B.1.8)}$$

$$= \left(\frac{\mathrm{d}}{\mathrm{d}t}\left(\frac{\Psi_2}{\Psi_1}\right)\right)^{-1}\frac{\frac{1}{i\pi}\mathrm{d}\log(q)}{\mathrm{d}q}\mathrm{d}q \quad \text{(B.1.9)}$$

$$= \frac{1}{i\pi}\left(\underbrace{\frac{\Psi_2'\Psi_1 - \Psi_1'\Psi_2}{\Psi_1^2}}_{W(\Psi_1,\Psi_2)/\Psi_1^2}\right)^{-1}\frac{\mathrm{d}q}{q} \quad \text{(B.1.10)}$$

$$= \frac{1}{i\pi}\frac{\Psi_1^2}{W(\Psi_1, \Psi_2)}\frac{\mathrm{d}q}{q} \quad \text{(B.1.11)}$$

where $W(\Psi_1, \Psi_2)$ denotes the Wronskian of the fundamental system.

B.1.2 Expressing the Kinematic Invariant in Terms of q-Series

To change the kinematic invariant to the nome we consider the known q-series for the (complementary) parameter given by

$$m = \left(\frac{\vartheta_2(q)}{\vartheta_3(q)}\right)^4 \qquad\qquad m' = \left(\frac{\vartheta_4(q)}{\vartheta_3(q)}\right)^4 \quad \text{(B.1.12)}$$

with

$$\vartheta_2(q) = \sum_{n=-\infty}^{\infty} q^{n-\frac{1}{2}}$$

$$\vartheta_3(q) = \sum_{n=-\infty}^{\infty} q^{n^2} \quad \text{(B.1.13)}$$

$$\vartheta_4(q) = \sum_{n=-\infty}^{\infty} (-1)^n q^{n^2} \; .$$

By using (B.1.2) and (B.1.12) we get the relation

$$y = -\underbrace{\frac{16t}{(t-9)(t-1)^3}}_{y_t} = \underbrace{\left(\frac{\vartheta_2(q)\vartheta_4(q)}{(\vartheta_3(q))^2}\right)^4}_{y_q} . \tag{B.1.14}$$

To get an expression for t in term of a q-series in the whole Euclidian regime the first thing to notice is, that the absolute value of (B.1.14) is smaller than one and that $|q| < 1$ (since $\tau \in \mathbb{H}$) for all $t < 0$. The strategy to obtain the q-series is:

1. Expand $y_t = -\frac{16t}{(t-9)(t-1)^3}$ (l.h.s of (B.1.14)) around $t = 0$ and invert it to the power series $t = \sum_{i>1} b_i y^i$. The resulting power series is a germ of the analytic continuation of $t(y_t)$

2. Invert y_t analytically and choose the branch whose expansion around $y = 0$ coincides with the series obtained by the inversion of the power series $y = \sum_i a_i t^i$ around $t = 0$.

3. Replace y_t by y_q and expand $t(y_q) = t(q)$ (substitute r.h.s. of (B.1.14)) in q and compare with the *The On-Line Encyclopedia of Integer Sequences®* (OEIS®)[2] if the coefficient sequence is a known q-series.

The first step can be easily done by a Taylor expansion of $y_t = -\frac{16t}{(t-9)(t-1)^3}$ in a vicinity of $t = 0$[3] and inverting it to the unique power series $\tilde{t}(y)^4$. The first few terms of the result are

$$\tilde{t}(y) = -\frac{9y}{16} - \frac{63y^2}{64} - \frac{4743y^3}{2048} - \frac{102609y^4}{16384} - \frac{19261161y^5}{1048576} + \mathcal{O}\left(y^6\right) . \tag{B.1.15}$$

This series defines the germ of the (multivalued) function $y^{-1} = t$ we are interested in. By solving

$$y = -\frac{16t}{(t-9)(t-1)^3} \tag{B.1.16}$$

with respect to $t(y)$ one finds four possible solutions (corresponding to the preimages/branches). We choose y^{-1} on the branch such that it has the same expansion around[5] $y = 0$ as $\tilde{t}$. It is given by

$$t(y) = 3 - \sqrt{\frac{2^{2/3}}{y^{2/3}} + \frac{2\sqrt[3]{2}}{\sqrt[3]{y}} + 4} + \frac{1}{2}\sqrt{\frac{16 - 64y}{\sqrt{\frac{2^{2/3}}{y^{2/3}} + \frac{2\sqrt[3]{2}}{\sqrt[3]{y}} + 4y}} - \frac{4 \cdot 2^{2/3}}{y^{2/3}} - \frac{8\sqrt[3]{2}}{\sqrt[3]{y}} + 32} . \tag{B.1.17}$$

The next step is to replace in (B.1.17) y by its product of ϑ-functions (B.1.14) and expand in q. The first few terms of the resulting series are

$$t(q) = -9q - 36q^2 - 90q^3 - 180q^4 - 351q^5 - 684q^6 + \mathcal{O}\left(q^7\right) . \tag{B.1.18}$$

---

[2] http://oeis.org/
[3] The convergence radius of this expansion is one.
[4] This can be done easily by using Mathematica's **InverseSeries**[] since $\lim_{t\to 0} y = 0$.
[5] This power series has convergence radius $1/4$, corresponding to $y(t_0|_{y'(t_0)=0}) = 1/4$.

Normalizing with -9 and comparing with **OEIS** yields three (almost) matching sequences (**A164617**, **A128640**, **A128641**) of known q-expansions. The one used in the following[6] is related to **A128640** and reads

$$t(q) = -9q \left(\frac{\Psi(-q^3)}{\Psi(-q)} \right)^4 = -\frac{9q\,((q^3; -q^3)_\infty)^4\,((q^6; q^6)_\infty)^4}{((q; -q)_\infty)^4\,((q^2; q^2)_\infty)^4} \,, \qquad \text{(B.1.19)}$$

where

$$\Psi(q) = (-q; q)_\infty \left(q^2; q^2 \right)_\infty \qquad \text{(B.1.20)}$$

denotes Ramanujan's Ψ function [7] and the q-Pochammer symbol has the product representation

$$(a; q)_\infty = \prod_{k=0}^{\infty} (1 - aq^k) \,. \qquad \text{(B.1.21)}$$

We may express $t(q)$ in terms *Dedekind-η* functions by using

$$\eta(\tau) = e^{\frac{i\pi\tau}{12}} \prod_{n=1}^{\infty} \left(1 - e^{2i\pi n\tau} \right) = q^{\frac{1}{12}} \prod_{n=1}^{\infty} \left(1 - q^{2n} \right) = q^{\frac{1}{12}} \left(q^2; q^2 \right)_\infty \,. \qquad \text{(B.1.22)}$$

The main difference to [105, 107] is, that by the virtue of $t(y)$ being a holomorphic function of y_q we can conclude that (B.1.19) holds for the whole Euclidian regime, where the periods are defined by (B.1.1) such that $|q| < 1$.

B.1.3 Expression of the Periods as q-Series

For the (complementary) complete elliptic integral of the first kind (K') K one has the expression

$$K = \frac{\pi}{2} \vartheta_3^2(q) \qquad\qquad K' = -\frac{\log(q)}{2} \vartheta_3^2(q) \,. \qquad \text{(B.1.23)}$$

Inserting this relation in (B.1.1) and using $t(q)$ (B.1.19) for the prefactor yields expressions in terms of q-series. The first few terms of the q-series are

$$\Psi_1 \propto \frac{\vartheta_3^2(q)}{(1 - t_q)^{3/4} \sqrt[4]{9 - t_q}} = \frac{1}{\sqrt{3}} - \sqrt{3}q + \sqrt{3}q^2 - \sqrt{3}q^3 + \sqrt{3}q^4 + \sqrt{3}q^6 + \mathcal{O}\left(q^7 \right) \qquad \text{(B.1.24)}$$

where $t_q = t(q)$ (B.1.19). Normalizing with $\sqrt{3}$ and comparing with **OEIS** reveals agreement with the sequence **A137608** given as

$$\frac{\vartheta_3^2(q)}{\sqrt{3}\,(1 - t_q)^{3/4} \sqrt[4]{9 - t_q}} = \frac{\Psi(-q)^3}{\Psi(-q^3)} \,. \qquad \text{(B.1.25)}$$

---

[6]One can check by expansion in q that it is equivalent to the expression given in [107].
[7]see e.g. [142] for an overview of its properties

B.1.4 Expressing the Kernel $\Psi_1^3/W(\Psi_1, \Psi_2)$ in Terms of $\overline{\mathrm{E}}$-Functions

Up to a multiplicative constant, this integration kernel reads

$$\frac{\Psi_1^3}{W(\Psi_1, \Psi_2)} \propto \frac{(9 - t_q)^{\frac{1}{4}} t_q \vartheta_3^6(q)}{(1 - t_q)^{5/4}} \tag{B.1.26}$$

where $t_q = t(q)$ is given in (B.1.19). Expanding this expression in terms of the nome q yields a power series, where the first few terms are

$$\frac{(9 - t_q)^{\frac{1}{4}} t_q \vartheta_3^6(q)}{(1 - t_q)^{5/4}} = -9\sqrt{3}q - 45\sqrt{3}q^2 - 81\sqrt{3}q^3 - 99\sqrt{3}q^4 - 216\sqrt{3}q^5 - 405\sqrt{3}q^6 + \mathcal{O}\left(q^7\right) . \tag{B.1.27}$$

Normalizing with respect to the first coefficients and comparing with **OEIS** shows that the obtained q-series is the known sequence **A214262**. Using the results of **OEIS** we have

$$-\frac{1}{9\sqrt{3}} \frac{(9 - t_q)^{\frac{1}{4}} t_q \vartheta_3^6(q)}{(1 - t_q)^{5/4}} = \frac{q\left((-q; -q)_\infty\right)^5 \left(-q^3; -q^3\right)_\infty \left((q^6; q^6)_\infty\right)^4}{\left((q^2; q^2)_\infty\right)^4} \tag{B.1.28}$$

$$= \sum_{k=1}^{\infty} \frac{k^2(-1)^k(-q)^k}{(-q)^k + (-q)^{2k} + 1} \tag{B.1.29}$$

$$= \sum_{k=1}^{\infty} \frac{k^2(-1)^k(-q)^k}{\left(r_3 - (-q)^k\right)\left(r_3^* - (-q)^k\right)} \tag{B.1.30}$$

$$= -\frac{i}{\sqrt{3}} \sum_{k=1}^{\infty} k^2(-1)^k \left(\frac{1}{1 - r_3(-q)^k} - \frac{1}{1 - r_3^*(-q)^k}\right) \tag{B.1.31}$$

$$= -\frac{i}{\sqrt{3}} \sum_{k=1}^{\infty} \sum_{l=1}^{\infty} k^2(-1)^k \left(r_3^l(-q)^{kl} - (r_3^*)^l(-q)^{kl}\right) \tag{B.1.32}$$

$$= -\frac{i}{\sqrt{3}} \left(\mathrm{ELi}_{-2,0}(-1, r_3, -q) - \mathrm{ELi}_{-2,0}(-1, r_3^*, -q)\right) \tag{B.1.33}$$

$$= \frac{1}{\sqrt{3}} \overline{\mathrm{E}}_{-2,0}(-1, r_3, -q) , \tag{B.1.34}$$

where r_3 denotes the third root of unity and the sum representation in the second line (B.1.29) is given on the **OEIS**. Partial fraction decomposition, as well as identifying a geometric series lead to (B.1.32). Including the constant stemming from Ψ_1 and W one has

$$\frac{\Psi_1^3}{W(\Psi_1, \Psi_2)} = -6i\pi^2 \frac{\mu^2}{m^2} \overline{\mathrm{E}}_{-2,0}(-1, r_3, -q) . \tag{B.1.35}$$

B.1.5 Expressing the Kernel $\Psi_1^4(t + 3)^4$ in Terms of $\overline{\mathrm{E}}$-Functions

We have by using (B.1.1) and replacing the elliptic integral by the ϑ-function (B.1.23)

$$\Psi_1(t + 3) \propto \frac{3(1 - t_q)^{\frac{1}{4}}(9 - t_q)^{3/4}\vartheta_3^2(q)}{2(t_q - 9)} - \frac{(1 - t_q)^{\frac{1}{4}}(9 - t_q)^{3/4}\vartheta_3^2(q)}{2(t_q - 1)} . \tag{B.1.36}$$

The comparison with **OEIS** shows that the expansion of both terms matches the sequence **A123331**.

Transforming $\frac{3(1-t_q)^{\frac{1}{4}}(9-t_q)^{3/4}\vartheta_3^2(q)}{2(t_q-9)}$ to $\overline{\mathrm{E}}$-Functions

The first few terms of the q-expansion of the first term are

$$\frac{3\left(1-t_q\right)^{\frac{1}{4}}\left(9-t_q\right)^{3/4}\vartheta_3^2(q)}{2\left(t_q-9\right)}=-\frac{\sqrt{3}}{2}-3\sqrt{3}q-6\sqrt{3}q^2-3\sqrt{3}q^3+3\sqrt{3}q^4-6\sqrt{3}q^6+\mathcal{O}\left(q^7\right)$$
(B.1.37)

and comparing the coefficients after normalizing with $3\sqrt{3}$ yields the known sequence **A123331**. Using the results therein, we have

$$\frac{1}{3\sqrt{3}}\frac{3\left(1-t_q\right)^{\frac{1}{4}}\left(9-t_q\right)^{3/4}\vartheta_3^2(q)}{2\left(t_q-9\right)}=-\frac{1}{6}-\sum_{k=1}^{\infty}\frac{(-1)^k(-q)^k}{(-q)^k+(-q)^{2k}+1}$$
(B.1.38)

$$=-\frac{1}{6}-\frac{1}{\sqrt{3}}\overline{\mathrm{E}}_{0,0}(-1,r_3,-q)$$
(B.1.39)

where we used, that the series is basically the same as in the treatment of the first kernel $\Psi_1^3/W(\Psi_1,\Psi_2)$.

Transforming $\frac{(1-t_q)^{\frac{1}{4}}(9-t_q)^{3/4}\vartheta_3^2(q)}{2(t_q-1)}$ to $\overline{\mathrm{E}}$-Functions

The q-expansion of the second summand reads

$$\frac{\left(1-t_q\right)^{\frac{1}{4}}\left(9-t_q\right)^{3/4}\vartheta_3^2(q)}{2\left(t_q-1\right)}=-\frac{3\sqrt{3}}{2}+3\sqrt{3}q-6\sqrt{3}q^2+3\sqrt{3}q^3-3\sqrt{3}q^4-6\sqrt{3}q^6+O\left(q^7\right)$$
(B.1.40)

and we see, that the coefficients are up to their signs the same as in the previous case. We therefore can take a similar series, namely

$$\frac{1}{3\sqrt{3}}\frac{\left(1-t_q\right)^{\frac{1}{4}}\left(9-t_q\right)^{3/4}\vartheta_3^2(q)}{2\left(t_q-1\right)}=-\frac{1}{2}-\sum_{k=1}^{\infty}\frac{(-q)^k}{-(-q)^k+(-q)^{2k}+1}$$
(B.1.41)

$$=-\frac{1}{2}+\frac{1}{\sqrt{3}}\overline{\mathrm{E}}_{0,0}\left(1,r_6^*,-q\right)$$
(B.1.42)

where the sixth root of unity enters due to the different denominator.

Putting everything together and including the prefactors yields

$$\Psi_1(q)(t_q+3)=\frac{6\pi\mu^2}{m^2}\left(\frac{1}{\sqrt{3}}-\overline{\mathrm{E}}_{0,0}\left(1,r_6^*,-q\right)-\overline{\mathrm{E}}_{0,0}\left(-1,r_3,-q\right)\right)$$
(B.1.43)

$$=\frac{6\pi\mu^2}{m^2}\left(\frac{1}{\sqrt{3}}+2\overline{\mathrm{E}}_{0,0}\left(1,r_3,-q\right)\right)$$
(B.1.44)

where we used the identity (B.3.1) shown in section (B.3.1).

B.1.6 Expressing the Kite Kernel $\Psi_1^3/((t-1)W(\Psi_1, \Psi_2))$ in Terms of $\overline{\mathrm{E}}$-Functions

For the kite integral we have in addition to the sunrise kernels the kernel

$$\frac{\Psi_1}{(t_q - 1)W_q(\Psi_1, \Psi_2)} \propto \frac{(t_q - 9)t_q \vartheta_3(q)^6}{(1 - t_q)^{9/4}(9 - t_q)^{3/4}} \ , \tag{B.1.45}$$

where we used (B.1.1) and replaced the elliptic integral by the ϑ-function (B.1.23). The first few terms of the q-expansion read

$$\frac{(t_q - 9)t_q \vartheta_3(q)^6}{(1 - t_q)^{9/4}(9 - t_q)^{3/4}} = 9\sqrt{3}q - 36\sqrt{3}q^2 + 81\sqrt{3}q^3 - 144\sqrt{3}q^4 + 216\sqrt{3}q^5 - 324\sqrt{3}q^6 + \mathcal{O}\left(q^7\right) \tag{B.1.46}$$

and normalizing with the leading coefficient $9\sqrt{3}$ yields the matching sequence **A122373** in the OEIS. Using the sum representation therein we have

$$\frac{1}{9\sqrt{3}} \frac{(t_q - 9)t_q \vartheta_3(q)^6}{(1 - t_q)^{9/4}(9 - t_q)^{3/4}} = \frac{-9}{8} \sum_{k=0}^{\infty} \frac{k^2(-q)^k}{(-q)^k + (-q)^{2k} + 1} - \frac{1}{8} \sum_{k=0}^{\infty} \frac{(-1)^k k^2(-q)^k}{(-q)^k + (-q)^{2k} + 1}$$

$$= -\frac{1}{8\sqrt{3}} \left(9\overline{\mathrm{E}}_{-2;0}\left(1; r_3; -q\right) + \overline{\mathrm{E}}_{-2;0}\left(-1; r_3; -q\right) \right) \tag{B.1.47}$$

where we used that it is basically the same sum as in section B.1.4. Inserting the constants we have

$$\frac{\Psi_{1,q}}{(t_q - 1)W_q(\Psi_1, \Psi_2)} = -\frac{6i\pi^2}{8} \frac{\mu^2}{m^2} \left(9\overline{\mathrm{E}}_{-2;0}\left(1; r_3; -q\right) + \overline{\mathrm{E}}_{-2;0}\left(-1; r_3; -q\right) \right) \ , \tag{B.1.48}$$

where r_3 denotes the third root of unity.

B.1.7 Expressing $\log(t_q)$, $\log(1 - t_q)$ and $\log(1 - t_q/9)$ in Terms of $\overline{\mathrm{E}}$-Functions

For the sunrise as well as the kite integral it is important to do derive the representation of certain logarithms of the kinematic invariant in terms $\overline{\mathrm{E}}$-functions. This will be done in the following by

1. Finding a representation of the argument of the logarithm as a product of q-Pochammer symbols by using **OEIS**.

2. Transform the resulting logarithm by using the in section B.2 discussed methods and in particular (B.2.13) and (B.2.12).

$\underline{\log(t_q)}$:

We use the representation (B.1.19) and have

$$\log(t_q) = \log\left(-\frac{9q\left((q^3;-q^3)_\infty\right)^4\left((q^6;q^6)_\infty\right)^4}{\left((q;-q)_\infty\right)^4\left((q^2;q^2)_\infty\right)^4}\right)$$
$$\overset{\text{B.2}}{=\joinrel=} -4(\overline{\text{E}}_{1;0}\left(r_6;1;-q\right)+\overline{\text{E}}_{1;0}\left(r_6;1;q\right)+\overline{\text{E}}_{1;0}\left(r_3;1;q\right))+\log(-9q) \quad\quad \text{(B.1.49)}$$
$$= -8\overline{\text{E}}_{1;0}\left(r_6;1;-q\right)-4\overline{\text{E}}_{1;0}\left(r_3;1;-q\right)+\log(-9q)$$
$$= -4\overline{\text{E}}_{1;0}\left(r_3;-1;-q\right)+\log(-9q)$$

where we synchronized the argument to $-q$ in the second to last line (see (7.3.54)) and summarized the $\overline{\text{E}}$-functions (see B.3.2). The identity which yields the last line is not covered in this appendix[8] but its validity has been verified up to order $\mathcal{O}(q^{800})$.

$\underline{\log(1-t_q)}$:

The expansion of $1-t_q$ coincides with the sequence **A132972** from which we get

$$\log(1-t_q) = 3\log\left(\frac{\left((-q;-q)_\infty\right)^3(q^6;q^6)_\infty}{\left((q^2;q^2)_\infty\right)^3(-q^3;-q^3)_\infty}\right) \quad\quad \text{(B.1.50)}$$
$$= 3(\overline{\text{E}}_{1;0}\left(-1;1;-q\right)-\overline{\text{E}}_{1;0}\left(r_6;1;-q\right))$$

where the argument was synchronized to $-q$[9].

$\underline{\log(1-t_q/9)}$:

For $1-t_q/9$ we find by comparison of the coefficients of the q-expansion that it corresponds to the known sequence **A164617** obtained by expanding a specific quotient of Ramanujan's Ψ and Φ functions. We have in terms of q-Pochammer symbols

$$1-t_q/9 = \frac{\left((-q^3;-q^3)_\infty\right)^3(q^6;q^6)_\infty}{(-q;-q)_\infty\left((q;-q)_\infty\right)^2\left((q^2;q^2)_\infty\right)^3\left((q^3;-q^3)_\infty\right)^2} \quad\quad \text{(B.1.51)}$$

and therefore

$$\log(1-t_q/9) = \log\left(\frac{\left((-q^3;-q^3)_\infty\right)^3(q^6;q^6)_\infty}{(-q;-q)_\infty\left((q;-q)_\infty\right)^2\left((q^2;q^2)_\infty\right)^3\left((q^3;-q^3)_\infty\right)^2}\right) \quad\quad \text{(B.1.52)}$$
$$= 3\overline{\text{E}}_{1;0}\left(-1;1;-q\right)+\overline{\text{E}}_{1;0}\left(r_6;1;-q\right)-4\overline{\text{E}}_{1;0}\left(r_3;1;-q\right) \quad\quad \text{(B.1.53)}$$

where the argument was synchronized to $-q$.

---

[8]It involves showing that a certain partitioning of terms q^{ij}/j for every $i\cdot j$ even cancels identically at every order in q.

[9]We get $\overline{\text{E}}$-functions with argument q and $-q$. Transformation to the same argument $-q$ is meant by "synchronizing" in the following.

B.2 Logarithms of q-Pochammer Symbols and ELi-Functions

In the following section I will show, that there is an easy translation of logarithms of q-Pochammer symbols into ELi- and $\overline{\text{E}}$-functions. This relationship is useful for practical computations, since every of the q-series found by comparison with **OEIS** can be expressed in terms of q-Pochammer symbols.

The q-Pochammer symbols of interest are

$$
\begin{aligned}
(\alpha q^a, \beta q^a)_\infty &= \prod_{k=0}^\infty \left(1 - \alpha q^a (\beta q^a)^k\right) \\
&= \prod_{k=0}^\infty \left(1 - \left(\left(\frac{\alpha}{\beta}\right)^{\frac{1}{a}} (\beta^{\frac{1}{a}} q)^{k+1}\right)^a\right)
\end{aligned}
\tag{B.2.1}
$$

where $a \in \mathbb{Z}$ and $\alpha, \beta, q \in \mathbb{C}$ such that the product converges. In the cases relevant to this thesis we always have $\alpha = \pm\beta = \pm 1$.

The first thing to notice is, that

$$
\begin{aligned}
\log\left((\alpha q^a, \beta q^a)_\infty\right) &\overset{\text{(B.2.1)}}{=} \log\left(\prod_{k=0}^\infty \left(1 - \alpha q^a (\beta q^a)^k\right)\right) \\
&= \sum_{k=0}^\infty \log\left(1 - \frac{\alpha}{\beta}(\beta q^a)^{k+1}\right) \\
&= -\sum_{n=1}^\infty \sum_{k=0}^\infty \frac{1}{n}\left(\frac{\alpha}{\beta}\right)^n (\beta q^a)^{n(k+1)} \\
&\overset{k \to k+1}{=} -\text{ELi}_{1;0}\left(\frac{\alpha}{\beta}; 1; \beta q^a\right) \ .
\end{aligned}
\tag{B.2.2}
$$

The problem with this representation is, that it translates into ELi's of higher order q^a dependence instead of q. This problem can be easily circumvented by consideration of the factorization

$$
\begin{aligned}
1 - \left(\left(\frac{\alpha}{\beta}\right)^{\frac{1}{a}} (\beta^{\frac{1}{a}} q)^{k+1}\right)^a &=: 1 - x_{\alpha,\beta}(q)^a \\
&= e^{i\pi} \prod_{1 \le n \le a} \left(x - e^{2i\pi \frac{n}{a}}\right) \\
&= e^{i\pi(1+a)} e^{\frac{2i\pi}{a}\sum_{n=1}^a n} \prod_{1 \le n \le a} \left(1 - x \underbrace{e^{-2i\pi \frac{n}{a}}}_{=:w_a^*(n)}\right) \\
&\overset{a \in \mathbb{Z}}{=} \prod_{1 \le n \le a} \left(1 - \left(\frac{\alpha}{\beta}\right)^{\frac{1}{a}} w_a^*(n)(\beta^{\frac{1}{a}} q)^{k+1}\right)
\end{aligned}
\tag{B.2.3}
$$

where $w_a^*(n)$ is a root of unity[10]. With this factorization we have

$$(\alpha q^a, \beta q^a)_\infty = \prod_{1 \le n \le a} \left(w_a^*(n) \left(\frac{\alpha}{\beta} \right)^{\frac{1}{a}} \beta^{\frac{1}{a}} q, \beta^{\frac{1}{a}} q \right)_\infty \tag{B.2.4}$$

and therefore

$$\log\left((\alpha q^a, \beta q^a)_\infty \right) \overset{(B.2.4)}{=\!=\!=} \sum_{1 \le n \le a} \log\left(\left(w_a^*(n) \left(\frac{\alpha}{\beta} \right)^{\frac{1}{a}} \beta^{\frac{1}{a}} q, \beta^{\frac{1}{a}} q \right)_\infty \right)$$

$$\overset{(B.2.2)}{=\!=\!=} - \sum_{1 \le n \le a} \mathrm{ELi}_{1,0}\left(w_a^*(n) \left(\frac{\alpha}{\beta} \right)^{\frac{1}{a}}; 1; \beta^{\frac{1}{a}} q \right). \tag{B.2.5}$$

The Special Case $\alpha = \pm\beta$ and the Representation with $\overline{\mathrm{E}}$

The sum (B.2.5) can in general not easily be written in terms of $\overline{\mathrm{E}}$ functions, due to the prefactor $\left(\frac{\alpha}{\beta} \right)^{\frac{1}{a}}$ in front of the roots of unity $w_a(n)$. But for $\alpha = \pm\beta$ it can. Here one has to notice:

1. $\overline{\mathrm{E}}_{0,1}\left((\pm 1)^{\frac{1}{a}} w_a(n), 1, q \right) = \mathrm{ELi}_{0,1}\left((\pm 1)^{\frac{1}{a}} w_a(n), 1, q \right) + \mathrm{ELi}_{0,1}\left(\left((\pm 1)^{\frac{1}{a}} w_a(n) \right)^*, 1, q \right)$

2. For every $(\pm 1)^{\frac{1}{a}} w_a(n) \notin \mathbb{R}$, the complex conjugate $\left((\pm 1)^{\frac{1}{a}} w_a(n) \right)^* \notin \mathbb{R}$ is also in the sum (B.2.5)

From that observation it follows directly for $\alpha = \pm\beta$

$$\log\left((\pm\beta q^a, \beta q^a)_\infty \right) = - \sum_{1 \le n \le a} \mathrm{ELi}_{1,0}\left(w_a^*(n) (\pm 1)^{\frac{1}{a}}; 1; \beta^{\frac{1}{a}} q \right) \tag{B.2.6}$$

$$= -\frac{1}{2} \sum_{\substack{1 \le n \le a \\ n | (\pm 1)^{\frac{1}{a}} w_a^*(n) \in \{\pm 1\}}} \overline{\mathrm{E}}_{1,0}\left((\pm 1)^{\frac{1}{a}} w_a^*(n); 1; \beta^{\frac{1}{a}} q \right) \tag{B.2.7}$$

$$- \sum_{\substack{1 \le n \le a \\ n | (\pm 1)^{\frac{1}{a}} w_a^*(n) \in \mathbb{H}}} \overline{\mathrm{E}}_{1,0}\left((\pm 1)^{\frac{1}{a}} w_a^*(n); 1; \beta^{\frac{1}{a}} q \right) \tag{B.2.8}$$

where $\mathbb{H}$ denotes the upper half plane.

Possible Reduction of the Argument

In the result (B.2.8) there is still one problem, since there is a $\beta^{\frac{1}{a}}$ term in front of the nome. Such a term is in general not wanted, since it spoils the multiplication properties. In some cases, it can easily be removed. For this we note, that the resulting q-series $(\alpha = \pm\beta)$ has the form

$$\log\left((\pm\beta q^a, \beta q^a)_\infty \right) = \sum_{j,l>0} \frac{1}{j} \left((\pm 1)^{\frac{j}{a}} \sum_{k=1}^{a} (w_a(k))^j \right) \left(\beta^{\frac{1}{a}} q \right)^{jl} \tag{B.2.9}$$

---

[10]Not necessarily a primitive one like the r_n's.

where $w_a(k)^j = e^{2i\pi kj/a}$ and[11]

$$\sum_{k=1}^{a}(w_a(k))^j = \begin{cases} a & \text{for } j = a \cdot n | n \in \mathbb{Z} \\ 0 & \text{else} \end{cases} \tag{B.2.10}$$

We can therefore write the result as:

$$\log\left((\pm\beta q^a, \beta q^a)_\infty\right) = \sum_{j,l>0} \frac{1}{aj}\left((\pm1)^j a\right)\left(\beta^{\frac{1}{a}}q\right)^{ajl} \tag{B.2.11}$$

and get the two cases:

$\underline{\beta = 1}$:

$$\log\left((\pm q^a, q^a)_\infty\right) = -\frac{1}{2} \sum_{\substack{1 \le n \le a \\ n|(\pm1)^{\frac{1}{a}}w_a^*(n) \in \{\pm1\}}} \overline{\mathrm{E}}_{1,0}\left((\pm1)^{\frac{1}{a}}w_a^*(n); 1; q\right)$$

$$- \sum_{\substack{1 \le n \le a \\ n|(\pm1)^{\frac{1}{a}}w_a^*(n) \in \mathbb{H}}} \overline{\mathrm{E}}_{1,0}\left((\pm1)^{\frac{1}{a}}w_a^*(n); 1; q\right) \tag{B.2.12}$$

$\underline{\beta = -1, a \text{ } \mathbf{odd}}$:

$$\log\left((\pm q^a, -q^a)_\infty\right) = -\frac{1}{2} \sum_{\substack{1 \le n \le a \\ n|(\pm1)^{\frac{1}{a}}w_a^*(n) \in \{\pm1\}}} \overline{\mathrm{E}}_{1,0}\left((\mp1)^{\frac{1}{a}}w_a^*(n); 1; -q\right)$$

$$- \sum_{\substack{1 \le n \le a \\ n|(\pm1)^{\frac{1}{a}}w_a^*(n) \in \mathbb{H}}} \overline{\mathrm{E}}_{1,0}\left((\mp1)^{\frac{1}{a}}w_a^*(n); 1; -q\right) . \tag{B.2.13}$$

We conclude this section by summarizing its results. The first takeaway is, that we can transform every q-Pochammer symbol where the powers of q are the same[12] into ELi-functions which might have an higher order of q in its argument. ELi-functions with higher order of q in its argument might conflict with the iterated integration used throughout this thesis. Therefore further restriction on the form of the q-Pochammer symbols had to be made, but the class which can be transformed directly into $\overline{\mathrm{E}}$-functions is still quite big and given by (B.2.12) and (B.2.13). They are enough for a derivation of all necessary results in this thesis. Nonetheless, this is probably a point where further generalizations are possible.

---

[11]Proof: For $j = a \cdot n$ clear; For $j \neq n \cdot a \Rightarrow e^{2i\pi j/a} \neq 1$, such that $\sum_{k=1}^{a}\left(e^{2i\pi\frac{j}{a}}\right)^k = \frac{1-e^{2i\pi j}}{1-e^{2i\pi\frac{j}{a}}} = 0$ where the geometric series was used.

[12]That condition might not be necessary, since e.g. identities like $(q,q^2)_\infty = 1/(-q,q)_\infty$ [142] can be used.

B.3 Identities of $\overline{\mathrm{E}}$-Functions

B.3.1 An $\overline{\mathrm{E}}$-Identity Involving the Third and Sixth Root of Unity

In the following the identity

$$\left(\overline{\mathrm{E}}_{n,n}(1, r_3, q) + \overline{\mathrm{E}}_{n,n}(-1, r_3, q)\right) + \left(\overline{\mathrm{E}}_{n,n}(1, r_3, q) + \overline{\mathrm{E}}_{n,n}(1, r_6^*, q)\right) = 0 \qquad \text{(B.3.1)}$$

where r_n denotes the *n-th* root of unity and which was used for the simplification of the integration kernels will be shown for the case $m = n = 0$[13]. The first summand can be written as

$$\overline{\mathrm{E}}_{0,0}(1, r_3, q) + \overline{\mathrm{E}}_{0,0}(-1, r_3, q) = \frac{1}{i} \sum_{i,j>0} \left(1 + (-1)^j\right) \underbrace{\left(r_3^i - (r_3^*)^i\right)}_{2i\Im\left(r_3^i\right)} q^{ij} \qquad \text{(B.3.2)}$$

$$= 4 \sum_{i,j>0} \sin\left(\frac{2\pi i}{3}\right) q^{2ij} \ . \qquad \text{(B.3.3)}$$

The second summand reads

$$\overline{\mathrm{E}}_{0,0}(1, r_3, q) + \overline{\mathrm{E}}_{0,0}(1, r_6^*, q) = \frac{1}{i} \sum_{i,j>0} \left(r_3^i - (r_3^*)^i + (r_6^*)^i - r_6^i\right) q^{ij} \qquad \text{(B.3.4)}$$

$$= 2 \sum_{i,j>0} \underbrace{\left(\sin\left(\frac{2\pi i}{3}\right) - \sin\left(\frac{2\pi i}{6}\right)\right)}_{=0 \text{ for } i=2n+1} q^{ij} \qquad \text{(B.3.5)}$$

$$= 2 \sum_{i,j>0} \underbrace{\left(2\cos\left(\frac{2\pi i}{3}\right) - 1\right)}_{\substack{= -2 \ \forall i | \mathrm{mod}(i,3) \neq 0 \\ = \ 1 \ \forall i | \mathrm{mod}(i,3) = 0}} \underbrace{\sin\left(\frac{2\pi i}{3}\right)}_{=0 \ \forall i | \mathrm{mod}(i,3)=0} q^{2ij} \qquad \text{(B.3.6)}$$

$$= -4 \sum_{i,j>0} \sin\left(\frac{2\pi i}{3}\right) q^{2ij} \qquad \text{(B.3.7)}$$

and we see, that at every order in q both summands cancel exactly.

B.3.2 A Useful Relation for $m + n$ Odd at Roots of Unity

Because of the definition of the $\overline{\mathrm{E}}$-function

$$\overline{\mathrm{E}}_{m;n}(x; y; q) = \mathrm{ELi}_{m;n}(x; y; q) + \mathrm{ELi}_{m;n}\left(\frac{1}{x}; \frac{1}{y}; q\right) \text{ for } m + n = 2k + 1 | k \in \mathbb{Z} \qquad \text{(B.3.8)}$$

and $(\zeta_i^k)^* = 1/\zeta_i^k$ with ζ_i^k being a root of unity, we immediately have

$$\overline{\mathrm{E}}_{m;n}\left(\zeta_i^k; \zeta_j^l; q\right) = \overline{\mathrm{E}}_{m;n}\left((\zeta_i^k)^*; (\zeta_j^l)^*; q\right) \qquad \text{(B.3.9)}$$

---

[13]Notice, that it is enough to show this identity at $(m, n) = (0, 0)$ since every other case is governed by *n*-fold iterated integration and differentiation.

B.4   An Algorithm for Symbolic Expansions of $\overline{\text{E}}$-functions

The results of the computations of the sunrise and the kite integral are given in terms of the ELi-functions, which are defined as a convergent power series in q with $|q| < 1$. While these series permit nice properties for analytical calculations like iterated integration, it is mandatory to have an fast expansion algorithm up to a certain order u in q, to obtain numerical results.

In this section some ideas on how to implement such an algorithm are discussed.

B.4.1   A brute force, straightforward algorithm

In principle, the expansion task is easily done by restricting the sums in the definitions of the ELi-functions to the upper bound u

$$\text{ELi}_{m_1,\ldots,m_l;n_1,\ldots,n_l;2o_1,\ldots,2o_{l-1}}(x_1,\ldots,x_l;y_1,\ldots,y_l;q) = \tag{B.4.1}$$

$$= \sum_{j_1}^{u} \cdots \sum_{j_l}^{u} \sum_{k_1}^{u} \cdots \sum_{k_l}^{u} \frac{x_1^{j_1}}{j_1^{m_1}} \cdots \frac{x_l^{j_l}}{j_l^{m_l}} \cdot \frac{y_1^{k_1}}{k_1^{n_1}} \cdots \frac{y_l^{k_l}}{k_l^{n_l}} \cdot \frac{q^{j_1 k_1 + \ldots + j_l k_l}}{\prod_{i=1}^{l-1}(\sum_{r=i}^{l} j_r k_r)^{o_i}} \tag{B.4.2}$$

and omitting terms of order $> \mathcal{O}(q^u)$.

Procedure BruteForceApproach

  Input: ELi-function of depth l; expansion order: u

  Result: q-series expansion of order $\mathcal{O}(q^u)$

  begin

    (* Define summands for ELi-function *)

    expansion0= $\left(\prod_{s=1}^{l} \frac{x_s^{j_s}}{j_s^{m_s}} \cdot \frac{y_s^{k_s}}{k_s^{n_s}} \cdot q^{j_s k_s} \right) \cdot \left(\prod_{i=1}^{l-1}(\sum_{r=i}^{l} j_r k_r)^{o_i} \right)^{-1}$;

    (*Sum over all j and k*)

    for t=1 to l **do**

      (* Minor change of summation limits to reduce number of terms $> \mathcal{O}(q^u)$ *)

      expansionN= $\sum_{k_t=1}^{u-l+1} \left(\sum_{j_t=1}^{\lfloor u/k_t \rfloor} \text{expansion0} \right)$;

      expansion0=expansionN ;

    expansionN $\leftarrow$ Omit terms of order $> \mathcal{O}(q^u)$

Even though this approach, as depicted in the BruteForceApproach procedure, is the most obvious, it has two mayor downsides:

1. The brute force approach BruteForceApproach only gives an exact series expansion without terms of order $> \mathcal{O}(q^u)$ for depth $l = 1$. The number of unwanted terms of order $> \mathcal{O}(q^u)$ grows tremendously fast for increasing $l > 1$. This can not be circumvented by minor changes in the summation limits.

2. The nested structure of the denominator $\left(\prod_{i=1}^{l-1}(\sum_{r=i}^{l} j_r k_r)^{o_i}\right)^{-1}$ does not allow any factorization of the expansion for $\vec{o} \neq \vec{0}$ and $l > 1$.

Therefore, any straightforward attempt to expand ELi-functions of higher depth to a reasonably high order (e.g. $l = 3$ up to $\mathcal{O}(q^{100})$) will result in long computation times caused by the computations of unwanted terms and their nested denominators.

B.4.2   An advanced algorithm

While it is not yet obvious how to circumvent the computation of unwanted terms, the analytical properties of the ELi-functions give rise to the possibility of factorizing the complete expansion procedure by getting rid of the nested denominators.
The essential relations to achieve a complete factorisation are

$$\mathrm{ELi}_{m_1,\ldots,m_l;n_1,\ldots,n_l;2(o_1+1),\ldots,2o_{l-1}}(x_1,\ldots,x_l;y_1,\ldots,y_l;q) = \tag{B.4.3}$$

$$= \int_0^q \frac{\mathrm{d}q'}{q'} \mathrm{ELi}_{m_1,\ldots m_l;n_1,\ldots,n_l;2o_1,\ldots,2o_{l-1}}(x_1,\ldots,x_l;y_1,\ldots,y_l;q') \tag{B.4.4}$$

$$\Leftrightarrow q\partial_q \mathrm{ELi}_{m_1,\ldots,m_l;n_1,\ldots,n_l;2o_1,\ldots,2o_{l-1}}(x_1,\ldots,x_l;y_1,\ldots,y_l;q) = \tag{B.4.5}$$

$$= \mathrm{ELi}_{m_1,\ldots,m_l;n_1,\ldots,n_l;2(o_1-1),\ldots,2o_{l-1}}(x_1,\ldots,x_l;y_1,\ldots,y_l;q) \tag{B.4.6}$$

and

$$\mathrm{ELi}_{m_1,\ldots m_l;n_1,\ldots,n_l;0,2o_2,\ldots,2o_{l-1}}(x_1,\ldots,x_l;y_1,\ldots,y_l;q) = \tag{B.4.7}$$

$$= \mathrm{ELi}_{m_1;n_1}(x_1;y_1;q) \cdot \mathrm{ELi}_{m_2,\ldots m_l;n_2,\ldots,n_l;2o_2,\ldots,2o_{l-1}}(x_2,\ldots,x_l;y_2,\ldots,y_l;q) . \tag{B.4.8}$$

By consecutive usage of (B.4.6) it is possible to reduce o_1 to zero and factor out an ELi of depth 1 with (B.4.8).

For the sake of illustration, the function $\mathrm{ELi}_{m_1,m_2;n_1,n_2;2o_1}(x_1,x_2;y_1,y_2;q)$ is therefore given by the o_1-fold iterated integration

$$\mathrm{ELi}_{m_1,m_2;n_1,n_2;2o_1}(x_1,x_2;y_1,y_2;q) = \tag{B.4.9}$$

$$= \int_0^q \left(\ldots \left(\int_0^{q_2} (\mathrm{ELi}_{m_1;n_1}(x_1;y_1;q_1)\mathrm{ELi}_{m_2;n_2}(x_2;y_2;q_1)) \frac{dq_1}{q_1}\right)\ldots\right) \frac{dq_{o_1}}{q_{o_1}} . \tag{B.4.10}$$

Since we are interested in the numerical evaluation of ELi-functions for $|q| < 1$ only, the q-expansion and iterated integration can be interchanged. If the series expansion of the product of ELi-function in (B.4.10) is given by

$$\mathrm{ELi}_{m_1;n_1}(x_1;y_1;q)\mathrm{ELi}_{m_2;n_2}(x_2;y_2;q) = a_2q^2 + a_3q^3 + a_4q^4 + \ldots + a_u q^u + \mathcal{O}(q^{u+1}) \tag{B.4.11}$$

the expansion of $\mathrm{ELi}_{m_1,m_2;n_1,n_2;2o_1}(x_1,x_2;y_1,y_2;q)$ is trivially obtained by

$$\mathrm{ELi}_{m_1,m_2;n_1,n_2;2o_1}(x_1,x_2;y_1,y_2;q) = \frac{a_1}{2^{o_1}}q^2 + \frac{a_3}{3^{o_1}}q^3 + \ldots + \frac{a_u}{u^{o_1}}q^u + \mathcal{O}(q^{u+1}) . \tag{B.4.12}$$

These considerations lead to the advanced recursive algorithm depicted in AdvancedApproach. This procedure works with ELi-functions of depth 1 only and is therefore free of any computations of the nested denominators.

Procedure AdvancedApproach

Input: ELi-function of depth l; expansion order: u
Result: q-series expansion of order $\mathcal{O}(q^u)$
begin

  if l==1 **then**
    (*Notice: The brute force approach is well suited for l==1*)

    expansionN=BruteForceApproach(ELi$_{m_1;n_1}(x_1;y_1;q)$);

  else
    (* usage of (B.4.6) and (B.4.10) *)

$$\text{expansion0} = \big(\tag{B.4.13}$$
$$\text{BruteForceApproach}(\text{ELi}_{m_1;n_1}(x_1;y_1;q)) \tag{B.4.14}$$
$$\times \text{AdvancedApproach}(\text{ELi}_{m_2,\dots,m_l;n_2,\dots,n_l;2o_2,\dots,2o_{l-1}}(x_2,\dots,x_l;y_2,\dots,y_l;q)) \tag{B.4.15}$$
$$\big); \tag{B.4.16}$$

    (* o_1-fold iterated integration via replacement *)
    expansionN=expansion0 /. $q^\alpha \to \frac{1}{\alpha^{o_1}}q^\alpha$;
  expansionN $\leftarrow$ Omit terms of order $> \mathcal{O}(q^u)$

The series expansion procedures described above are easily modified to work with $\overline{\text{E}}$-functions as well. But since any $\overline{\text{E}}$-function can be written as a linear combination of ELi-functions, this is the natural point for parallelized q-series expansion of $\overline{\text{E}}$-functions.

B.5 Explicit Expressions for Hyperlogarithms and E-functions in Terms of $\overline{\text{E}}$-functions

This expressions are obtained by computing the iterated integrals as described in section 7.4.1. The here listed explicit expressions are published in [124] and taken from there. They are included since they are referred to in section 7.6.1 as an explanation for the increasing error by constant order in the q-expansion at higher orders in the ε-expansion.

$$
\begin{aligned}
G(1;y) &= 3\left[\overline{\text{E}}_{1;0}(-1;1;-q) - \overline{\text{E}}_{1;0}(r_6;1;-q)\right], \\
G(0,1;y) &= 3\left[\overline{\text{E}}_{2;1}(-1;1;-q) - \overline{\text{E}}_{2;1}(r_6;1;-q)\right] \\
&\quad -12\left[\overline{\text{E}}_{0,1;-1,0;2}(r_3,-1;-1,1;-q) - \overline{\text{E}}_{0,1;-1,0;2}(r_3,r_6;-1,1;-q)\right], \\
G(1,1;y) &= 9\left[\overline{\text{E}}_{0,1;-1,0;2}(-1,-1;1,1;-q) - \overline{\text{E}}_{0,1;-1,0;2}(-1,r_6;1,1;-q)\right. \\
&\quad \left. -\overline{\text{E}}_{0,1;-1,0;2}(r_6,-1;1,1;-q) + \overline{\text{E}}_{0,1;-1,0;2}(r_6,r_6;1,1;-q)\right].
\end{aligned} \tag{B.5.1}
$$

$$G\left(0,0,1;y\right) = 3\left[\overline{\mathrm{E}}_{3;2}\left(-1;1;-q\right) - \overline{\mathrm{E}}_{3;2}\left(r_6;1;-q\right)\right] - 12\left[\overline{\mathrm{E}}_{0,1;-1,0;4}\left(r_3,-1;-1,1;-q\right)\right.$$
$$\left.-\overline{\mathrm{E}}_{0,1;-1,0;4}\left(r_3,r_6;-1,1;-q\right)\right] - 12\left[\overline{\mathrm{E}}_{0,2;-1,1;2}\left(r_3,-1;-1,1;-q\right)\right.$$
$$\left.-\overline{\mathrm{E}}_{0,2;-1,1;2}\left(r_3,r_6;-1,1;-q\right)\right] + 48\left[\overline{\mathrm{E}}_{0,0,1;-1,-1,0;2,2}\left(r_3,r_3,-1;-1,-1,1;-q\right)\right.$$
$$\left.-\overline{\mathrm{E}}_{0,0,1;-1,-1,0;2,2}\left(r_3,r_3,r_6;-1,-1,1;-q\right)\right],$$

$$G\left(0,1,1;y\right) = 9\left[\overline{\mathrm{E}}_{0,1;-1,0;4}\left(-1,-1;1,1;-q\right) - \overline{\mathrm{E}}_{0,1;-1,0;4}\left(-1,r_6;1,1;-q\right)\right.$$
$$\left.-\overline{\mathrm{E}}_{0,1;-1,0;4}\left(r_6,-1;1,1;-q\right) + \overline{\mathrm{E}}_{0,1;-1,0;4}\left(r_6,r_6;1,1;-q\right)\right]$$
$$-36\left[\overline{\mathrm{E}}_{0,0,1;-1,-1,0;2,2}\left(r_3,-1,-1;-1,1,1;-q\right) - \overline{\mathrm{E}}_{0,0,1;-1,-1,0;2,2}\left(r_3,-1,r_6;-1,1,1;-q\right)\right.$$
$$\left.-\overline{\mathrm{E}}_{0,0,1;-1,-1,0;2,2}\left(r_3,r_6,-1;-1,1,1;-q\right) + \overline{\mathrm{E}}_{0,0,1;-1,-1,0;2,2}\left(r_3,r_6,r_6;-1,1,1;-q\right)\right],$$

$$G\left(1,0,1;y\right) = 9\left[\overline{\mathrm{E}}_{0,2;-1,1;2}\left(-1,-1;1,1;-q\right) - \overline{\mathrm{E}}_{0,2;-1,1;2}\left(-1,r_6;1,1;-q\right)\right.$$
$$\left.-\overline{\mathrm{E}}_{0,2;-1,1;2}\left(r_6,-1;1,1;-q\right) + \overline{\mathrm{E}}_{0,2;-1,1;2}\left(r_6,r_6;1,1;-q\right)\right]$$
$$-36\left[\overline{\mathrm{E}}_{0,0,1;-1,-1,0;2,2}\left(-1,r_3,-1;1,-1,1;-q\right) - \overline{\mathrm{E}}_{0,0,1;-1,-1,0;2,2}\left(-1,r_3,r_6;1,-1,1;-q\right)\right.$$
$$\left.-\overline{\mathrm{E}}_{0,0,1;-1,-1,0;2,2}\left(r_6,r_3,-1;1,-1,1;-q\right) + \overline{\mathrm{E}}_{0,0,1;-1,-1,0;2,2}\left(r_6,r_3,r_6;1,-1,1;-q\right)\right],$$

$$G\left(1,1,1;y\right) = 27\left[\overline{\mathrm{E}}_{0,0,1;-1,-1,0;2,2}\left(-1,-1,-1;1,1,1;-q\right)\right.$$
$$-\overline{\mathrm{E}}_{0,0,1;-1,-1,0;2,2}\left(-1,-1,r_6;1,1,1;-q\right) - \overline{\mathrm{E}}_{0,0,1;-1,-1,0;2,2}\left(-1,r_6,-1;1,1,1;-q\right)$$
$$+\overline{\mathrm{E}}_{0,0,1;-1,-1,0;2,2}\left(-1,r_6,r_6;1,1,1;-q\right) - \overline{\mathrm{E}}_{0,0,1;-1,-1,0;2,2}\left(r_6,-1,-1;1,1,1;-q\right)$$
$$+\overline{\mathrm{E}}_{0,0,1;-1,-1,0;2,2}\left(r_6,-1,r_6;1,1,1;-q\right) + \overline{\mathrm{E}}_{0,0,1;-1,-1,0;2,2}\left(r_6,r_6,-1;1,1,1;-q\right)$$
$$\left.-\overline{\mathrm{E}}_{0,0,1;-1,-1,0;2,2}\left(r_6,r_6,r_6;1,1,1;-q\right)\right]. \tag{B.5.2}$$

The E-functions needed for the evaluation of the first two Laurent-coefficients of the sunrise are:

$$\mathrm{E}_{1;0}(-1;1;-q) = \overline{\mathrm{E}}_{1;0}(-1;1;-q) - \log(2) \tag{B.5.3}$$

$$\mathrm{E}_{2;0}(r_3;-1;-q) = \overline{\mathrm{E}}_{2;0}(r_3;-1;-q) - \frac{1}{2}i\left(\mathrm{Li}_2(r_3) - \mathrm{Li}_2\left(\frac{1}{r_3}\right)\right) \tag{B.5.4}$$

$$\mathrm{E}_{1;0}(r_3;1;-q) = \overline{\mathrm{E}}_{1;0}(r_3;1;-q) + \frac{1}{2}\left(-\log\left(1-\frac{1}{r_3}\right) - \log(1-r_3)\right) \tag{B.5.5}$$

$$\mathrm{E}_{3;1}(r_3;-1;-q) = \overline{\mathrm{E}}_{3;1}(r_3;-1;-q) - \frac{1}{2}i\left(\mathrm{Li}_3(r_3) - \mathrm{Li}_3\left(\frac{1}{r_3}\right)\right) \tag{B.5.6}$$

$$\mathrm{E}_{0,1;-2,0;4}(r_3,r_3;-1,-1;-q) = \overline{\mathrm{E}}_{0,1;-2,0;4}(r_3,r_3;-1,-1;-q)$$
$$+ \frac{1}{2}\left(-\log\left(1-\frac{1}{r_3}\right) - \log(1-r_3)\right)\overline{\mathrm{E}}_{2;0}(r_3;-1;-q) \tag{B.5.7}$$

$$\mathrm{E}_{0,1;-2,0;4}(r_3,r_3;-1,1;-q) = \overline{\mathrm{E}}_{0,1;-2,0;4}(r_3,r_3;-1,1;-q)$$
$$+ \frac{1}{2}\left(-\log\left(1-\frac{1}{r_3}\right) - \log(1-r_3)\right)\overline{\mathrm{E}}_{2;0}(r_3;-1;-q) \tag{B.5.8}$$

$$\mathrm{E}_{0,1;-2,0;4}(r_3,-1;-1,1;-q) = \overline{\mathrm{E}}_{0,1;-2,0;4}(r_3,-1;-1,1;-q) - \log(2)\overline{\mathrm{E}}_{2;0}(r_3;-1;-q). \tag{B.5.9}$$

Bibliography

[1] G. Passarino and M. Veltman, "One-loop corrections for e^+e^- annihilation into $\mu^+\mu^-$ in the Weinberg model," <u>Nuclear Physics B</u> **160** no. 1, (1979) 151 – 207.

[2] T. Binoth, E. N. Glover, P. Marquard, and J. van der Bij, "Two loop corrections to light by light scattering in supersymmetric QED," <u>JHEP</u> **0205** (2002) 060, `arXiv:hep-ph/0202266 [hep-ph]`.

[3] O. Tarasov, "Connection between Feynman integrals having different values of the space-time dimension," <u>Phys.Rev.</u> **D54** (1996) 6479–6490, `arXiv:hep-th/9606018 [hep-th]`.

[4] O. Tarasov, "Generalized recurrence relations for two loop propagator integrals with arbitrary masses," <u>Nucl.Phys.</u> **B502** (1997) 455–482, `arXiv:hep-ph/9703319 [hep-ph]`.

[5] S. Weinzierl, "The Art of computing loop integrals," `arXiv:hep-ph/0604068 [hep-ph]`.

[6] W. Pauli and F. Villars, "On the Invariant Regularization in Relativistic Quantum Theory," <u>Rev. Mod. Phys.</u> **21** (Jul, 1949) 434–444. `http://link.aps.org/doi/10.1103/RevModPhys.21.434`.

[7] E. R. Speer, <u>Generalized Feynman Amplitudes</u>. Princeton University Press, 1969.

[8] C. Bollini and J. Giambiagi, "Dimensional Renormalization: The Number of Dimensions as a Regularizing Parameter," <u>Nuovo Cim.</u> **12** no. 1, (1972) 20–26.

[9] G. 't Hooft and M. Veltman, "Regularization and Renormalization of Gauge Fields," <u>Nucl.Phys.</u> **B44** (1972) 189–213.

[10] G. 't Hooft, "Dimensional regularization and the renormalization group," <u>Nucl.Phys.</u> **B61** (1973) 455–468.

[11] K. G. Wilson, "Quantum field theory models in less than four-dimensions," <u>Phys.Rev.</u> **D7** (1973) 2911–2926.

[12] D. Kreimer and K. Yeats, "Diffeomorphisms of quantum fields," `arXiv:1610.01837 [math-ph]`.

[13] A. Grozin, Lecture on QED and QCD: Practical Calculation and Renormalization of One- and Multi-Loop Feynman Diagrams. World Scientific Publishing Co., Inc., River Edge, NJ, USA, 2007.

[14] T. Kinoshita, "Mass singularities of Feynman amplitudes," J.Math.Phys. **3** (1962) 650–677.

[15] T. Lee and M. Nauenberg, "Degenerate Systems and Mass Singularities," Phys.Rev. **133** (1964) B1549–B1562.

[16] M. Argeri and P. Mastrolia, "Feynman Diagrams and Differential Equations," Int.J.Mod.Phys. **A22** (2007) 4375–4436, `arXiv:0707.4037 [hep-ph]`.

[17] K. Chetyrkin and F. Tkachov, "Integration by Parts: The Algorithm to Calculate beta Functions in 4 Loops," Nucl.Phys. **B192** (1981) 159–204.

[18] A. Grozin, "Integration by parts: An Introduction," Int.J.Mod.Phys. **A26** (2011) 2807–2854, `arXiv:1104.3993 [hep-ph]`.

[19] V. A. Smirnov, Analytic Tools for Feynman Integrals. 250. Springer Berlin Heidelberg, 2012.

[20] S. Laporta and E. Remiddi, "The Analytical value of the electron (g-2) at order α^3 in QED," Phys.Lett. **B379** (1996) 283–291, `arXiv:hep-ph/9602417 [hep-ph]`.

[21] A. Smirnov and A. Petukhov, "The Number of Master Integrals is Finite," Lett.Math.Phys. **97** (2011) 37–44, `arXiv:1004.4199 [hep-th]`.

[22] R. N. Lee and A. A. Pomeransky, "Critical points and number of master integrals," JHEP **11** (2013) 165, `arXiv:1308.6676 [hep-ph]`.

[23] R. N. Lee, "Presenting LiteRed: a tool for the Loop InTEgrals REDuction," `arXiv:1212.2685 [hep-ph]`.

[24] R. N. Lee, "LiteRed 1.4: a powerful tool for reduction of multiloop integrals," J. Phys. Conf. Ser. **523** (2014) 012059, `arXiv:1310.1145 [hep-ph]`.

[25] S. Laporta, "High precision calculation of multiloop Feynman integrals by difference equations," Int.J.Mod.Phys. **A15** (2000) 5087–5159, `arXiv:hep-ph/0102033 [hep-ph]`.

[26] S. Laporta and E. Remiddi, "Analytic treatment of the two loop equal mass sunrise graph," Nucl. Phys. **B704** (2005) 349–386, `arXiv:hep-ph/0406160 [hep-ph]`.

[27] A. Smirnov, "Algorithm FIRE – Feynman Integral REduction," JHEP **0810** (2008) 107, `arXiv:0807.3243 [hep-ph]`.

[28] C. Studerus, "Reduze-Feynman Integral Reduction in C++," Comput.Phys.Commun. **181** (2010) 1293–1300, `arXiv:0912.2546 [physics.comp-ph]`.

[29] A. V. Smirnov, "FIRE5: a C++ implementation of Feynman Integral REduction," Comput.Phys.Commun. **189** (2014) 182–191, `arXiv:1408.2372 [hep-ph]`.

[30] A. von Manteuffel and C. Studerus, "Reduze 2 - Distributed Feynman Integral Reduction," `arXiv:1201.4330 [hep-ph]`.

[31] A. Georgoudis, K. J. Larsen, and Y. Zhang, "Azurite: An algebraic geometry based package for finding bases of loop integrals," `arXiv:1612.04252 [hep-th]`.

[32] C. Bogner and S. Weinzierl, "Feynman graph polynomials," Int. J. Mod. Phys. **A25** (2010) 2585–2618, `arXiv:1002.3458 [hep-ph]`.

[33] N. Nakanishi, Graph theory and Feynman integrals. Mathematics and its applications. Gordon and Breach, 1971.

[34] M. Peskin and D. Schroeder, An Introduction to Quantum Field Theory. Advanced book classics. Addison-Wesley Publishing Company, 1995.

[35] E. Panzer, "Feynman integrals and hyperlogarithms," ArXiv e-prints (June, 2015) , `arXiv:1506.07243 [math-ph]`.

[36] H. Cheng and T. T. Wu, EXPANDING PROTONS: SCATTERING AT HIGH-ENERGIES. 1987.

[37] E. Remiddi and J. A. M. Vermaseren, "Harmonic polylogarithms," Int. J. Mod. Phys. **A15** (2000) 725–754, `arXiv:hep-ph/9905237 [hep-ph]`.

[38] T. Gehrmann and E. Remiddi, "Two loop master integrals for $\gamma \longrightarrow 3$ jets: The Planar topologies," Nucl.Phys. **B601** (2001) 248–286, `arXiv:hep-ph/0008287 [hep-ph]`.

[39] T. Gehrmann and E. Remiddi, "Two loop master integrals for $\gamma \longrightarrow 3$ jets: The Nonplanar topologies," Nucl.Phys. **B601** (2001) 287–317, `arXiv:hep-ph/0101124 [hep-ph]`.

[40] J. Ablinger, J. Blümlein, and C. Schneider, "Harmonic sums and polylogarithms generated by cyclotomic polynomials," Journal of Mathematical Physics **52** no. 10, (Oct., 2011) 102301, `arXiv:1105.6063 [math-ph]`.

[41] A. B. Goncharov, "Multiple polylogarithms, cyclotomy and modular complexes," Math. Res. Lett. **5** no. 4, (1998) 497–516, `arXiv:1105.2076 [math.AG]`.

[42] F. C. S. Brown, "Multiple zeta values and periods of moduli spaces $\mathfrak{M}\_0, n$," ArXiv Mathematics e-prints (June, 2006) , `math/0606419`.

[43] F. Brown, "Iterated integrals in quantum field theory," in Geometric and Topological Methods for Quantum Field Theory: Proceedings, 6th Summer School, Villa de Leyva, Colombia, 6-23 Jul 2009, pp. 188–240. 2013.

[44] J. A. Lappo-Danilevski, " Théorie algorithmique des corps de Riemann," Matem. Sb. **34** (1927) 113–148. `http://mi.mathnet.ru/msb7440`.

[45] A. Kotikov, "Differential equations method: New technique for massive Feynman diagrams calculation," Phys.Lett. **B254** (1991) 158–164.

[46] E. Remiddi, "Differential equations for Feynman graph amplitudes," Nuovo Cim. **A110** (1997) 1435–1452, `arXiv:hep-th/9711188 [hep-th]`.

[47] J. M. Henn, "Lectures on differential equations for Feynman integrals," J. Phys. **A48** (2015) 153001, `arXiv:1412.2296 [hep-ph]`.

[48] R. N. Lee, "Reducing differential equations for multiloop master integrals," JHEP **04** (2015) 108, `arXiv:1411.0911 [hep-ph]`.

[49] M. Argeri, S. Di Vita, P. Mastrolia, E. Mirabella, J. Schlenk, U. Schubert, and L. Tancredi, "Magnus and Dyson Series for Master Integrals," JHEP **03** (2014) 082, `arXiv:1401.2979 [hep-ph]`.

[50] L. Tancredi, "Integration by parts identities in integer numbers of dimensions. A criterion for decoupling systems of differential equations," Nucl. Phys. **B901** (2015) 282–317, `arXiv:1509.03330 [hep-ph]`.

[51] J. Ablinger, A. Behring, J. Blümlein, A. De Freitas, A. von Manteuffel, and C. Schneider, "Calculating Three Loop Ladder and V-Topologies for Massive Operator Matrix Elements by Computer Algebra," Comput. Phys. Commun. **202** (2016) 33–112, `arXiv:1509.08324 [hep-ph]`.

[52] A. Primo and L. Tancredi, "On the maximal cut of Feynman integrals and the solution of their differential equations," Nucl. Phys. **B916** (2017) 94–116, `arXiv:1610.08397 [hep-ph]`.

[53] C. Meyer, "Transforming differential equations of multi-loop Feynman integrals into canonical form," `arXiv:1611.01087 [hep-ph]`.

[54] O. Gituliar and V. Magerya, "Fuchsia: a tool for reducing differential equations for Feynman master integrals to epsilon form," `arXiv:1701.04269 [hep-ph]`.

[55] L. Adams, E. Chaubey, and S. Weinzierl, "Simplifying differential equations for multi-scale Feynman integrals beyond multiple polylogarithms," `arXiv:1702.04279 [hep-ph]`.

[56] Wolfram Research, Inc., "Mathematica," 2014. Version 10.0, Champaign, IL.

[57] S. Moch, P. Uwer, and S. Weinzierl, "Nested sums, expansion of transcendental functions and multiscale multiloop integrals," J. Math. Phys. **43** (2002) 3363–3386, `arXiv:hep-ph/0110083 [hep-ph]`.

[58] T. Huber and D. Maitre, "HypExp 2, Expanding Hypergeometric Functions about Half-Integer Parameters," Comput. Phys. Commun. **178** (2008) 755–776, `arXiv:0708.2443 [hep-ph]`.

[59] E. Panzer, "On hyperlogarithms and Feynman integrals with divergences and many scales," JHEP **03** (2014) 071, `arXiv:1401.4361 [hep-th]`.

[60] F. Brown and D. Kreimer, "Angles, Scales and Parametric Renormalization," Lett. Math. Phys. **103** (2013) 933–1007, `arXiv:1112.1180 [hep-th]`.

[61] A. von Manteuffel, E. Panzer, and R. M. Schabinger, "A quasi-finite basis for multi-loop Feynman integrals," JHEP **02** (2015) 120, `arXiv:1411.7392 [hep-ph]`.

[62] A. von Manteuffel, E. Panzer, and R. M. Schabinger, "On the Computation of Form Factors in Massless QCD with Finite Master Integrals," Phys. Rev. **D93** no. 12, (2016) 125014, `arXiv:1510.06758 [hep-ph]`.

[63] K.-T. Chen, "Iterated path integrals," Bull. Amer. Math. Soc. **83** no. 5, (09, 1977) 831–879. `http://projecteuclid.org/euclid.bams/1183539443`.

[64] L. Lewin, Structural Properties of Polylogarithms, vol. 37 of Mathematical Surveys and Monographs. American Mathematical Society, 1991.

[65] J. M. Borwein, D. M. Bradley, D. J. Broadhurst, and P. Lisonek, "Special Values of Multiple Polylogarithms," Transactions of the American Mathematical Society **353** no. 3, (2001) 907–941.

[66] D. Maitre, "HPL, a mathematica implementation of the harmonic polylogarithms," Comput. Phys. Commun. **174** (2006) 222–240, `arXiv:hep-ph/0507152 [hep-ph]`.

[67] D. Maitre, "Extension of HPL to complex arguments," Comput. Phys. Commun. **183** (2012) 846, `arXiv:hep-ph/0703052 [hep-ph]`.

[68] T. Gehrmann and E. Remiddi, "Numerical evaluation of two-dimensional harmonic polylogarithms," Comput. Phys. Commun. **144** (2002) 200–223, `arXiv:hep-ph/0111255 [hep-ph]`.

[69] J. Ablinger, "Computer Algebra Algorithms for Special Functions in Particle Physics," ArXiv e-prints (May, 2013) , `arXiv:1305.0687 [math-ph]`.

[70] J. Vollinga and S. Weinzierl, "Numerical evaluation of multiple polylogarithms," Comput. Phys. Commun. **167** (2005) 177, `arXiv:hep-ph/0410259 [hep-ph]`.

[71] E. Panzer, "Algorithms for the symbolic integration of hyperlogarithms with applications to Feynman integrals," Comput. Phys. Commun. **188** (2015) 148–166, `arXiv:1403.3385 [hep-th]`.

[72] C. Bogner, "MPL—A program for computations with iterated integrals on moduli spaces of curves of genus zero," Comput. Phys. Commun. **203** (2016) 339–353, `arXiv:1510.04562 [physics.comp-ph]`.

[73] F. Brown, "The Massless higher-loop two-point function," Commun. Math. Phys. **287** (2009) 925–958, `arXiv:0804.1660 [math.AG]`.

[74] F. C. S. Brown, "On the periods of some Feynman integrals," ArXiv e-prints (Oct., 2009) , `arXiv:0910.0114 [math.AG]`.

[75] C. Bogner and M. Lüders, "Multiple polylogarithms and linearly reducible Feynman graphs," Contemp. Math. **648** (2015) 11–28, `arXiv:1302.6215 [hep-ph]`.

[76] J. M. Henn, "Multiloop integrals in dimensional regularization made simple," Phys. Rev. Lett. **110** (2013) 251601, `arXiv:1304.1806 [hep-th]`.

[77] H. Frellesvig and C. G. Papadopoulos, "Cuts of Feynman Integrals in Baikov representation," JHEP **04** (2017) 083, `arXiv:1701.07356 [hep-ph]`.

[78] F. Dulat and B. Mistlberger, "Real-Virtual-Virtual contributions to the inclusive Higgs cross section at N3LO," `arXiv:1411.3586 [hep-ph]`.

[79] S. Caron-Huot and J. M. Henn, "Iterative structure of finite loop integrals," JHEP **06** (2014) 114, `arXiv:1404.2922 [hep-th]`.

[80] J. Bosma, M. Sogaard, and Y. Zhang, "Maximal Cuts in Arbitrary Dimension," `arXiv:1704.04255 [hep-th]`.

[81] C. Meyer, "Algorithmic transformation of multi-loop master integrals to a canonical basis with CANONICA," `arXiv:1705.06252 [hep-ph]`.

[82] N. Arkani-Hamed, J. L. Bourjaily, F. Cachazo, and J. Trnka, "Local Integrals for Planar Scattering Amplitudes," JHEP **06** (2012) 125, `arXiv:1012.6032 [hep-th]`.

[83] A. von Manteuffel and L. Tancredi, "A non-planar two-loop three-point function beyond multiple polylogarithms," `arXiv:1701.05905 [hep-ph]`.

[84] P. Belkale and P. Brosnan, "Periods and Igusa Local Zeta Functions," International Mathematics Research Notices no. 49, (2003) 2655–2670.

[85] S. Bloch, H. Esnault, and D. Kreimer, "On Motives associated to graph polynomials," Commun. Math. Phys. **267** (2006) 181–225, `arXiv:math/0510011 [math-ag]`.

[86] C. Bogner and S. Weinzierl, "Periods and Feynman integrals," J. Math. Phys. **50** (2009) 042302, `arXiv:0711.4863 [hep-th]`.

[87] A. Primo and L. Tancredi, "Maximal cuts and differential equations for Feynman integrals. An application to the three-loop massive banana graph," `arXiv:1704.05465 [hep-ph]`.

[88] R. E. Cutkosky, "Singularities and Discontinuities of Feynman Amplitudes," Journal of Mathematical Physics **1** no. 5, (1960) 429–433, `http://dx.doi.org/10.1063/1.1703676`. `http://dx.doi.org/10.1063/1.1703676`.

[89] M. J. G. Veltman, "Unitarity and causality in a renormalizable field theory with unstable particles," Physica **29** (1963) 186–207.

[90] E. Remiddi, "Dispersion Relations for Feynman Graphs," Helv. Phys. Acta **54** (1982) 364.

[91] S. Bloch and D. Kreimer, "Cutkosky Rules and Outer Space," `arXiv:1512.01705 [hep-th]`.

[92] S. Abreu, R. Britto, C. Duhr, and E. Gardi, "Cuts from residues: the one-loop case," `arXiv:1702.03163 [hep-th]`.

[93] S. Müller-Stach, S. Weinzierl, and R. Zayadeh, "Picard-Fuchs equations for Feynman integrals," Commun. Math. Phys. **326** (2014) 237–249, `arXiv:1212.4389 [hep-ph]`.

[94] R. Bonciani, V. Del Duca, H. Frellesvig, J. M. Henn, F. Moriello, and V. A. Smirnov, "Two-loop planar master integrals for Higgs$\to$ 3 partons with full heavy-quark mass dependence," JHEP **12** (2016) 096, `arXiv:1609.06685 [hep-ph]`.

[95] D. J. Broadhurst, J. Fleischer, and O. V. Tarasov, "Two loop two point functions with masses: Asymptotic expansions and Taylor series, in any dimension," Z. Phys. **C60** (1993) 287–302, `arXiv:hep-ph/9304303 [hep-ph]`.

[96] S. Bauberger, F. A. Berends, M. Bohm, and M. Buza, "Analytical and numerical methods for massive two loop selfenergy diagrams," Nucl. Phys. **B434** (1995) 383–407, `arXiv:hep-ph/9409388 [hep-ph]`.

[97] S. Bauberger, M. Böhm, G. Weiglein, F. A. Berends, and M. Buza, "Calculation of two-loop self-energies in the electroweak Standard Model," Nucl. Phys. Proc. Suppl. **37B** no. 2, (1994) 95–114, `arXiv:hep-ph/9406404 [hep-ph]`.

[98] M. Caffo, H. Czyz, S. Laporta, and E. Remiddi, "The Master differential equations for the two loop sunrise selfmass amplitudes," Nuovo Cim. **A111** (1998) 365–389, `arXiv:hep-th/9805118 [hep-th]`.

[99] B. A. Kniehl, A. V. Kotikov, A. Onishchenko, and O. Veretin, "Two-loop sunset diagrams with three massive lines," Nucl. Phys. **B738** (2006) 306–316, `arXiv:hep-ph/0510235 [hep-ph]`.

[100] S. Groote, J. G. Korner, and A. A. Pivovarov, "Laurent series expansion of sunrise type diagrams using configuration space techniques," Eur. Phys. J. **C36** (2004) 471–482, `arXiv:hep-ph/0403122 [hep-ph]`.

[101] S. Groote, J. G. Korner, and A. A. Pivovarov, "On the evaluation of a certain class of Feynman diagrams in x-space: Sunrise-type topologies at any loop order," Annals Phys. **322** (2007) 2374–2445, `arXiv:hep-ph/0506286 [hep-ph]`.

[102] S. Groote, J. G. Korner, and A. A. Pivovarov, "A Numerical Test of Differential Equations for One- and Two-Loop sunrise Diagrams using Configuration Space Techniques," Eur. Phys. J. **C72** (2012) 2085, `arXiv:1204.0694 [hep-ph]`.

[103] D. H. Bailey, J. M. Borwein, D. Broadhurst, and M. L. Glasser, "Elliptic integral evaluations of Bessel moments," J. Phys. **A41** (2008) 205203, `arXiv:0801.0891 [hep-th]`.

[104] L. Adams, C. Bogner, and S. Weinzierl, "The two-loop sunrise graph with arbitrary masses," J. Math. Phys. **54** (2013) 052303, `arXiv:1302.7004 [hep-ph]`.

[105] L. Adams, C. Bogner, and S. Weinzierl, "The two-loop sunrise graph in two space-time dimensions with arbitrary masses in terms of elliptic dilogarithms," J. Math. Phys. **55** no. 10, (2014) 102301, `arXiv:1405.5640 [hep-ph]`.

[106] L. Adams, C. Bogner, and S. Weinzierl, "The two-loop sunrise integral around four space-time dimensions and generalisations of the Clausen and Glaisher functions towards the elliptic case," J. Math. Phys. **56** no. 7, (2015) 072303, `arXiv:1504.03255 [hep-ph]`.

[107] L. Adams, C. Bogner, and S. Weinzierl, "The iterated structure of the all-order result for the two-loop sunrise integral," J. Math. Phys. **57** no. 3, (2016) 032304, `arXiv:1512.05630 [hep-ph]`.

[108] L. Adams and S. Weinzierl, "Feynman integrals and iterated integrals of modular forms," `arXiv:1704.08895 [hep-ph]`.

[109] C. Bogner, A. Schweitzer, and S. Weinzierl, "Analytic continuation and numerical evaluation of the kite integral and the equal mass sunrise integral," `arXiv:1705.08952 [hep-ph]`.

[110] S. Bloch and P. Vanhove, "The elliptic dilogarithm for the sunset graph," J. Number Theor. **148** (2015) 328–364, `arXiv:1309.5865 [hep-th]`.

[111] S. Bloch, M. Kerr, and P. Vanhove, "Local mirror symmetry and the sunset Feynman integral," `arXiv:1601.08181 [hep-th]`.

[112] E. Remiddi and L. Tancredi, "Schouten identities for Feynman graph amplitudes; The Master Integrals for the two-loop massive sunrise graph," Nucl. Phys. **B880** (2014) 343–377, `arXiv:1311.3342 [hep-ph]`.

[113] E. Remiddi and L. Tancredi, "Differential equations and dispersion relations for Feynman amplitudes. The two-loop massive sunrise and the kite integral," Nucl. Phys. **B907** (2016) 400–444, `arXiv:1602.01481 [hep-ph]`.

[114] M. Trott, The Mathematica Guidebook: Programming with CD-ROM. Springer-Verlag New York, Inc., Secaucus, NJ, USA, 1st ed., 2002.

[115] V. Prasolov and I. Solov_ev, Elliptic Functions and Elliptic Integrals. Memoirs of the American Mathematical Society. American Mathematical Soc., 1997.

[116] T. S. Developers, SageMath, the Sage Mathematics Software System (Version 7.5.1), 2017. `http://www.sagemath.org`.

126

[117] D. Husemöller, <u>Elliptic Curves</u>. Graduate Texts in Mathematics. Springer New York, 2006.

[118] E. Remiddi, "Differential equations for the two loop equal mass sunrise," <u>Acta Phys.Polon.</u> **B34** (2003) 5311–5322, `arXiv:hep-ph/0310332 [hep-ph]`.

[119] A. I. Davydychev and J. B. Tausk, "A Magic connection between massive and massless diagrams," <u>Phys. Rev.</u> **D53** (1996) 7381–7384, `arXiv:hep-ph/9504431 [hep-ph]`.

[120] H. J. Lu and C. A. Perez, "Massless one loop scalar three point integral and associated Clausen, Glaisher and L functions,".

[121] Z. Bern, L. J. Dixon, and D. A. Kosower, "Dimensionally regulated pentagon integrals," <u>Nucl. Phys.</u> **B412** (1994) 751–816, `arXiv:hep-ph/9306240 [hep-ph]`.

[122] B. F. Stienstra, Jan, "On the Picard-Fuchs Equation and the Formal Brauer Group of Certain Elliptic K3-Surfaces.," <u>Mathematische Annalen</u> **271** (1985) 269–304. `http://eudml.org/doc/163967`.

[123] R. S. Maier, "On Rationally Parametrized Modular Equations," <u>ArXiv Mathematics e-prints</u> (Nov., 2006) , `math/0611041`.

[124] L. Adams, C. Bogner, A. Schweitzer, and S. Weinzierl, "The kite integral to all orders in terms of elliptic polylogarithms," <u>J. Math. Phys.</u> **57** (2016) 122302, `arXiv:1607.01571 [hep-ph]`.

[125] A. Sabry, "Fourth order spectral functions for the electron propagator," <u>Nuclear Physics</u> **33** (1962) 401 – 430.

[126] D. J. Broadhurst, "The Master Two Loop Diagram With Masses," <u>Z. Phys.</u> **C47** (1990) 115–124.

[127] S. Bauberger and M. Bohm, "Simple one-dimensional integral representations for two loop selfenergies: The Master diagram," <u>Nucl. Phys.</u> **B445** (1995) 25–48, `arXiv:hep-ph/9501201 [hep-ph]`.

[128] J. Zhao, "Analytic continuation of multiple polylogarithms," <u>Analysis Mathematica</u> **33** no. 4, (2007) 301–323. `http://dx.doi.org/10.1007/s10476-007-0404-7`.

[129] B. S. Institution, <u>The C standard: incorporating Technical Corrigendum 1 : BS ISO/IEC 9899/1999</u>. John Wiley, 2003.

[130] G. Passarino, "Elliptic Polylogarithms and Basic Hypergeometric Functions," <u>Eur. Phys. J.</u> **C77** no. 2, (2017) 77, `arXiv:1610.06207 [math-ph]`.

[131] F. Olver, N. I. of Standards, and T. (U.S.), <u>NIST Handbook of Mathematical Functions Hardback and CD-ROM</u>. Cambridge University Press, 2010.

[132] J. Carlson, S. Müller-Stach, and C. Peters, <u>Period Mappings and Period Domains</u>. Cambridge Studies in Advanced Mathematics. Cambridge University Press, 2003.

[133] R. Hwa and V. Teplitz, <u>Homology and Feynman Integrals</u>. The Mathematical physics monographs series. Benjamin, 1966.

[134] T. Binoth and G. Heinrich, "An automatized algorithm to compute infrared divergent multiloop integrals," <u>Nucl. Phys.</u> **B585** (2000) 741–759, `arXiv:hep-ph/0004013 [hep-ph]`.

[135] C. Bogner and S. Weinzierl, "Resolution of singularities for multi-loop integrals," <u>Comput. Phys. Commun.</u> **178** (2008) 596–610, `arXiv:0709.4092 [hep-ph]`.

[136] A. V. Smirnov and M. N. Tentyukov, "Feynman Integral Evaluation by a Sector decomposiTion Approach (FIESTA)," <u>Comput. Phys. Commun.</u> **180** (2009) 735–746, `arXiv:0807.4129 [hep-ph]`.

[137] S. Borowka, J. Carter, and G. Heinrich, "Numerical Evaluation of Multi-Loop Integrals for Arbitrary Kinematics with SecDec 2.0," <u>Comput. Phys. Commun.</u> **184** (2013) 396–408, `arXiv:1204.4152 [hep-ph]`.

[138] S. Borowka and G. Heinrich, "Massive non-planar two-loop four-point integrals with SecDec 2.1," <u>Comput. Phys. Commun.</u> **184** (2013) 2552–2561, `arXiv:1303.1157 [hep-ph]`.

[139] S. C. Borowka, <u>Evaluation of multi-loop multi-scale integrals and phenomenological two-loop applications</u>. PhD thesis, Munich, Tech. U., 2014. `arXiv:1410.7939 [hep-ph]`. `https://inspirehep.net/record/1324960/files/arXiv:1410.7939.pdf`.

[140] S. Borowka, G. Heinrich, S. P. Jones, M. Kerner, J. Schlenk, and T. Zirke, "SecDec-3.0: numerical evaluation of multi-scale integrals beyond one loop," <u>Comput. Phys. Commun.</u> **196** (2015) 470–491, `arXiv:1502.06595 [hep-ph]`.

[141] M. Abramowitz and I. A. Stegun, <u>HANDBOOK OF MATHEMATICAL FUNCTIONS</u>. Dover Publications, Inc., 1965.

[142] B. Berndt, <u>Ramanujan's Notebooks</u>. No. pt. 1. Springer New York, 2012.